A Data-driven Approach using Surrogate Models and Non-deterministic Optimization Techniques for Calibration of Soil Parameters and Sensitivity Analysis: Application to a Rockfill Dam

by

GULLNAZ SHAHZADI

MANUSCRIPT-BASED THESIS PRESENTED TO ÉCOLE DE TECHNOLOGIE SUPÉRIEURE IN PARTIAL FULFILLMENT FOR THE DEGREE OF DOCTOR OF PHILOSOPHY
Ph.D.

MONTREAL, AUGUST 07 2023

ÉCOLE DE TECHNOLOGIE SUPÉRIEURE
UNIVERSITÉ DU QUÉBEC

BOARD OF EXAMINERS

THIS THESIS HAS BEEN EVALUATED

BY THE FOLLOWING BOARD OF EXAMINERS

Mr. Azzeddine Soulaimani, Thesis supervisor
Department of Mechanical Engineering, Ecole de technologie superieure

Mr. François Duhaime, Chair, Board of Examiners
Department of Construction Engineering, Ecole de technologie superieure

Mr. Hakim Bouzid, Member of the Jury
Department of Mechanical Engineering, Ecole de technologie superieure

M. Marc Smith, Member of the Jury
Dams and infrastructures department, WSP, Montreal, Canada

M. Amin Hariri-Ardebili, External Examiner
National Institute of Standards and Technology (NIST), Gaithersburg, USA

THIS THESIS WAS PRESENTED AND DEFENDED

IN THE PRESENCE OF A BOARD OF EXAMINERS AND THE PUBLIC

ON JULY 10 2023

AT ÉCOLE DE TECHNOLOGIE SUPÉRIEURE

ACKNOWLEDGEMENTS

I would like to express my deep appreciation and sincere gratitude to my supervisor, Prof. Azzeddine Soulaïmani, for his persistent guidance and support. Working under his esteemed supervision has been an incredible opportunity that I am truly grateful for his willingness to assist me whenever I needed it has been truly remarkable. My time as his student has been the most memorable experience of my academic career.

I am genuinely grateful to my mentor, Dr. Amjad Ali, Sir Nisar Ahmed Shakoor, and all my supporters for their continuous and significant encouragement and support from the beginning of my studies here in Canada. Their unwavering support has made a significant impact on my studies and has helped me to become more confident in my academic pursuits.

I am immensely grateful to the members of my research group, GRANIT, who are my esteemed colleagues in mechanical engineering at Ecole Technologies Superior. Their unwavering support and company have been valuable to me, and I extend my heartfelt appreciation to Shubham Chaudhry, Azzedine Abdedou, and Ali Elmbrok Salem Ahmid for their exceptional contributions. I extend my sincere gratitude to the esteemed members of my Ph.D. examiner committee, including our guest examiners Prof. Hakim Bouzid, M. Marc Smith, M.Amin Hariri-Ardebili, and the president Prof. François Duhaime. Your invaluable time and efforts are deeply appreciated, and I am humbled to have you as my committee. This privilege is an honour, and I thank you for your indispensable contribution.

Last but not least, I am grateful to my family, particularly my parents and brothers, for their constant emotional support during my Ph.D. program. Their care has truly been priceless to me. My husband, Rana Rabnawaz, has been an incredible source of encouragement and kindness during the challenging times we faced together. I will always cherish his patience and care. Additionally, I want to express my deep appreciation for my son Mumin, who made many sacrifices to allow me to focus fully on my work. My family means the world to me, even more than meta-heuristics.

Une approche basée sur les données utilisant des modèles de substitution et des techniques d'optimisation non déterministes pour l'étalonnage des paramètres du sol et l'analyse de sensibilité : application à un barrage en enrochement

GULLNAZ SHAHZADI

RÉSUMÉ

Le développement de modèles numériques avancés pour la conception et l'évaluation de la sécurité de structures complexes telles que les barrages en enrochement dépend fortement de la disponibilité de ressources de calcul importantes. La structure complexe des barrages en enrochement, qui se compose de diverses zones avec des paramètres de sol variables, rend les modèles très incertains. Des variations mineures de certains paramètres du sol peuvent avoir un impact significatif sur l'ensemble de la structure, ce qui rend difficile la détermination des paramètres géomécaniques nécessaires à une modélisation efficace. Cependant, les tests en laboratoire ou in situ et les relations empiriques de la littérature sont les approches générales pour estimer ces paramètres. Néanmoins, ces mesures ne reflètent pas fidèlement la situation réelle.

Dans ce contexte, une analyse d'incertitude et une analyse de sensibilité globale ont été réalisées pour évaluer l'effet des paramètres constitutifs du sol sur le comportement d'un barrage en enrochement. Les modèles de substitution se rapprochent efficacement de la relation entre les paramètres de sol d'entrée et les déplacements, réduisant ainsi les coûts de calcul des études paramétriques. L'expansion du chaos polynomial et les réseaux de neurones profonds sont utilisés pour construire des modèles de substitution pour calculer les indices de Sobol nécessaires pour identifier l'impact des paramètres du sol sur le comportement du barrage. Deux paramètres, le module de cisaillement et les poids spécifiques, sont considérés comme des variables aléatoires d'entrée plus sensibles à partir desquelles des incertitudes surviennent.

Cette thèse propose une approche très efficace axée sur les données qui utilise des réseaux de neurones profonds et des algorithmes d'optimisation pour identifier avec précision les paramètres du sol pour un barrage en enrochement situé au Québec. Une analyse approfondie des mesures de déplacement de l'inclinomètre a été réalisée à l'aide d'un modèle d'éléments finis 2D, le domaine de calcul étant méticuleusement divisé en sous-domaines pour tenir compte de l'hétérogénéité des matériaux. Afin d'accélérer les calculs, des modèles de substitution ont été utilisés à la place du modèle d'éléments finis (FEM) complet. Pour résoudre le problème de minimisation, des algorithmes d'optimisation stochastique tels que l'algorithme génétique (GA), l'optimisation de l'essaim de particules (PSO) et l'évolution différentielle (DE) ont été soigneusement évalués et comparés.

Une autre contribution de cette thèse est de présenter une nouvelle technique pour améliorer les analyses de sécurité et de stabilité en identifiant des paramètres grâce à une méthode d'optimisation hybride. Un modèle de substitution de réseau neuronal profond est établi et une formulation de fonction multi-objectifs est utilisée pour mesurer la différence entre les déplacements prédits et réels. Les paramètres du sol sont identifiés à l'aide d'un algorithme

hybride Particle Swarm-Genetic Algorithm appliqué aux données de quatre inclinomètres installés dans deux sections différentes du barrage. L'étude compare l'efficacité des modèles Mohr-Coulomb (MC) et Hardening Soil (HS), montrant que le modèle HS fournit les valeurs des déplacements les plus proches des données mesurées sur site. La recherche se termine par la présentation des paramètres optimaux pour le barrage de la Romaine-2 et met en évidence l'efficacité des réseaux profonds et de l'optimisation hybride dans la résolution de problèmes inverses.

Mots-clés: Analyse de sensibilité, analyse d'incertitude, modélisation de substitution, expansion du chaos polynomial, réseau de neurones profonds, analyse inverse, techniques d'optimisation, fonctions multi-objectifs

A Data-driven Approach using Surrogate Models and Non-deterministic Optimization Techniques for Calibration of Soil Parameters and Sensitivity Analysis: Application to a Rockfill Dam

GULLNAZ SHAHZADI

ABSTRACT

The development of advanced numerical models for designing and assessing the safety of complex structures such as rockfill dams heavily relies on the availability of significant computational resources. The intricate structure of rockfill dams, which consists of various zones with varying soil parameters, makes the models highly uncertain. Minor variations in some soil parameters can significantly impact the expected behaviour of the structure, making it challenging to determine the geomechanical parameters required for effective modelling. However, laboratory or in situ tests and empirical relationships from the literature are the general approaches to estimating these parameters. Nonetheless, these measures do not accurately depict the insitu characteristics of the dam.

In this context, uncertainty and global sensitivity analysis have been carried out to determine the influence of constitutive soil parameters on the behaviour of a rockfill dam. In parametric studies, surrogate models are helpful in approximating the relationship between inputs (soil parameters) and outputs (displacement) and thus effectively reduce computational costs. Surrogate models, built using methods such as polynomial chaos expansion and deep neural networks, calculate the Sobol indices required for identifying the impact of soil parameters on dam behaviour. Two parameters, Shear modulus and specific weights, are considered more sensitive input random variables from which uncertainties occur.

This thesis proposes a highly effective data-driven approach that utilizes deep neural networks and optimization algorithms to estimate in situ values of soil parameters for a rockfill dam located in Quebec. Extensive analysis of inclinometer displacement measurements was carried out using a 2D finite element model, with the computational domain being meticulously divided into subdomains to account for the variability of material properties. In order to expedite computations, surrogate models were employed in lieu of the complete FEM model. To solve the minimization problem, stochastic optimization algorithms such as Genetic algorithm (GA), Particle Swarm Optimization (PSO), and Differential evolution (DE) were thoroughly evaluated and compared.

Another contribution of this thesis is to present a novel technique for enhancing safety and stability analyses by identifying parameters through a hybrid optimization method. A deep neural network surrogate model is established and a multi-objective function formulation is used to weigh the difference between predicted and actual displacements. The soil parameters are identified using a hybrid Particle Swarm-Genetic Algorithm applied to data from four inclinometers installed in two different cross-sections of the dam. The study compares the effectiveness of the Mohr-Coulomb (MC) and Hardening Soil (HS) models, showing that the HS model provides the closest values to the measured onsite data. The research concludes by

presenting the optimal soil parameters for the Romaine-2 dam and highlights the effectiveness of DNNs and hybrid optimization in solving inverse problems.

Keywords: Senstivity analysis, uncertainty analysis, surrogate modelling, polynomial chaos expansion, deep neural network, inverse analysis, optimization techniques, multi-objective functions

TABLE OF CONTENTS

LIST OF TABLES

LIST OF FIGURES

Page

LIST OF ALGORITHMS

Page

LIST OF ABBREVIATIONS

FEM	Finite Element Method
MC	Mohr-Coulomb
HS	Hardening Soil
HSS	Hardening soil with small strains
PCE	Polynomial chaos expansion
DNN	Deep neural network
ML	Machine Learning
AI	Artificial Intelligence
DL	Deep Learning
LR	Linear Regression
SVM	Support Vector Machine
ANN	Artificial Neural Networks
RF	Random Forest
ReLu	Rectifier linear units
tanh	Hyperbolic Tangent Function
GA	Genetic Algorithm
PSO	Particle Swarm optimization
DE	Differential evolution
PSOGA	Hybrid Particle Swarm Optimization and Genetic Algorithm
SVR	Support vector regression

LIST OF SYMBOLS AND UNITS OF MEASUREMENTS

C	Cohesion in Mohr-Coulomb failure
cu	Undrained shear strength
E	Young's modulus
E^{ref}	Reference Elastic modulus
E_{50}^{ref}	Reference secant stiffness in standard drained triaxial test in HS soil model
E_{50}	Secant stiffness in standard drained triaxial test in HS soil model
E_{ur}	Unloading and reloading stiffness in HS soil model
E_{oed}	Oedometer stiffness in HS soil model
E_{oed}^{ref}	Reference oedometer stiffness in HS soil model
E_t	Tangent Young's modulus
F	Poisson's ratio parameter in Hyperbolic model
f	Yield function
$\bar{f}$	Function of stress
G_{ref}	Shear modulus
q	Deviatoric stress
q_f	Ultimate deviatoric stress
ϕ	Friction angle in Mohr-Coulomb failure criteria
φ_m	Mobilized friction angle
φ_{cv}	Critical friction angle

$\triangle\varphi$	Change of friction angle with confining stress in Hyperbolic model
σ_1	Major principal stress; axial stress in triaxial setting
σ_2	Intermediate principal stress
σ_3	Minor principal stress; radial stress in triaxial setting
σ_{1d}	Maximum principal stress in dry condition
σ_{3w}	Isotropic confinement stress after wetting
$\triangle\sigma_x$	Horizontal stress increment (x axis) in plane strain formulation
$\triangle\sigma_y$	Vertical stress increment (y axis) in plane strain formulation
$\sigma_1 - \sigma_3$	Deviatoric stress
ϵ	Strain
ψ	Dilatancy angle
ϵ_1	Vertical strain
E_i	Initial stiffness
p_{ref}	Confining pressure
R_f	Failure ratio
γ^p	Plastic strain
$\mathcal{E}_v^p$	Plastic volume change
m	Power for the stress-level dependency of stiffness
Ψ_{mob}	Mobilized dilatancy angle
e_{max}	Maximum void ratio

e_{init}	Initial void ratio
K_0^{nc}	Coefficient of lateral earth pressure
p_p	Pre-consolidation stress
$\mathbf{W}$	Weighted diagonal matrix

INTRODUCTION

0.1 Research context

In the late 19th and early 20th centuries, rockfill has been widely used as an engineering material for the construction of dams. Initially, performance was excellent, but excessive deformation limited its use in high embankments or dams (Sherard & Cooke, 1987; Oldecop & Alonso, 2001; Alonso & Cardoso, 2010). However, with improved compaction techniques, the use of rockfill in high dams (such as rockfill dams) accelerated, and several kinds of research have been done on the deformation behaviours of rockfill (Rahmani & Panah, 2020; Xiao *et al.*, 2020; Zhou, Ma & Zhang, 2019). A rockfill dam is an embankment dam constructed primarily using compacted rock materials. It is designed to impound water and create a reservoir by confining the water within the dam's structure. Rockfill dams have two principal parts: the central rockfill zone and the impervious zone. Nowadays, these Dams are among the most popular and highest dams in the world. However, the safety of the dams is the essential factor. Nevertheless, the analysis of rockfill dams is difficult due to the uncertainties and variability in material properties.

Over the years, the finite element method (FEM) has become one of the most advanced engineering numerical modelling methods used in design. This successful use of the FEM can be attributed to its ability to provide better accuracy and effectively deal with complex geometries, boundary conditions, and material (rock/soil) nonlinearities (Wei, Xiaolin, Chuangbing & Xinghong, 2010; Saberi, Annan & Konrad, 2018). To accurately model a dam, all the material properties of the constitutive models in every zone within the dam structure must be known. Still, this can be challenging as limited information regarding the soil materials used in the dam structures and restricted recorded instrumentation data from in situ. Additionally, obtaining soil samples for testing, particularly from the central impervious part, is typically complex, costly effecting and may impact the dam's performance and safety. Hydro-Québec, a diligent and well-informed owner, strictly enforces compliance with the Dam Safety Act (Konard, Soulaimani, Lefebvre,

Leger & Nguyen, 2014a,b). Thus, the dam owners require predicting the behaviour of each high-capacity dam to improve the design for upcoming constructions. Therefore, the dam must be modelled accurately, and a proper constitutive model has to be chosen for every part of the dam. In addition, it is required to calibrate the parameters in various sections of the dam and discuss the impact of each parameter's variation.

Currently, earth-rockfill embankments are well-equipped with instruments that gather valuable data for dam owners and their consultants. This data includes pore pressures, deformations, total stresses, and seepage. It is, therefore judicious to collect this information and use it to evaluate the behavioural law used to model the mechanical behaviour of the different types of rockfill structures. One question that comes to mind is whether a method exists to identify the dam's material properties from the recorded data obtained from these instruments. However, the understanding of behaviour is not as advanced for the new mixed structures built in the last ten years, such as embankment dams with an upstream concrete mask (Toulnustouc (Rochon, Morneau & Lefebvre, 2001)) and rockfill dams with an asphalt core (Romaine-2 (Longtin *et al.*, 2012)). Inverse analysis, also known as back analysis, is undoubtedly considered the most effective technique for parameter identification (Zentar, Hicher & Moulin, 2001). It enables the calibration of soil parameters by meticulously analyzing the relationship between a conceptual model and the physical system. The parameters are adjusted automatically by minimizing the measure of the difference between the finite element results and the measured data. However, factors such as the number of parameters, choice of constitutive model, numerical modelling, and framework for inverse analysis can affect calibration accuracy.

It would also be interesting to examine the possibility of distinguishing displacement's vertical and horizontal components. In addition, It is necessary to understand how input parameters affect outputs to understand the performance of these structural systems during the construction and impoundment phases. Therefore, uncertainty and sensitivity analysis has become a vital

task to evaluate. This research will concentrate on numerical modelling and identification of parameters of appropriate soil models for an asphaltic core rockfill dam, which will enhance the accuracy of dam behaviour prediction, leading to improved dam design and safety assessment.

0.2 Thesis objectives

This thesis contributes to analyzing the sensitivity, propagation of uncertainties and calibration of the soil parameters through numerical models of a rockfill dam. To model a dam, all the properties of soil constitutive models in each zone of the dam structure are required. However, due to the complexity or age of the dams, soil parameters are not always available or obtained through mathematical expressions.

The specific objectives of this work are as follows:

1. Carry out a literature review, as exhaustive as possible, of the different parametric uncertainty propagation, sensitivity and calibration methods.
2. Develop an interface between the FEM model and Python code to generate a simulated data set.
3. Implement the classical techniques for propagation uncertainty by executing sampling methods such as Monte Carlo (MC) through the numerical model of a rockfill dam.
4. Implement a non-intrusive stochastic approach Polynomial chaos expansion (PCE) and a deep neural network-based data-driven surrogate model to analyze the propagation of parametric uncertainties that overcome the limitations of other techniques.
5. Conduct the sensitivity analysis and compute the sobol indices to identify the impact of soil parameters on dam response.
6. Exploit the different approaches implemented and developed for identifying the soil parameters through the application of the dam with real data, allowing the establishment of a reliable data-driven framework using the non-intrusive surrogate approach with a

considerably reduced computational effort. Also, compare the results for optimal parameters with available measurements.

0.3 Proposed approach

Briefly, the thesis proposes the methodology and framework that significantly contribute to uncertainty propagation, sensitivity and inverse analysis. The following contributions are made in order to address the significant and challenging issues:

1. A numerical model of the highest rockfill dam is built layer by layer using appropriate constitutive soil models. Also, an interface between the numerical model and the programming code is created to perform the simulations. The credibility of the numerical simulations was assessed by comparing them with the experimental data sets.
2. In this research, the sobol sampling technique (Sobol, 1993) has been used to generate the simulation data sets. The convergence study is conducted using the Monte Carlo method to get an accurate sample size.
3. A data set of the numerical simulations at specific positions in the dam is generated and compared with the measured data.
4. An original contribution, the sensitivity and uncertainty analysis, has been conducted for an application of rockfill dam after construction using surrogate modelling techniques, polynomial chaos expansion and deep neural network. Their results are compared with the classical Monte Carlo (MC) sampling technique. The results show that surrogate models play a significant role in reducing the computational cost of numerical models. The work is published in

   Water (Special issue: Soft Computing and Machine Learning in Dam Engineering); https://doi.org/10.3390/w13131830
5. Secondly, the FEM model for two different cross-sections of the dam containing horizontal and vertical inclinometers has been built to get the numerical simulations for all inclinometers

at the exact positions of measured data. A comparative study is performed to account for the heterogeneity of the materials by decomposing the computational domain into subdomains. A data-driven approach using deep neural networks and non-deterministic optimization algorithms has been proposed to identify the soil parameters leading to the results that best approximate the measured. The originality of this work is in the evaluation process in the following journal,

KSCE Journal of Civil Engineering, https://www.springer.com/journal/12205

6. In continuity, a comparative study of constitutive soil models, the Mohr-Coulomb (MC) and Hardening Soil (HS) model, is conducted and the soil parameters are identified through a hybrid optimization technique by reducing the error of multi-objective function. This work has been submitted for evaluation in the journal,

   Structures https://www.sciencedirect.com/journal/structures

0.4 Thesis organization

This thesis is formatted into three articles. The first chapter is dedicated to the literature review and an article already published is presented in the second chapter. There are two submitted articles presented in the third and fourth chapters. Chapter 1 illustrates the comprehensive literature review of the following subjects,

- Romaine-2 dam
- Finite element modelling (FEM)
- Constitutive soil models: Mohr-Coulomb (MC) and Hardening Soil (HS) model
- Surrogate modelling: Polynomial chaos expansion (PCE) and Deep neural network (DNN)
- Uncertainty analysis
- Sensitivity analysis
- The inverse analysis
- Optimization techniques and their implementation

Chapter 2 explicitly compares deep neural network and Polynomial chaos expansion-based surrogate models for the sensitivity and uncertainty propagation for the Romaine-2 dam. In moving on to Chapter 3, a data-driven approach with deep neural network and optimization techniques has been proposed to identify the optimal parameters of the Mohr-coulomb constitutive soil model for different subdomains in the dam. The measured data were recorded on four different inclinometers installed in two different cross-sections of the dam. Chapter 4 is exclusively dedicated to the comparative analysis of constitutive soil models for inverse analysis. The hybrid optimization technique is applied to minimize the multi-objective function; the accuracy and efficiency of constitutive soil models are compared. It is found that the HS model analysis results are the closest to the values measured onsite. Chapter 5 presents a discussion of the results and recommendations for future works.

CHAPTER 1

LITERATURE REVIEW AND FUNDAMENTAL CONCEPTS

1.1 Introduction

The literature review discussed in this chapter highlights the challenges associated with modelling the structure and analyzing the behaviour by identifying soil parameters, with a significant emphasis on the Romaine-2 dam. The methods used to identify the soil parameters, and to analyze their uncertainty and sensitivity, are explicitly described and reviewed in this chapter.

1.2 Rockfill and asphalt core dams

Canada is unquestionably a top 10 global dam builder, with over 10,000 dams. Of these, 933 are classified as "large" dams, boasting a reservoir of over 3 million m^3. Quebec province is responsible for a third of these large dams, comprising 6,000 dams and dikes. It is worth noting that Hydro Quebec manages 10% of these dams. Fig.1.1 indicates that 72% of Hydro Quebec dams are embankment dams (earth and rockfill dams). Rockfill dams are common due to their versatility and cost-effectiveness and are increasingly utilized for various purposes, such as irrigation, power generation, and flood control. These dams are typically constructed on multiple sites and foundations using compacted rockfill. An impermeable core or layer is installed on the dam's upstream face to prevent seepage through the porous core. The impervious components are typically reinforced concrete, asphaltic concrete, or clay. Moreover, the construction process of the dam can be streamlined through mechanization, significantly reducing labour costs.

The ICOLD Bulletin 84 (Stateler & Sundaram, 2013) provides an extensive account of earth dams constructed between 1948 and 1991, utilizing various bituminous core types, such as hand-placed and machine-placed. In 1962 Germany achieved a significant milestone by building the first earth dam with a machine-compacted asphalt core (Höeg, Valstad & AM Ruud, 2007). Since then, over 100 asphalt core dams have been erected worldwide, including in China, Brazil, Iran, and Canada, as documented by Hydropower and Dam's journal (Konard *et al.*,

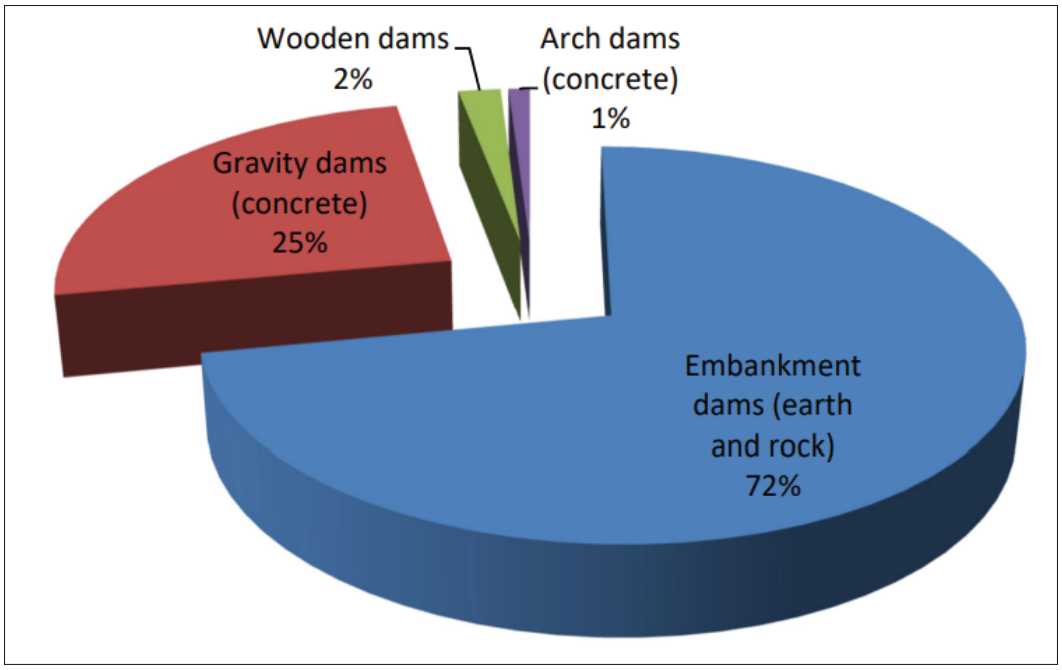

Figure 1.1 This data displays the proportion of dams controlled by Hydro Quebec categorized by their type

2014a). The reports indicate that asphalt-concrete core dams operate satisfactorily thanks to their impermeability, flexibility, resistance to erosion, and self-healing properties (Saxegaard, 2003). The asphalt-concrete core can respond to induced deformation as a whole or due to foundation settlement, primarily due to its viscoelastic plastic features (Creegan & Monismith, 1996; Gopi, 2010). Furthermore, the asphalt-concrete core is strong enough to withstand earthquake excitations without cracking or material degradation (Hoeg, 2005).

1.2.1 Romaine-2 dam

The Romaine-2 dam, situated on the Romaine River in Quebec's North shore region, was constructed in 2014. It is one of North America's tallest dams and is considered the most significant hydroelectric development globally, utilizing the asphalt core rockfill design (Jean, 2011). The decision to use asphalt core rockfill dam structures was based on their economic viability over earth core dams, considering the distance required to reach appropriate till borrow areas in the Romaine-2 region.

Designing the retaining structures for Romaine-2 was challenging. For the past half-century, Hydro-Quebec has relied on glacial till as its waterproofing material for embankment dams. However, the company was determined to develop new dam designs, particularly for locations where natural waterproofing materials are either unavailable or of inferior quality (Jean, 2011). Multiple specialized studies were thoroughly reviewed to ensure an economically sound and state-of-the-art design for the rockfill dam while maintaining strict standards. Additionally, the design elements of the Norwegian structures were thoroughly analyzed and compared to ensure confidence in constructing the Romaine-2. The specialized studies program conducted four interrelated activities to guide design and engineering decisions, as illustrated in Fig.1.2. A

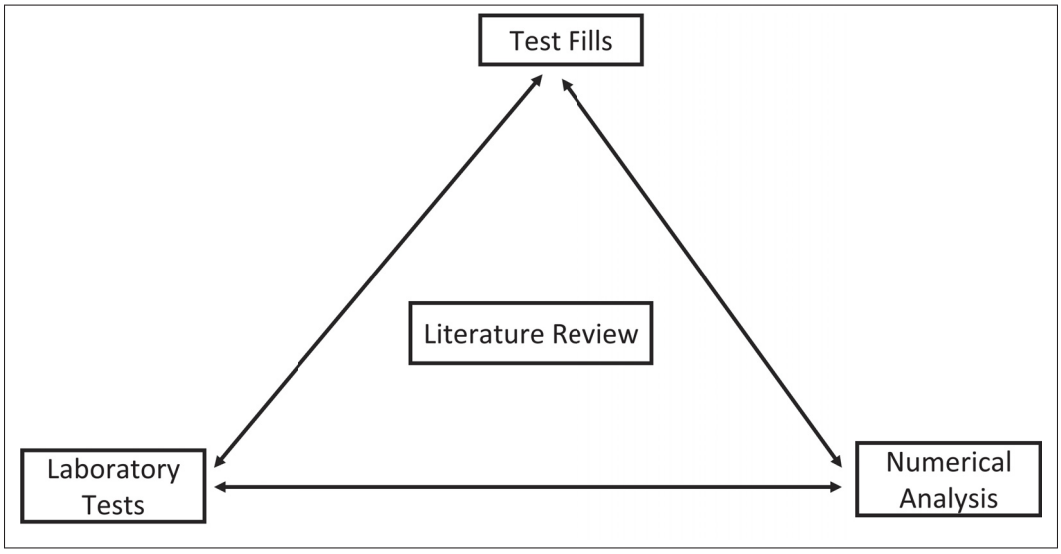

Figure 1.2 Four specialized interrelated activities

comprehensive literature review was conducted to identify the crucial design and construction elements of asphalt core rockfill dams. The study included global experiences from countries such as China, Germany, Norway, and Austria. In addition, data and insights from the Nemiscau-1 project, a small asphalt core rockfill dam in North America, were used to incorporate international standards into construction practices in Quebec (Longtin *et al.*, 2012). Furthermore, the primary goals of conducting laboratory tests on the asphaltic core and rockfill material were to identify their origin and formulate a preliminary mix for bituminous concrete used in construction. The objective was to determine the mechanical properties of the dam fills and core, which will

serve as inputs for numerical modelling. In order to assess the influence of rockfill properties on placement and compaction methods, as well as to compare Norwegian dam construction practices to those of Hydro Quebec, the test fill objectives were established. Additionally, the mechanical properties of the rockfill were determined to define input parameters for numerical modelling. The primary goal of the numerical analysis was to evaluate and understand the magnitude and mechanism of movements within the structure (Konard *et al.*, 2014a,b). This research program identified the optimal rockfill placements and compaction requirements to guarantee the dam's and its core's high performance.

Six dikes, with a height of up to 80 meters, were constructed as part of the project. A hydrological study conducted at a supply level of 243.8 meters found that the reservoir area spans approximately 81 km^2. The dam, measuring 514 meters long and with a maximum height of 110 meters, is a zoned rockfill dam with an asphalt-concrete core. A comprehensive analysis of the plan for the dam and dikes of the Romaine-2 project is presented in Fig.1.3. The dam's fill volume is approximately 4,475,500 m^3, and the spillway has a capacity of 2976 m^3/s during flood conditions (Vannobel, Smith, Lefebvre, Karray & Éthier, 2013).

The cross-section of the Romaine-2 dam is illustrated in Fig.1.4. The asphalt core boasts a variable width, measuring 85 cm at the base and 50 cm at the top. It is flanked on both sides by a support zone M of crushed stone with a maximum particle size of 80 mm. The transition zone N comprises crushed stone with a maximum particle size of 200 mm. The O internal shell zone can accommodate rock particles of up to 600 mm, while the P external shell zone can accommodate particles of up to 1200 mm (Smith, 2015). Ensuring the safety of a dam requires a highly emphasized monitoring program. The Romaine-2 dam, designed by Hydro Quebec, is the world's largest asphalt core rockfill dam. The innovative requirements for rockfill placement and compaction, along with a thin impervious barrier, make the instrumentation provided for the dam significant.

The monitoring program comprises various instruments such as vertical inclinometers (INV-01 and INV0-2) on both sides of the core, vertical and horizontal inclinometers (INV-03, INV-04,

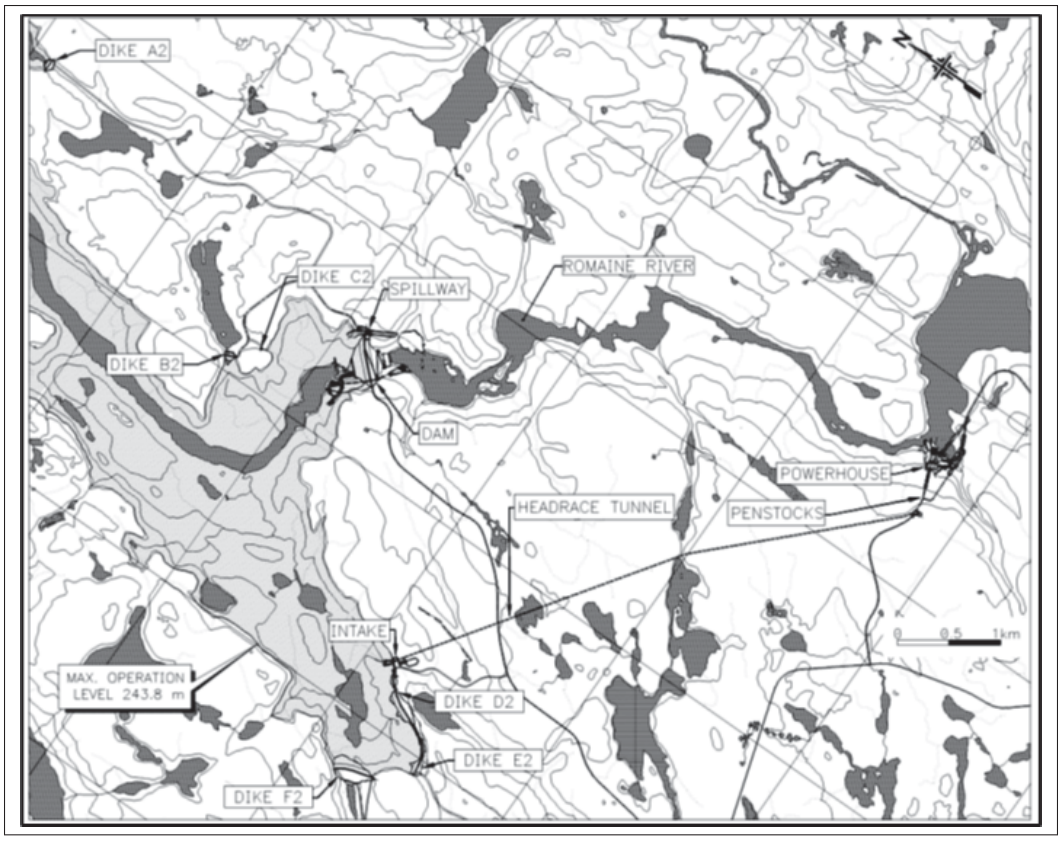

Figure 1.3 An overview of the layout for the dam and dikes of the Romaine-2 development taken from Longtin *et al.*(2012, p. 2)

INH-01, and INH-02) in the downstream shells (Vannobel *et al.*, 2013). To visualize the vertical and horizontal inclinometer positions, refer to Fig.1.4. This installation offered comprehensive information that helps to understand the dam's ongoing performance (Stateler & Sundaram, 2013). With the use of advanced instrumentation, it became possible to conduct numerical back analysis and gain a deeper understanding of the factors influencing the behaviour of the structure (Adamo, Al-Ansari, Sissakian, Laue & Knutsson, 2021). This aims to expand knowledge about modelling and create digital tools to help engineers better comprehend, interpret, and model the typical behaviour of retaining structures. This will aid in accurately diagnosing issues, estimating damage progression, and designing effective corrective measures or recommendations.

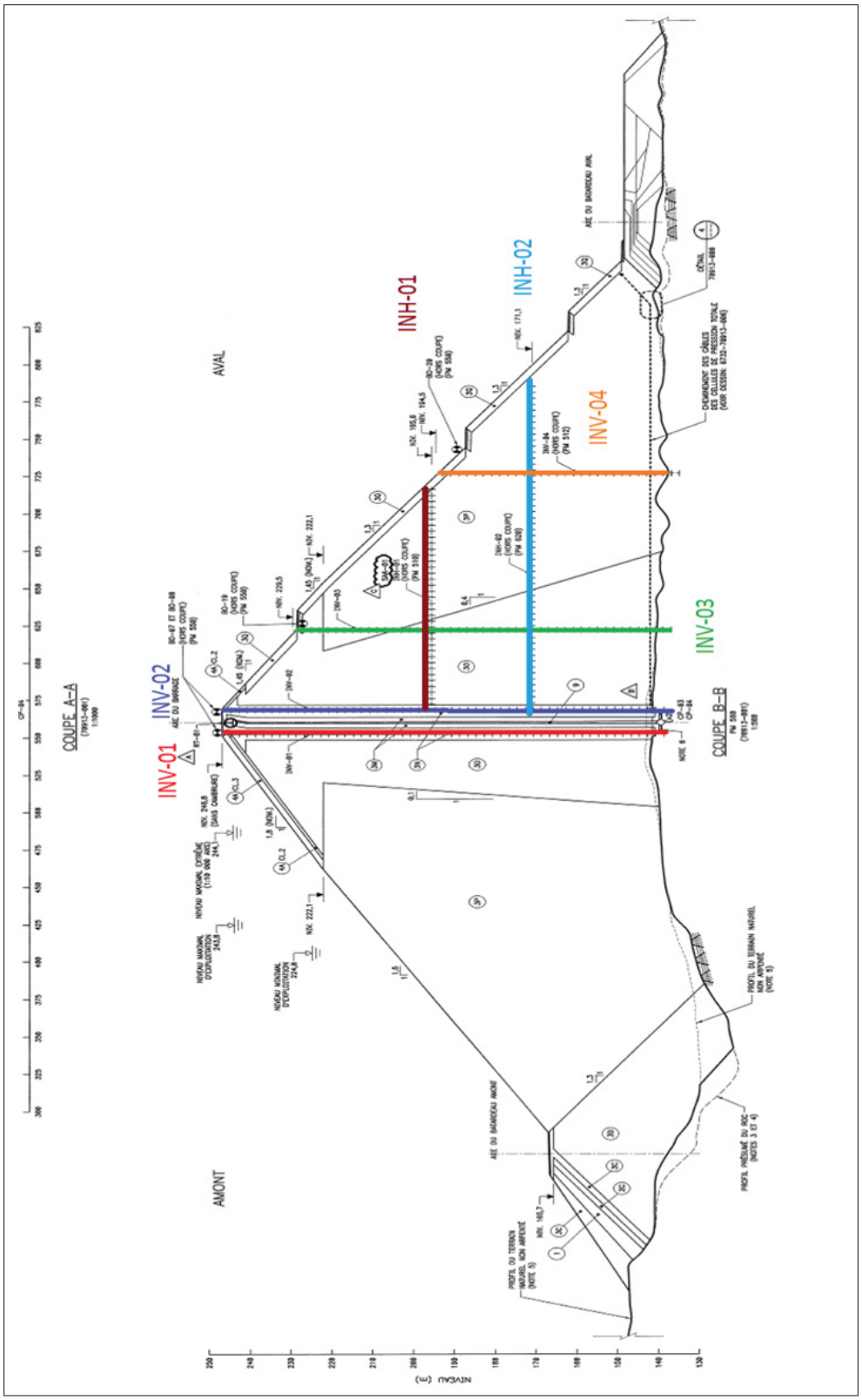

Figure 1.4 Cross section of Romaine-2 dam (cad drawing)

1.3 Finite element modelling (FEM)

Geotechnical engineering has significantly benefited from the advancements in numerical modelling techniques, particularly finite elements. These methods have been proven to be a more cost-effective approach to scientific research than experimental techniques. Despite the advancements in numerical modelling techniques, accurately describing the behaviour of dams during construction and impoundment stages continues to be challenging. Even though there are several constitutive soil models available, each comes with its own set of limitations in hypothesis. It must be emphasized that constitutive soil model parameters and their determination through tests may not accurately reflect real-life field conditions.

When it comes to granular materials or rockfills, choosing the right constitutive model is crucial as it greatly impacts the effectiveness of numerical modelling. The process of selecting such a model requires intricate and elaborate arrangements. Various modelling techniques are utilized in geotechnical studies of rockfill dams to mimic the behaviour of the rockfill; finite element methods are most common (Varadarajan, Sharma & AK Gupta, 2003; Xing, Gong & Hai-Feng Fu, 2006; Costa & Alonso, 2009; Pramthawee, Jongpradist & Kongkitkul, 2011; Akbari Hamed, 2017). However, the outcomes of FEM modelling methods depend on various factors considered during calculations, including physical input parameters, initial conditions, and boundary conditions. In some cases, these processes are subject to uncertainties that must be considered to achieve the most precise results. Barcelona's basic model was used to simulate the mechanical behaviour of the core, shoulder, and filter materials of the Lechago dam (built in Spain) and achieved agreement between the laboratory results and the numerical simulations (Costa & Alonso, 2009). A constitutive model that accounts for the elastoplasticity of rockfill was employed to study its properties. The rockfill parameters were defined using extensive triaxial tests, and the researchers found that the model could accurately predict rockfill behaviour (Varadarajan, Sharma, Abbas & Dhawan, 2006). The utilization of the Duncan change model is common in rockfill simulations (Duncan & Chang, 1970; Xing *et al.*, 2006). The input parameters in this model are straightforward and have clear physical significance. As a result, the Duncan and Chang model has been employed by researchers to examine the static and seismic

loading behaviours that occur when constructing rockfill dams, as well as during impoundment (Xing *et al.*, 2006; Özkuzukiran, Özkan, Özyazicioğlu & Yildiz, 2006; Dakoulas, 2012). The deformation and stability of dams were assessed by studying the traits of weak rockfill during its placement and compaction in three Chinese dam projects. Further, the results were compared with field measurements. Several numerical simulations have assessed the performance of asphalt concrete core dams (Akhtarpour & Khodaii, 2009; Hoeg, 2005; Vannobel *et al.*, 2013).

1.4 Constitutive soil models

A constitutive model is a set of equations intended to reproduce soil behaviour using stress-strain relations. However, the multi-physical nature of soils is complex, exhibiting both elastic and plastic non-linear deformations. Depending on the loading history, the soil can compact or expand, and its stiffness varies significantly with the stress state, which in turn depends on the pore pressure. After several decades of research, sophisticated constitutive laws are currently available to model the various behaviours of soils. In addition, various constitutive equations developed by (Varadarajan *et al.*, 2003; Xing *et al.*, 2006; Costa & Alonso, 2009; Pramthawee *et al.*, 2011) are frequently utilized to reproduce the behaviour of rockfill materials. The equations or constitutive models listed below are commonly employed.

1.4.1 Mohr Coulomb (MC)

It is a perfectly plastic elastic model widely used for pulverulent soils (sand) and cohesive soils in the short and long term (clay and silt). The load surface can be presented in the principal stress space by the following equation:

$$F(\sigma_{ij}) = (\sigma_1 - \sigma_3) - (\sigma_1 + \sigma_3)\sin\phi - 2\boldsymbol{C}\cos\phi = 0 \tag{1.1}$$

σ_1 and σ_3 represent the major and minor principal stresses; the compression is positive. The plastic potential function is defined by Eq.(1.2). The shape of the loading surface in the deviatory plane is a hexagon Fig.1.5. The flow law is associated when the friction angle ϕ and the dilatancy

angle ψ are equal. Otherwise, the flow law is non-associated.

$$G(\sigma_{ij}) = (\sigma_1 - \sigma_3) - (\sigma_1 + \sigma_3)\sin\psi \tag{1.2}$$

In the linear-elastic perfectly plastic Mohr coulomb model, there are a total of five parameters

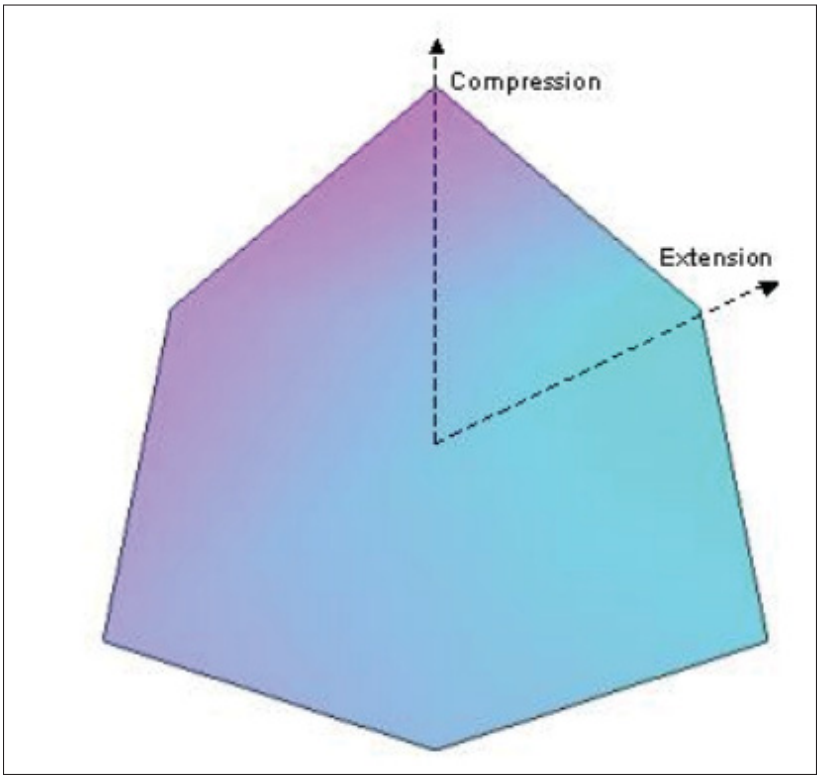

Figure 1.5 Mohr-Coulomb criterion in the deviation plane

which are very familiar in geotechnical. These parameters are determined from general laboratory tests (triaxial or oedometer).

In general, three tests are carried out at different confining pressures to determine all the parameters. Corresponding to stress states at failure, the cohesion and friction angle can also be calculated in the Mohr plane. Fig.1.6 represents a simulation of a triaxial compression test by the Mohr-Coulomb law. Similar to Duncan & Chang (1970), the Mohr coulomb model also neglects the intermediate principal stress. The linear region is determined by Hooke's law of

Table 1.1 Basic parameters of Mohr Coulomb model

Parameters	Symbols	Units
young's modulus	E	KNm^{-2}
Poisson coefficient	ν	$--$
Cohesion	C	KNm^{-2}
Friction angle	ϕ	$degree$
Dilatancy angle	ψ	$degree$

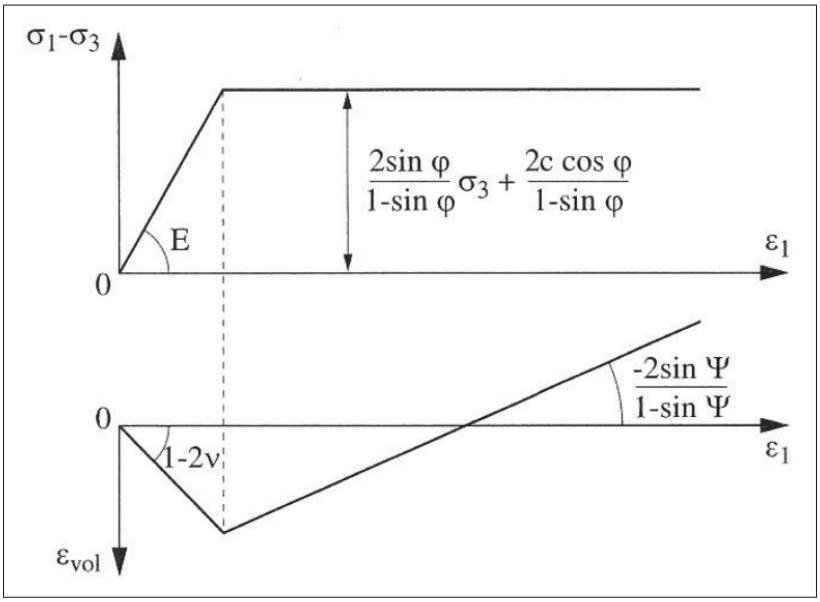

Figure 1.6 Modelling of a triaxial compression test by the Mohr-Coulomb law, taken from Hicher & Shao(2002, p. 118)

isotropic elasticity, whereas the plastic region is associated with the MC failure criterion (Ti, Huat, Noorzaei, Jaafar & Sew, 2009). The stiffness modulus is not constant for real soil and depends on the stress. When conducting triaxial testing on soil samples, the stress-strain curve's initial slope (E_0) and the secant modulus at 50% strength (E_{50}) are typically recorded. E_0 is suitable for materials with an extended linear elastic range, while E_{50} is preferred for soil loading (Brinkgreve *et al.*, 2016). However, when dealing with unloading concerns, such as tunnelling or excavations, it is necessary to use the unload-reload modulus (E_{ur}) instead of E_{50}, shown in

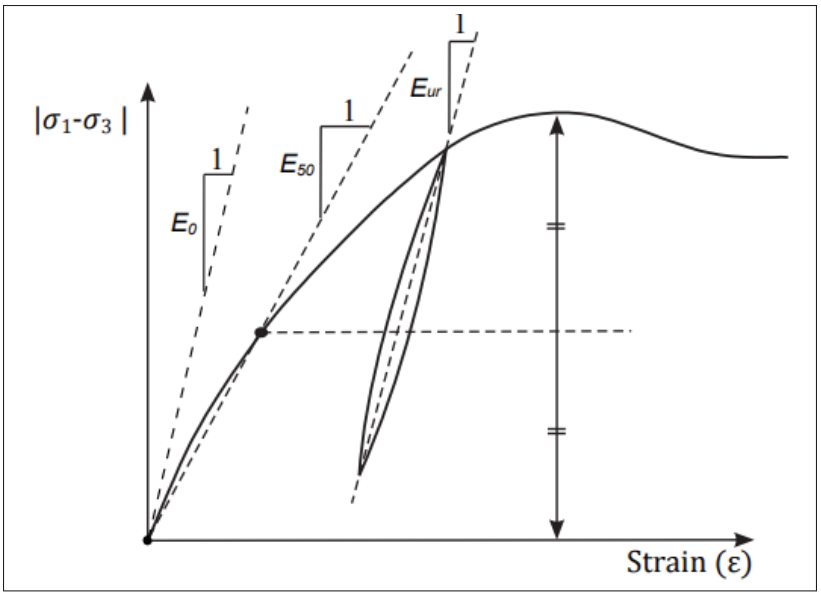

Figure 1.7 The initial stiffness, secant modulus and unload-reload modulus, taken from Brinkgreve *et al.* (2016, p. 37)

Fig.1.7. For the MC model, in many cases, it is suggested to consider a Poisson's ratio between 0.3 and 0.4 (Brinkgreve *et al.*, 2016); hence a Poisson's ratio of 0.35 is generally assumed.

1.4.2 Hardening Soil model (HS)

The HS model was initially designed by Schanz & Vermeer (1996), with further development by Schanz, Vermeer & Bonnier (1999), using Vermeer's Double Hardening model as the foundation. Additionally, the HS integrates concepts from Kondner (1963); Duncan & Chang (1970); Janbu (1963).

Unlike the elastic perfectly-plastic model, the hardening plasticity model's yield surface is not fixed in principal stress space. It can expand due to plastic deformation. Shear and compression hardening are the two primary hardening forms in this model. Shear hardening results from permanent strains caused by primary deviatoric loading, while compression hardening results from permanent plastic strains caused by direct compression in the oedometer and isotropic loading. The Hardening Soil model confidently relies on the hyperbolic correlation between

the deviatoric stress q and the vertical strain ϵ_1 in primary triaxial loading. This correlation is consistently observed in drained triaxial tests, and the resulting curves can be accurately represented by:

$$\epsilon_1 = \frac{1}{E_i} \frac{q}{1 - \frac{q}{q_a}} \tag{1.3}$$

for $q < q_f$, where q_a and E_i are the shear strength and initial stiffness. The initial stiffness E_i is related to the confining stress-dependent stiffness modulus E_{50} by,

$$E_i = \frac{2E_{50}}{2 - R_f} \tag{1.4}$$

$$E_{50} = E_{50}^{ref} \left(\frac{c \cos(\phi) - \sigma_3^{'} \sin(\phi)}{c \cos(\phi) + p_{ref} \sin(\phi)} \right)^m \tag{1.5}$$

The secant stiffness in a standard drained triaxial test is represented by E_{50}^{ref} and is associated with the reference confining pressure. The default value for p_{ref} in PLAXIS (Plaxis, 2017) is 100 stress units. However, the actual stiffness is affected by the minor principal stress, $\sigma_3^{'}$, which is the confining pressure in a triaxial test. It's important to note that $\sigma_3^{'}$ is negative when subjected to compression. The extent of stress dependency is determined by the power m. To simulate logarithmic compression behaviour, like the one observed in soft clays, m should be set at 1.0. Norwegian sands and silts have m values around 0.5, according to (Janbu, 1963), while (Von Soos, 1990) reports various values ranging from 0.5 to 1.0. The definitions of q_f, the ultimate deviatoric stress, and the quantity q_a specified in Eq.(1.5) are as follows:

$$q_f = (c \cot \phi - \sigma_3^{'}) \frac{2 \sin(\phi)}{1 - \sin(\phi)} \tag{1.6}$$

$$q_a = \frac{q_f}{R_f} \tag{1.7}$$

R_f represents the failure ratio, while C, $\sigma_3^{'}$ and ϕ refer to the cohesion, minor principal stress and friction angle, respectively. When it comes to unloading and reloading stress paths, a different

stiffness modulus is utilized, as

$$E_{ur} = E_{ur}^{ref}\left(\frac{c\cos(\phi) - \sigma_3^{'}\sin(\phi)}{c\cos(\phi) + p_{ref}\sin(\phi)}\right)^{m} \tag{1.8}$$

The reference Young's modulus, corresponding to the unloading and reloading reference pressure, is denoted by E_{ur}^{ref}. Also, the oedometer stiffness is presented as,

$$E_{oed} = E_{oed}^{ref}\left(\frac{c\cos(\phi) - \sigma_3^{'}\sin(\phi)}{c\cos(\phi) + p_{ref}\sin(\phi)}\right)^{m} \tag{1.9}$$

The value of E_{oed}^{ref} represents the tangent stiffness modulus at vertical stress of $\sigma_1 = p^{ref}$ as illustrated in Fig.1.8.

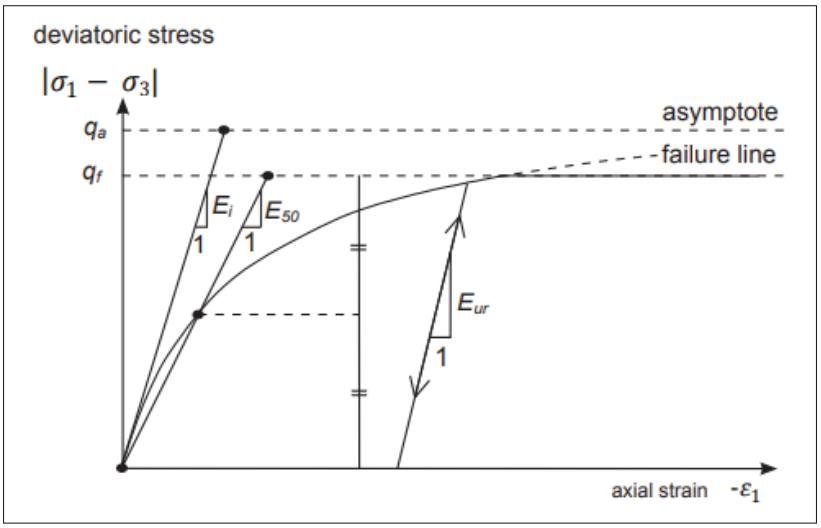

Figure 1.8 The hyperbolic stress-strain relationship is observed during the primary loading of a drained triaxial test, taken from Brinkgreve *et al.* (2016, p. 69)

A yield function that involves shear hardening is expressed as:

$$\tilde{f} = \bar{\tilde{f}} - \gamma^{p} \tag{1.10}$$

The function $\bar{f}$ depends on stress, while γ^p is based on plastic strain. These relationships are expressed in Eq.(1.11) and (1.12), respectively.

$$\bar{f} = \frac{1}{E_{50}} \frac{q}{1 - \frac{q}{q_a}} - \frac{2q}{E_{ur}} \tag{1.11}$$

$$\gamma^p = \mathcal{E}_1^p - \mathcal{E}_2^p - \mathcal{E}_3^p \tag{1.12}$$

$$\mathcal{E}_v^p = \mathcal{E}_1^p + \mathcal{E}_2^p + \mathcal{E}_3^p \tag{1.13}$$

$$\gamma^p = (2\mathcal{E}_1^p - \mathcal{E}_v^p) \approx 2\mathcal{E}_1^p \tag{1.14}$$

where $\mathcal{E}_1^p$ refers to the axial plastic strain. According to studies by (Brinkgreve *et al.*, 2016; Obrzud, 2010), the plastic volume change $\mathcal{E}_v^p$ is relatively negligible. Hence, we can assume that γ^p is approximately equal to $2\mathcal{E}_1^p$ in the abovementioned equation. To estimate the axial elastic strain,

$$\mathcal{E}_1^e = \frac{q}{E_{ur}} \tag{1.15}$$

let's suppose the yield condition $f = 0$, then $\bar{f} = \gamma^p$,

$$\mathcal{E}_1^p = \frac{1}{2}\bar{f} = \frac{1}{2}\left(\frac{1}{E_{50}} \frac{q}{1 - \frac{q}{q_a}} - \frac{2q}{E_{ur}}\right) \tag{1.16}$$

When equations (1.15) and (1.16) are combined, equation (1.17) is derived, which is used in the triaxial test, where the axial strain is the sum of both the elastic and plastic components, as expressed:

$$\mathcal{E}_1 = \mathcal{E}_1^e + \mathcal{E}_1^p = \frac{q}{E_{ur}} + \frac{1}{2}\left(\frac{1}{E_{50}} \frac{q}{1 - \frac{q}{q_a}} - \frac{2q}{E_{ur}}\right) = \frac{1}{2E_{50}} \frac{q}{1 - \frac{q}{q_a}} \tag{1.17}$$

Eq.(1.14) provides the measure of plastic shear strain, and the explanation for volumetric plastic strain is presented in detail. The plastic flow rule is firmly established based on the plastic potential defined in Eq.(1.18) by (Obrzud, 2010). Eq.(1.19) makes calculating the rate of plastic

volumetric strain for triaxial tests possible, demonstrating a linear correlation.

$$g_1 = \frac{\sigma_1 - \sigma_3}{2} + \frac{\sigma_1 + \sigma_3}{2} \sin \Psi_m \tag{1.18}$$

$$\mathcal{E}_1{}^{\cdot p} = \sin \Psi_m \gamma^{\cdot p} \tag{1.19}$$

$$\sin \Psi_m = \frac{\sin \varphi_m - \sin \varphi_{cv}}{1 - \sin \varphi_m \sin \varphi_{cv}} \tag{1.20}$$

The mobilized friction angle is denoted by φ_m.

$$\sin \varphi_m = \frac{\sigma_1^{'} - \sigma_3^{'}}{\sigma_1^{'} + \sigma_3^{'} - 2 \cot \varphi} \tag{1.21}$$

The parameter known as the critical state friction angle, with its symbol φ_{cv}, is defined as,

$$\sin \varphi_{cv} = \frac{\sin \varphi - \sin \Psi}{1 - \sin \varphi \sin \Psi} \tag{1.22}$$

The present hardening model shares specific parameters with the non-hardening Mohr-Coulomb (MC) model, such as the failure parameters C, ϕ, and ψ. The soil parameters of the HS model are listed in the following table, In the HS model, the dilatancy cut-off is taken into consideration.

Table 1.2 Basic parameters of Hardening soil model

Parameters	**Symbols**	**Units**
Cohesion	C	KNm^{-2}
Angle of internal friction	ϕ	$degree$
Dilatancy angle	ψ	$degree$
Tension cut-off and tensile strength	σ_t	KNm^{-2}
Secant stiffness in standard drained triaxial test	E_{50}^{ref}	KNm^{-2}
Tangent stiffness for primary oedometer loading	E_{oed}^{ref}	KNm^{-2}
unloading/reloading stiffness $E_{ur}^{ref} = 3E_{50}^{ref}$	E_{ur}^{ref}	KNm^{-2}
Power for stress-level dependency of stiffness	m	[-]
Failure ratio $\frac{q_f}{q_a}$	R_f	[-]

When materials undergo extensive shearing and reach a critical density, they stop dilating, as depicted in Fig.1.9. The initial void ratio e_{init} and maximum void ratio e_{max} values are assigned

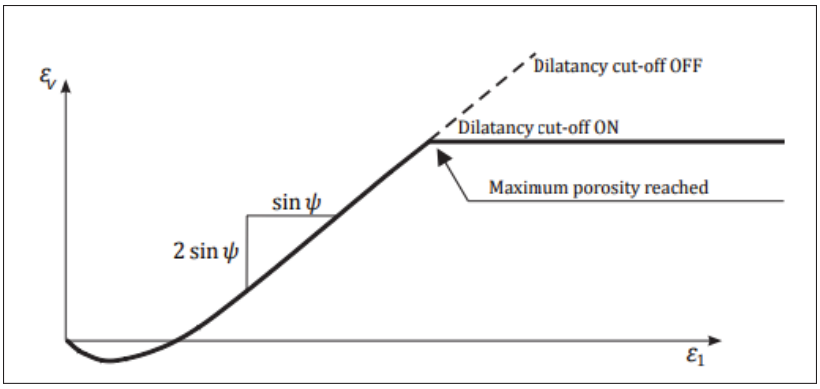

Figure 1.9 The strain curve is obtained from a typical drained triaxial test that incorporates a dilatancy cut-off, taken from Brinkgreve *et al.* (2016, p. 78)

to determine this behaviour. When the maximum void ratio is reached, the mobilized dilatancy angle Ψ_{mob} is set to zero (Brinkgreve *et al.*, 2016).

For $e < e_{max}$

$$\sin \Psi_{mob} = \frac{\sin \varphi_{mob} - \sin \varphi_{cv}}{1 - \sin \varphi_{mob} \sin \varphi_{cv}} \tag{1.23}$$

For $e > e_{max}$, $\Psi_{mob} = 0$.

In addition, The correlation between void ratio and volumetric strain is demonstrated as

$$-(\mathcal{E}_v - \mathcal{E}_v^{init}) = \ln \left(\frac{1+e}{1+e_{init}}\right) \tag{1.24}$$

Fig.1.11 presents a shear yield surface that overlooks the plastic volume strain during isotropic compression. (Brinkgreve *et al.*, 2016) introduce a second yield surface that closes the elastic region in the $p - axis$ direction to overcome this limitation. This cap yield surface allows for a model with independent parameters, namely E_{50}^{ref} and E_{oed}^{ref}. The triaxial modulus E_{50}^{ref} regulates the shear yield surface, while the oedometer modulus E_{oed}^{ref} controls the cap yield surface.

The yield cap is defined as,

$$\mathfrak{f}^{c} = \frac{q^{\sim 2}}{M^2} + p^2 - p_p^2 \tag{1.25}$$

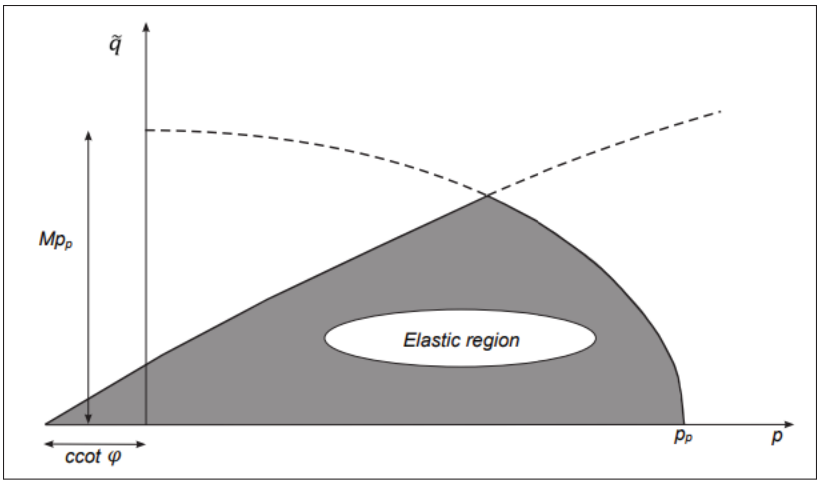

Figure 1.10 The yield surface in the $p-q$-plane. Additionally, the elastic region can be further minimized by implementing a tension cut-off, taken from Brinkgreve *et al.* (2016, p. 80)

The equation above defines various parameters, including M, which is linked to K_0^{nc}, the coefficient of lateral earth pressure during consolidation. p_p represents the pre-consolidation stress, while the remaining parameters are also defined as,

$$p = -\frac{(\sigma_1 + \sigma_2 + \sigma_3)}{3} \tag{1.26}$$

$$q^{\sim} = \sigma_1 + (\delta - 1)\sigma_3 - (\delta)\sigma_3 \tag{1.27}$$

$$\delta = \frac{3 + \sin\varphi}{3 - \sin\varphi} \tag{1.28}$$

Fig.1.10 presents the entire yield lines, while Fig.1.11 displays the yield surfaces in the principal stress space. The MC model distinctly demonstrates hexagonal shapes for the shear locus and yield cap, as illustrated in Fig.1.11.

Schanz *et al.* (1999) have highlighted the advantages of utilizing the HS constitutive model. The HS model's yield surface can expand due to plastic straining, unlike an elastic-perfectly plastic model with a stable yield surface in the principal stress space. Furthermore, the HS model

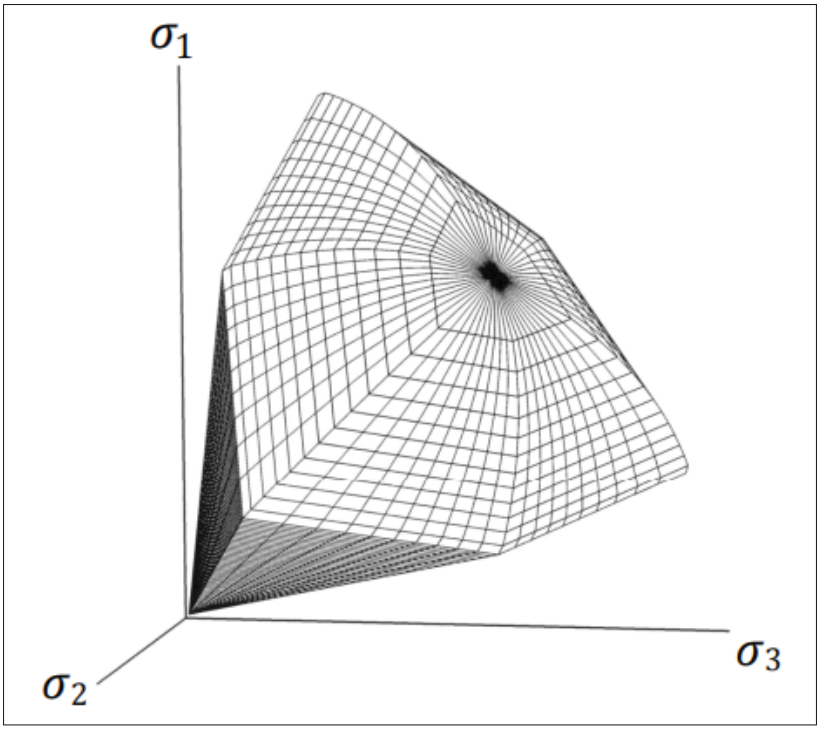

Figure 1.11 A depiction of the complete yield contour of the HS model in the principal stress space for soil without cohesion, taken from Brinkgreve *et al.*(2016, p. 81)

includes both shear and compression hardening to simulate irreversible strain caused by primary deviatoric loading and plastic strain caused by direct compression in oedometer loading.

Nevertheless, the HS constitutive model has some limitations, as listed by Obrzud (2010). Firstly, the model is unable to reproduce softening impacts. Secondly, the model fails to replicate the hysteretic soil behaviour during cyclic loading. Despite the soil's limited elastic strain range, the model assumes elastic material behaviour during unloading and reloading.

1.5 Surrogate modelling

Surrogate models are highly effective analytical models that can accurately imitate the input-output behaviour of complex systems. By conducting computationally intensive simulations at carefully chosen sample points, these models offer a simplified representation of a complex

system with less precision in a specific domain while still providing accurate approximations of the complex simulations' behaviour. As a result, surrogate models are a powerful tool for reducing computational demands and creating a more streamlined approach to analyzing complex systems (Davis, Cremaschi & Eden, 2017). The surrogate-based methods are widely used in geotechnical applications due to their efficiency and cost savings (Huang, Radi & El Hami, 2016; Guo & Dias, 2020; Sargsyan, 2017; Stephens, Gorissen, Crombecq & Dhaene, 2011; Forrester, Sobester & Keane, 2008).

1.5.1 Polynomial chaos expansion (PCE)

The polynomial chaos (PC) technique offers an alternative to sampling-based approaches for analyzing uncertainties. PC methods fall under stochastic expansion methods, which rely on Wiener homogeneous chaos theory (Wiener, 1938) to study the propagation of uncertainties. By expanding the model response into a series of chaos polynomials as a function of random input variables, this method provides an approximation of the reaction in the form:

$$\bar{Y} = \sum_{k=1}^{N_P} \beta_k \Phi_k(\zeta) \tag{1.29}$$

The multivariate bases, $\Phi_k(\zeta)$, are created using the univariate bases, $\phi_j(\zeta_j)$, which are chosen based on the probability density function of the input random variable ζ_j because the convergence of these bases strongly depends on it (Xiu & Karniadakis, 2002). The coefficients of a polynomial chaos approximation undergo evaluation through intrusive techniques in their initial stages, detailed in 2.2.1.1. These techniques rely on the Galerkin projection, which modifies the governing equations, leading to the need for solving a system of coupled equations. The unknowns in this system are the coefficients, β_j (Dinescu, Smirnov, Hirsch & Lacor, 2010; Ghanem, 1999). While this method has good convergence, its intrusive nature can present a challenge in specific configurations where extensive developments are necessary (Zokagoa, 2011). To overcome this drawback, non-intrusive methods have been developed that treat the deterministic model as a black box. The fundamental concept of these methods is to estimate

the coefficients based on a reduced number of solutions derived from the deterministic model. This set of solutions comprises evaluations of the model's response from a specific range of values for the random input variables (Loeven, Witteveen & Bijl, 2007).

Non-intrusive methods can be categorized into two main types: projection and regression. The projection methods utilize the orthogonality property of polynomial basis functions to determine the coefficients for approximating the model's response (Ghiocel & Ghanem, 2002). However, this technique can be pretty demanding regarding computational effort, especially when the number of uncertain input parameters increases significantly (Blatman & Sudret, 2010b). However, the collocation method simplifies the process by using regression to determine the coefficients that best approximate the output response. This is achieved through a limited number of evaluations of the deterministic model, resulting in a system of algebraic equations. The matrix in this system contains the values of the polynomial bases evaluated at the collocation points, while the vector holds the responses of the model (Berveiller, Sudret & Lemaire, 2006). When using regression-based non-intrusive methods, the selection of collocation points is a critical step that strongly affects the efficiency and convergence of the method. The literature proposes various techniques to choose these points optimally, which may inspire new collocation methods. For instance, the probabilistic collocation method considers collocation points as roots of orthogonal polynomial bases (Loeven *et al.*, 2007). In contrast, the collocation point method combines different sampling techniques with an oversampling coefficient to distribute the points across the parametric domain (Hosder, Walters & Balch, 2007; Abdedou & Soulaimani, 2019).

The efficiency of stochastic approximations based on polynomial expansions of chaos depends on several criteria, such as the polynomial order and the number of random variables, which determine the size of the expansion. The construction of multivariate polynomial bases involves introducing the notion of the multi-index and using the tensor product between the univariate terms of the orthogonal base (Miller, Berg, Davison, Sudicky & Forsyth, 2018; Sudret, 2014). Chaos polynomial methods offer an attractive feature of estimating the statistical moments of the output response from previously calculated coefficients without additional computational effort (Salehi, Raisee, Cervantes & Nourbakhsh, 2018). These coefficients also enable direct

calculation of the Sobol sensitivity indices, identifying the random variables contributing the most to the output response's variability (Homma & Saltelli, 1996a). Compared to classical sampling methods, these approaches substantially reduce computational effort, as they do not require additional computations for sensitivity analysis (Shahzadi & Soulaïmani, 2021; Rahman, 2011). The application of PCE in dam engineering has gained widespread popularity in recent years. The PCE model for surrogate modelling of embankment dams was introduced by (Ghanem, Saad & Doostan, 2007), later used to perform a reliability analysis on sliding stability (Guo, Dias, Carvajal, Peyras & Breul, 2018). (Hariri-Ardebili, Mahdavi, Abdollahi & Amini, 2021) comprehensively quantified the uncertainty in dam engineering problems through PCE. In addition, an adaptive PCE for sensitivity and reliability analysis of aging dams was applied while investigating copula dependency among random variables (Amini, Abdollahi, Hariri-Ardebili & Lall, 2021). (Shahzadi & Soulaïmani, 2021) constructed a surrogate model for rockfill dams by combining PCE with deep neural networks. (Sevieri, Andreini, De Falco & Matthies, 2019) developed a generalized PCE-based probabilistic procedure in a Bayesian framework, incorporating parameter identification and seismic fragility analysis for concrete gravity dams.

1.5.2 Machine Learning in modern computational geotechnics

Geotechnical materials are inherently complex, making it challenging for researchers to use theoretical solutions to solve design problems and assessment issues. Geotechnical Engineers are increasingly turning to soft computing techniques to tackle such problems (Goh & Zhang, 2014; Zhang, Goh & Zhang, 2016; Ray *et al.*, 2021). ML algorithms have significant potential to uncover correlations among information without any prior assumptions (Goh, Zhang, Zhang, Xiao & Xiang, 2018; van Natijne, Lindenbergh & Bogaard, 2020; Zhang *et al.*, 2021a). Recent advancements in computing efficiency have led to increased exploration of artificial intelligence (AI), deep learning(DL) and deep neural network (DNN) (Da'u & Salim, 2020; Nguyen, Kashani, Ngo & Bordas, 2019). AI is a science that studies ways to create intelligent programs capable of creatively solving problems. At the same time, ML is a subset of AI that enables systems to learn and improve from experience without explicit programming. DNN, a specific type

of ML, can represent the world as a hierarchy of concepts without manual feature extraction. DNN predictions' accuracy gradually increases with dataset expansion, making it an efficient tool for extracting useful information and making reliable decisions in geoengineering (Zhang *et al.*, 2022; Zhang, Xie, Zhang, Qiu & Wu, 2021b). However, geotechnical engineering is still experiencing a significant lack of DNN applications. This is primarily due to the highly dynamic and unpredictable nature of rocks and soil, which presents numerous challenges for researchers. ML techniques such as Linear Regression analysis (LR), Support Vector Machine (SVM), Artificial Neural Networks (ANN) and Random Forest (RF) acquire knowledge from experiences, eliminating the need for hypothesizing about primary rules governing the problem (Bishop, 2006). These techniques have demonstrated remarkable effectiveness in handling nonlinear and plastic issues related to rock and soil. Many studies have explored the application of ML in geotechnics, including predicting soil shear strength, developing statistical correlations relating to geotechnical soil parameters of a specific region, pile capacity, foundation settlement, slope stability, tunnels and predicting the ultimate bearing capacity of cohesionless soils, (Yousefpour & Fallah, 2018; Adarsh, Dhanya, Krishna, Merlin & Tina, 2012; Puri, Prasad & Jain, 2018; Shahzadi & Soulaïmani, 2021). Several ML techniques are compared to analyze the uncertainty in the soil parameters of the dam (Hariri-Ardebili, Chen & Mahdavi, 2022).

1.5.2.1 Deep neural network (DNN)

Deep learning has become immensely popular in both supervised and unsupervised problem-solving. This is due to its ability to eliminate the need for extensive feature engineering or domain expertise in processing raw data. The method employs representation learning techniques that involve multiple levels of representation. Input data is transformed into a higher-level, more abstract representation layer by layer, using simple yet non-linear modules (Goodfellow, Bengio & Courville, 2016). Deep neural networks have proven to be highly effective in solving problems in various domains, including science, business, and government (Alzubaidi *et al.*, 2021; Samek, Montavon, Lapuschkin, Anders & Müller, 2021). They are often used as a tool to solve classification and regression issues. A standard neural network comprises interconnected

processors called neurons, which produce a sequence of real-value activations. The calculation from the previous layer to the next layer in a deep neural network can typically be represented as follows:

$$Y = \sum(input * weights) + bias \tag{1.30}$$

where, Y is an output vector. Every node has a non-linear activation function that can approximate highly complex functions. This function decides the node's output based on input data. The goal is to transform the input signal into an output signal for the node, which will then act as input for the following layer. A simple one-layer DNN is shown in the Fig.1.12.

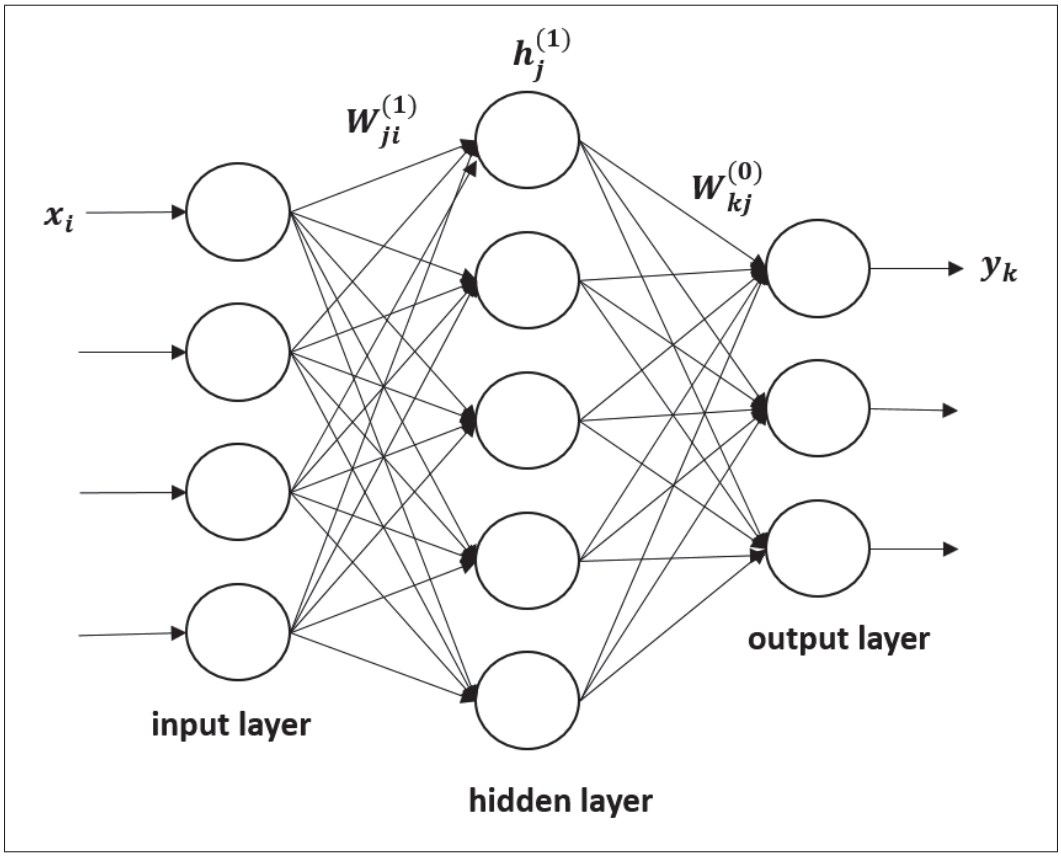

Figure 1.12 One-layer neural network

The three most commonly used activation functions are sigmoid, tanh, and ReLU. The sigmoid activation function is in the form, $f(x) = \frac{1}{1+e^{-x}}$, hyperbolic tangent function (tanh) are defined $f(x) = \frac{1-e^{-2x}}{1+e^{-2x}}$ and Rectifier linear units (ReLu) is presented as $f(x) = max(0, x)$. Sigmoid and

tanh restrict the input to (0,1) and (-1,1), respectively. ReLU activates only the input values with negative values, making the network sparse and increasing computational efficiency.

Recent research in geotechnics suggests that deep neural network(DNN) presents a promising solution for addressing uncertainties in various geotechnical aspects. ANN has been widely applied in geotechnical areas such as underground openings (Sterling & Lee, 1992), braced excavation (Sou-Sen & Hsien-Chuang, 2004; Zhang *et al.*, 2021b), slope stability (Asteris *et al.*, 2022), earth retaining structures (Pham, Tran & Vu, 2021), modelling tunnel boring machine performance (Xu, Liu, Wang & Wang, 2021), and predicting geotechnical parameters (Wang, 2022).

1.6 Uncertainty analysis

Uncertainty pervades many characteristics of geotechnical engineering, particularly in the classification of material properties of rockfill and earth dam foundation systems. Uncertainty in geotechnics is presented in all aspects (Phoon *et al.*, 2022; Iyengar, Rajaram, Decker & Mavris, 2023; Cao, Jiang & Zu, 2022). In general, some of this uncertainty may be due to the difficulty in making accurate measurements. Some may be due to uncertainty in the models, equations, and understanding of the systems involved. Additional uncertainty can result from the spatial variability of the system (Hacıefendioğlu, Bayraktar & Başağa, 2010). Moreover, in some instruments, especially those designed for likewise observations (Kovári & Amstad, 1993) the errors in the measurements are not independent. For instance, if an inclinometer device measures horizontal displacements along a borehole, the displacement value is based on all the previously measured displacements. Also, some instruments are the cause of errors in the measured data. Using non-intrusive chaos polynomial methods has become widespread for analyzing uncertainty propagation and constructing stochastic surrogate models that efficiently estimate statistical moments and distribution functions with low computational cost (Hariri-Ardebili *et al.*, 2021; Abdedou & Soulaimani, 2019).

1.7 Sensitivity analysis

Engineers have shown interest in using sensitivity analysis to comprehend the complex behaviour related to soil parameters. Sensitivity analysis is a powerful method for identifying crucial input parameters significantly impacting model outcomes. The main purpose of employing Sobol indices in sensitivity analysis is to determine the parameters that significantly impact the output response variability (Homma & Saltelli, 1996b). Sensitivity analysis methods are categorized into two main types, local and global sensitivity analysis (Saltelli *et al.*, 2008). Local sensitivity analysis measures the impact of an input parameter on a model in a specific area. In contrast, global sensitivity analysis looks at the uncertainty in the output caused by uncertainty in the input (Cacuci, Ionescu-Bujor & Navon, 2005). Global sensitivity analysis treats each input as an independent variable by varying all inputs simultaneously. This technique involves five essential steps: defining the computational model, identifying relevant inputs and their limits, generating input samples using a sampling design method, evaluating the generated input parameters, and analyzing uncertainty while calculating the importance of each input through a sensitivity estimator. Various techniques, such as Monte Carlo sampling, have been developed to obtain Sobol indices. Variance-based global sensitivity analysis determines the parameters that affect dam stability the most (Dimov & Georgieva, 2010; Segura, Miquel, Paultre & Padgett, 2021). However, these sensitivity analysis techniques often require a large number of simulations (Branbo, Hassan *et al.*, 2020). Surrogate-based methods are the most commonly used due to their efficiency and cost-effectiveness. Polynomial chaos expansion with Sobol's indices is the most cost-effective method for conducting parameter sensitivity analysis of the dam model (YiFei, MaoSen, Tran-Ngoc, Khatir & Wahab, 2023). A global sensitivity analysis was conducted to determine the effect of soil parameters on rockfill dam behaviour by calculating the Sobol indices (Das & Soulaïmani, 2019; Shahzadi & Soulaïmani, 2021).

1.8 Inverse analysis

Inverse analysis in the geotechnical community started in the early 80s. (Gioda & Maier, 1980; Gioda & Sakurai, 1987) took the initiative to use inverse analysis to identify the rock mass

parameters for a tunnel excavation application. The inverse analysis become popular in the geotechnical community for identifying soil parameters for several applications of dams, tunnel excavation, consolidation, and test embankment on soft clay deposits (Santos Rodríguez, 2015; Das & Soulaimani, 2021; Hariri-Ardebili *et al.*, 2022; Amini *et al.*, 2021). (Calvello & Finno, 2004) calibrated soil parameters for different models using the results from triaxial comparison tests performed on specimens and recalibrated using inclinometer data that recorded the displacements of excavation. Malecot and his group (Malecot, Flavigny & Boulon, 2004) used inverse analysis to calibrate the soil parameters of the Mohr-Coulomb (MC) model of synthetic sheet pile wall for horizontal displacements. The optimization techniques based on genetic algorithm and gradient were used and the results were compared. Later, Levasseur (Levasseur, Malécot, Boulon & Flavigny, 2008) and Rechea (Rechea, Levasseur & Finno, 2008) used genetic algorithms to optimize inverse analysis. Moreover, Levasseur utilized a genetic algorithm post-process and introduced the concept of using a principal component analysis to better deal with problems that are not unique and associated with the nature of geomechanics (Levasseur, Malecot, Boulon & Flavigny, 2009, 2010). An inverse analysis was presented to identify the soil parameters of the hardening soil model of a real supported excavation performed in five stages (Finno & Calvello, 2005). A comparative study of optimization algorithms (genetic algorithm and self learning simulation) was presented to identify the soil parameters in a deep excavation (Hashash, Levasseur, Osouli, Finno & Malecot, 2010a). He suggests that the genetic algorithm assists in the best selection of soil parameters for the constitutive model, as compared to this self-learning simulation, allowing us to discover new soil behaviour. In order to improve the accuracy, a hybrid Genetic algorithm as an application of simple synthetic tunnel excavation was established for back analysis (Santos Rodríguez, 2015). The inverse analysis combines the PCE with an optimization technique for the concrete dam (YiFei *et al.*, 2023). The research review shows that most of the back analysis effort has been focused on optimization techniques and their applications to challenging real problems in the last decade. Indeed, the attempt to create more robust and computationally efficient inverse analysis procedures is still vigorously pursued. Like all inverse problems, parameters identification problems are often ill-posed, which shows

that at least one of the given properties in Hadamard's definition (Engl, Hanke & Neubauer, 1996) is violated for all admissible data,

1. The solution exists
2. The solution is unique.
3. The solution depends continuously on data.

The abovementioned properties are discussed in detail (Xiang, Swoboda & Cen, 2003).

1.8.1 Existence

In order to achieve a solution, it is imperative that the numerical model accurately describes the physical problem and the measurements are sufficient. If a suitable numerical model cannot be determined, the immediate issue remains unsolved and the identification of parameters cannot be addressed. Mathematically, if a set is bounded convex and the function is continuous, at least one solution must exist.

1.8.2 Uniqueness

In order to ensure a unique solution, it is necessary to have sufficient information in the measurement data. While this is not always a requirement, the contraction mapping theorem (Chicone *et al.*, 1999) provides mathematical proof of the guarantee of uniqueness.

1.8.3 Stability

The discussion of the third property is directly related to evaluating the continuity of the fitness function (objective function). Sometimes, the continuity of the objective function may be disrupted. In such cases, regulations can be implemented to restore its smoothness and compensate for any loss of continuity. This is probably the reason that parameter identification problems are usually unstable (Engl *et al.*, 1996).

1.9 Optimization techniques and their implementation

Optimization techniques have become gradually popular and essential in different engineering applications considering the advancement in computing systems (Eykhoff, 1974). Back analysis problems can be reduced to minimize or maximize a function, the difference between measured and calculated data. There are several optimization techniques available to search for the best solution to a given problem. However, selecting a robust algorithm that provides the optimal solution can be a complex process. These optimization techniques are categorized based on gradients. Genetic algorithm, Swarm particle optimization, Ant algorithm and Simulated annealing are some of the non-gradient optimization techniques preferred for non-smooth functions (Eykhoff, 1974; Fletcher, 1981; Goldberg, 1989a). Different optimization techniques are utilized in inverse analysis to identify the soil parameters of dams (Vahdati, Levasseur, Mattsson & Knutsson, 2013; Vahdati, 2014; Dou, Li & Kang, 2017).

1.9.1 Genetic Algorithm

The search method of Genetic algorithms (GA) employs principles of natural evolution, such as genetics and selection. Evolution is closely linked to Charles Darwin (Darwin, 1857), who introduced the idea of natural selection to improve an organism's fitness through slight, heritable deviations. Later Gregor Mendel identified the basis of genetic inheritance, which formalized Darwin's theories (Mendel, 1865). Although, the concept of creating an artificial algorithm that can imitate nature's evolutionary process was first introduced by Holland (Holland, 1975). However, his students at the University of Michigan (Goldberg, 1989b) explained this vision. As a result of their research, the following characteristics were uncovered.

- Chromosomes play a crucial role in the process of evolution.
- Evolution only occurs during the moment of reproduction.
- Selection is the definitive process of choosing individuals for reproduction.
- Individuals with high fitness are the sole candidates to be selected for reproduction.
- The process of crossover, which combines the chromosomes of the selected parents, produces new offspring.

- Mutation is the only way to introduce new genetic material into the population.
- The genes contained within chromosomes hold all the necessary information for producing the best individuals possible, and nothing else can

The primary advantage of utilizing genetic algorithms is their ability to handle complex and diverse problems. However, this robustness often comes at the cost of increased computational expenses compared to traditional optimization methods. Genetic algorithms possess several unique characteristics, such as

- working with coded parameter sets rather than individual parameters
- searching from a population of points rather than a single point
- utilizing objective function information instead of derivatives or auxiliary knowledge
- implementing probabilistic transition rules instead of deterministic ones

It is better to use with success in all scientific fields. It is recognized to be highly efficient in dealing with large, discrete, nonlinear and poorly understood optimization problems (Pal, Wije Wathugala & Kundu, 1996). Although, the method does not guarantee the optimum solution to a problem. Nevertheless, genetic mechanisms, such as reproductions, crossings and mutations, permit localizing an optimum set of solutions close to the optimum in a given search space (Gallagher, Sambridge & Drijkoningen, 1991).

1.9.2 Particle Swarm Optimization

Swarm intelligence is the term used to describe the synchronized behaviour of decentralized systems made up of multiple individuals who work together through self-organization (Cui & Gao, 2012). Particle swarm optimization (PSO) has undoubtedly demonstrated its effectiveness in a wide range of fields, such as structural design (Perez & Behdinan, 2007), hydrogeology (Martínez, Gonzalo, Álvarez, Kuzma & Pérez, 2010), environmental sciences (Najafzadeh & Tafarojnoruz, 2016; Ferdowsi, Mousavi, Mohamad Hoseini, Faramarzpour & Gandomi, 2022) and geotechnical engineering (Hajihassani, Jahed Armaghani & Kalatehjari, 2018; Yin, Jin, Shen & Hicher, 2018), among others. It has also been instrumental in the epidemic modelling of Sars-Cov-2 (Godio,

Pace & Vergnano, 2020; Al-Qaness, Ewees, Fan & Abd El Aziz, 2020), reservoir engineering (Shams, Ahmed & Sayyouh, 2020), computer vision (Nakane *et al.*, 2020) and artificial neural networks (Abdolrasol *et al.*, 2021) etc. Particle swarm optimization (PSO) was suggested by (Gao, 2006), while Cheng, Li, Sun & Au (2012) used a hybrid approach for handling pile driving back analysis. An ANN for displacement back analysis of earth-rockfill dams was utilized by (Yu, Zhang & Yuan, 2007). Hashash preferred optimization-based inverse analysis for excavation response (Hashash, Levasseur, Osouli, Finno & Malecot, 2010b). An inverse analysis for parameter identification performed in the simulation of excavation support systems using optimization algorithms (Rechea, Levasseur & Finno, 2007). Lastly, (Moreira *et al.*, 2013) used an evolution strategy for back analysis of geomechanical parameters in underground work.

1.10 Objective function formulation for optimization techniques

Optimization techniques' most critical and challenging task is defining an objective function according to the problem requirements. There are numerous ways to define an objective function. (Eykhoff, 1974) presented the most extended methods. The objective function can be defined as minimizing the difference between the measurements and the numerical values. This dissertation presents some methods, such as

- The least square method
- The Markov method
- Maximum likelihood method
- Maximum likelihood method with basic information
- Relative error objective function
- Objective function with instrumentation error
- Objective function to smooth the oscillations in measured data

The least square method is one of the most straightforward but comprehensive methods to define an objective function. In the identification of parameters, the best parameters are those that

minimize the objective function, which is defined as

$$f_{obj} = \sum_{i=1}^{N} (Y_i - \bar{\mathbf{Y}}_i) \tag{1.31}$$

Where N is the number of measurements, Y_i show the measurement data and $\bar{\mathbf{Y}}_i$ are the calculated values. In matrix notation,

$$f_{obj} = [Y - \bar{\mathbf{Y}}]^T [Y - \bar{\mathbf{Y}}] \tag{1.32}$$

Markov is regarded as a generalization of the least-squares method where the weighted diagonal matrix $\mathbf{W}$ reflects the measurement quality.

$$f_{obj} = [Y - \bar{\mathbf{Y}}]^T \mathbf{W} [Y - \bar{\mathbf{Y}}] \tag{1.33}$$

The measurement process's associated error is indicated by $\mathbf{W}$, with higher weights given to more reliable measurements. The definition of $\mathbf{W}$ is generally associated with the standard deviation of the apparatus utilized to obtain the measurements. However, it can be adjusted as needed to incorporate other factors that may affect the accuracy of the measurement extraction process, such as the technician's expertise or specific environmental conditions.

The maximum likelihood method assigns the differences between measurements and the model to the observational procedure, treating it as a random variable with a determined probability density function. This statistical approach provides a more comprehensive criterion than those based on least-squares and Markov methods, making the objective function defined by the maximum likelihood method more reliable. However, a deeper understanding of the issue is necessary to define it adequately. The solution to the problem maximizes the probability of obtaining the actual observed data or the likelihood estimation (Edwards, 1974; Tarantola, 2005).

Let $\mathbf{X}$ be the set of parameters and $\mathbf{Y}$ be the set of measurements; to determine the likelihood of a hypothesis, one must consider the conditional probability of $\mathbf{Y}$ given a set of parameters $\mathbf{X}$.

This leads to the criterion being expressed as:

$$\mathbb{L} \propto f(\mathbf{Y}|\mathbf{X}) \tag{1.34}$$

$$\mathbb{L} = Kf(\mathbf{Y}|\mathbf{X}) \tag{1.35}$$

K is the constant of proportionality.

According to (Carrera, 1988), this formulation possesses theoretical and conceptual advantages:

- It is unnecessary to establish the probability of a hypothesis, as it has become a disputed notion within probability theory.
- The model doesn't necessarily have to replicate the accurate system precisely (Baram & Sandell, 1978).

Assuming that the error of the measurements follows the Gaussian distribution, the likelihood function can be rewritten as,

$$f(\mathbf{Y}|\mathbf{X}) = \frac{1}{\sqrt{(2\pi)^N|\sigma|}} \exp\left(\frac{-1}{2}(Y-\bar{\mathbf{Y}})^T(\sigma)^{-1}(Y-\bar{\mathbf{Y}})\right) \tag{1.36}$$

where N is the number of measurements, σ is the covariance matrix, representing the error structure associated with measurements (Bishop, 2006). The solution to the problem is the one that maximizes the probability of obtaining the field measurements observed. In other words, the best parameter estimation is found by maximizing the likelihood L in Eq.1.36. The log-likelihood can be expressed as,

$$S = -2\ln\mathbb{L} = (Y-\bar{\mathbf{Y}})^T(\sigma)^{-1}(Y-\bar{\mathbf{Y}}) + \ln|\sigma| + N\ln(2\pi) - 2\ln K \tag{1.37}$$

On the assumption that the covariance matrix is fixed and the last three terms of Eq.(1.37) are constant. The objective function using the maximum likelihood method can be finally defined as:

$$f_{obj} = [Y-\bar{\mathbf{Y}}]^T(\sigma)^{-1}[Y-\bar{\mathbf{Y}}] \tag{1.38}$$

The "weighted" matrix has a clear statistical meaning in Eq.(1.38) represented by the inverted measurements covariance matrix. In the case where measurements are independent among them, $(\sigma)^{-1}$ is a diagonal matrix, and the objective function obtained by the maximum likelihood method (Eq.(1.38)) is equivalent to the one acquired by the Markov method (Eq.(1.33)). In addition, if the values on the diagonal $(\sigma)^{-1}$ are the same, the objective function achieved through the maximum likelihood method (Equation (1.38)) is equal to that obtained from the least-squares method (Equation (1.32)).

To expand the horizon of the objective function, it is possible to integrate prior information into the problem (such as the a priori parameter values X). The updated objective function must include a term that considers the error in estimating the prior parameter. Consequently, Eq.(1.35) can be altered to Eq.(1.39), where the likelihood is proportional to the joint probability of the measurements and the initial parameter values.

$$\mathbb{L} = Kf(\mathbf{Y}|\mathbf{X}, \mathbf{X}^0) = Kf(\mathbf{Y}|\mathbf{X})f(\mathbf{X}^0) \tag{1.39}$$

The probability functions $f(\mathbf{Y}|\mathbf{X})$ and $f(\mathbf{X}^0)$ are considered Gaussians or normal. Therefore,

$$f(\mathbf{Y}|\mathbf{X}) = \mathbb{L} = \frac{1}{\sqrt{(2\pi)^N|\sigma|}} \exp\left(\frac{-1}{2}(Y - \bar{\mathbf{Y}})^T(\sigma)^{-1}(Y - \bar{\mathbf{Y}})\right) \tag{1.40}$$

and

$$f(\mathbf{X}^0) = \frac{1}{\sqrt{(2\pi)^n|\sigma_0|}} \exp\left(\frac{-1}{2}(\mathbf{X}^0 - \mathbf{X})^T(\sigma_0)^{-1}(\mathbf{X}^0 - \mathbf{X})\right) \tag{1.41}$$

where, N represents the number of measurements, n the number of parameters, σ_0 represents the covariance matrix of priori parameters, and $(\mathbf{X}^0 - \mathbf{X})$ represents a vector of differences between prior and estimated parameters.

Working with supporting function S in Eq.(1.37) is more beneficial than working with function L (1.39). To define the new supporting function, Eq.(1.40) and Eq.(1.41) can be utilized as

follows:

$$S = (Y-\bar{\mathbf{Y}})^T(\sigma)^{-1}(Y-\bar{\mathbf{Y}})+(\mathbf{X}^0-\mathbf{X})^T(\sigma_0)^{-1}(\mathbf{X}^0-\mathbf{X})+\ln\sigma+\ln\sigma_0+N\ln(2\pi)+n\ln(2\pi)-2\ln K \tag{1.42}$$

Assume that the covariance matrices σ and σ_0 are constant along with fixed last three terms in Eq.(1.42), the objective function utilizing the maximum likelihood method with prior knowledge can be defined as follows:

$$f_{obj} = [Y - \bar{\mathbf{Y}}]^T\sigma^{-1}[Y - \bar{\mathbf{Y}}] + [\mathbf{X}^0 - \mathbf{X}]^T\sigma_0^{-1}[\mathbf{X}^0 - \mathbf{X}] + \ln|\sigma| + \ln|\sigma_0| \tag{1.43}$$

The aforementioned objective functions are usually applied to cases where the exact measurements are used (i.e. displacements). However, in cases where different kinds of measurements or significant differences in the magnitude of the measurements are involved, an objective function defined by the concept of relative error is considered appropriate. Using the structure of the maximum likelihood method (Eq.(1.38)) and defining the components of as in (Eq.(1.44)), an objective function in Eq.(1.45) is appropriately defined for cases where different kinds of measurements or significant differences among the magnitude of the measurements are involved.

$$R = \frac{(Y_i - \bar{\mathbf{Y}}_i)^2}{(Y_i)^2} \tag{1.44}$$

$$f_{obj} = [R]^T(\sigma_{cv})^{-1}[R] \tag{1.45}$$

The matrix (σ_{cv}) contains the squared coefficient of variation of the measurements. It represents the error structure related to the measurements, and its analysis is crucial for accurate results.

The mean square error method is a straightforward definition of an objective function.

$$f_{obj} = \frac{1}{N}\sum_{i=1}^{N}(Y_i - \bar{Y}_i)^2 \tag{1.46}$$

In this equation, N represents the total number of measurement points, Y_i stands for the measured data, and $\bar{Y}_i$ represents the numerical prediction. To generalize this equation weights C_i are added.

$$f_{obj} = \frac{1}{N}\sum_{i=1}^{N} C_i (Y_i - \bar{Y}_i)^2 \tag{1.47}$$

For accurate measurements, giving more importance to reliable data is crucial. Inevitable uncertainties can affect the performance of inclinometers, causing significant fluctuations in the measured displacement plots. These fluctuations can complicate the optimization process, making it challenging to arrive at a reliable solution. To tackle this issue, the weights C_i are formulated as:

$$C_i = \tanh(\frac{1}{\delta_i}) \tag{1.48}$$

$$\delta_i = \beta(\frac{Y_i - \bar{Y}_m}{\gamma_m + \varepsilon})^2 \tag{1.49}$$

$\bar{Y}_m$ represents the mean displacement along the inclinometers, γ_m indicates standard deviation of measured data, β represents an empirical parameter ($\beta = 3$ is a typical value), and ε reflects an avoidance factor. It is likely that C_i will tend to zero when δ_i indicates a large amount of uncertainty regarding the measured data. For small δ_i, however, C_i is close to 1. It is possible to combine multi-error functions into a single composite function by using the weighted sum method (Murata & Ishibuchi, 1995). According to (Gunantara, 2018), the higher the weight, the higher the priority of the function.

1.11 Conclusion

This chapter presents a literature review on the different lines of research that is the subject of this thesis. An exhaustive presentation of the various works that have dealt with soil models, methods for analyzing non-intrusive techniques for surrogate models and inverse analysis. Some other notions relating to fundamental concepts of the different approaches have been presented, particularly the methods of polynomials of chaos, deep neural network, formulation of objective functions and the optimization technique will be the subject of a detailed presentation in the following chapters.

CHAPTER 2

DEEP NEURAL NETWORK- AND POLYNOMIAL CHAOS EXPANSION-BASED SURROGATE MODELS FOR SENSITIVITY AND UNCERTAINTY PROPAGATION: AN APPLICATION TO A ROCKFILL DAM

Gullnaz Shahzadi[1] , Azzeddine Soulaïmani[1]

[1] Department of Mechanical Engineering, Ecole de Technologie Supérieure, 1100 Notre-Dame W., Montreal (QC), Canada H3C 1K3

This article has been published in:
Water 2021, 13(13), 1830; https://doi.org/10.3390/w13131830

Abstract

Computational modelling plays a significant role in the design of rockfill dams. Various constitutive soil parameters are used to design such models, which often involve high uncertainties due to the complex structure of rockfill dams comprising various zones of different soil parameters. This study performs an uncertainty analysis and a global sensitivity analysis to assess the effect of constitutive soil parameters on the behaviour of rockfill dams. A Finite Element code (Plaxis) is utilized for the structure analysis. A database of the computed displacements at inclinometers installed in the dam is generated and compared to in situ measurements. Surrogate models are significant tools to approximate the relationship between input soil parameters and displacements and thereby reduce the computational costs of parametric studies. Polynomial chaos expansion and deep neural networks are used to build surrogate models to compute the Sobol indices required to identify the impact of soil parameters on dam behaviour.

keywords

Sensitivity analysis, Polynomial Chaos Expansion, Uncertainty, Deep neural networks, rockfill dams

2.1 Introduction

To meet the new challenges faced by geotechnical engineers, the use of innovative computer-based models has been growing exponentially. The complex structures and uncertainties comprised in the design of rockfill dams are a major challenge in predicting dam behavior (Bowles *et al.*, 1996; Calvello & Finno, 2004). Numerical methods, computational statistics and machine learning play a significant role in building improved, reliable rockfill dam models, helping to predict their behavior and reduce the cost of construction. The use of sensitivity analysis has attracted the interest of engineers seeking to understand the complex behavior associated with soil parameters. The main rationale for a sensitivity analysis using Sobol indices is to identify the most significant parameters in the variability of the output response (Homma & Saltelli, 1996b). Sensitivity analysis methods are usually categorized into local and global sensitivity analysis (Saltelli *et al.*, 2008). Local sensitivity analysis quantifies the local impact of an input parameter on a model, whereas global sensitivity analysis is focused on the uncertainty in the output due to the uncertainty in the input (Cacuci *et al.*, 2005). Numerous techniques have been developed for obtaining Sobol indices through variants of the Monte Carlo sampling technique (Dimov & Georgieva, 2010) and variance-based global sensitivity analysis are performed to identify the most affecting parameters to the dam stability (Segura *et al.*, 2021), although these techniques for sensitivity analysis often require a large number of simulations (Branbo *et al.*, 2020). The surrogate-based methods are the type more widely used, due to their efficiency and cost savings (Huang *et al.*, 2016; Guo & Dias, 2020; Sargsyan, 2017; Stephens *et al.*, 2011; Forrester *et al.*, 2008). Polynomial Chaos expansion based surrogate models have been used recently for the sensitivity analysis of dams (Hariri-Ardebili *et al.*, 2021).

This work evaluates surrogate-based and variance-based global sensitivity analysis in the design of a rockfill dam. Finite element method models (FEM) with appropriate soil parameters are often utilized for dam modeling and design (Duncan, 1996; Owen & Hinton, 1980; Pietruszczak, 2010). Various constitutive models exist, each involving a different set of parameters, tested and used in several geotechnical problems (Pramthawee *et al.*, 2011). In this study, A two-dimensional plane-strain finite element-based model is used in Plaxis to compute the displacements and

stresses for a vertical cross-section of the dam which employs a simple constitutive soil model, the Mohr-Coulomb (MC) (Wood, 1990). The soil parameters cohesion(C), specific weight (ρ), shear modulus (G_{ref}), Poisson coefficient (ν), and friction angle (ϕ) are the input parameters for the MC model (Labuz & Zang, 2012). Moreover, the Mohr-Coulomb constitutive model is widely used in geotechnical engineering practice due to its simple nature, and fewer parameters are required as compared to other more complex constitutive models such as the Hardening-Soil model (HS) (Schanz *et al.*, 1999). The Sobol sampling method is applied to generate the samples of soil parameters as the input (Dige & Diwekar, 2018; Burhenne, Jacob & Henze, 2011). Subsequently, the parameters are assigned to the numerical model and the displacements are calculated at the positions of each of the inclinometers. Once the database of the inputs and outputs has been produced, the dam response can be estimated with respect to the uncertainty associated with the input parameters. The Polynomial chaos expansion (PCE) and deep neural networks (DNN) techniques (Breiman, 1996; Goodfellow *et al.*, 2016; Bishop, 2006; Hsieh, 2009) are used to build the surrogate models to evaluate the Sobol indices. The surrogate models are trained by utilizing an error function measuring the difference between the computed and measured displacements on the inclinometers.

2.2 Methodology

The methodology is comprised of two main phases: surrogate model approximation and sensitivity-uncertainty analysis.

2.2.1 Surrogate models

In the current challenging and technically competitive environment, surrogate models can increase efficiency and reduce the computational costs of a problem or design process. Several surrogate-modeling techniques have been applied to uncertainty analysis, sensitivity analysis, and optimization. Polynomial chaos, a probabilistic approach, and Deep neural networks are used in this study.

2.2.1.1 Polynomial Chaos Expansion (PCE)

Consider a physical model represented by a function $y = M(x)$, where $x \in \mathfrak{R}^n$, $y \in \mathfrak{R}^m$, and n is the number of input quantities and m the number of outputs. For simplicity, the m=1 case will be considered in the following description. The uncertainties in the input variables and their propagation to the output lead to the description of x and y as random variables $X = (X_1, X_2, X_3, ..., X_n)$ and Y, respectively (Blatman & Sudret, 2010a; Xiu & Karniadakis, 2002; Hariri-Ardebili & Sudret, 2020). For a specific value of x, the corresponding response (a realization) y is actually computed by executing a deterministic numerical solver for the non-intrusive variant of PCE. The joint probability density function (PDF) of the random vector X is denoted by ρ_x. Assuming that the input random variables X_i are independent, then ρ_x a multiplication of the marginal probabilities, $\rho_x(X) = \prod_{i=1}^{n} \rho_i(X_i)$. A polynomial Chaos Expansion approximates the response Y as a linear combination of orthonormal polynomials $\varphi_\alpha(X)$:

$$\bar{Y}(X) = \sum_{\alpha=1}^{NP} b_\alpha \varphi_\alpha(X) \tag{2.1}$$

where b_α are the expansion coefficients forming the vector $b = (b_1, b_2, b_3, ..., b_{NP})^T$. In a full PCE, the number of expansion factors NP depends on the polynomial order p and the number of random input parameters n, and is given by $NP = \frac{(n+p)!}{p!\,n!}$. The multivariate basis of polynomials $\varphi_\alpha(X)$ can be constructed as a tensor product of univariate orthonormal polynomials $\varphi_{p_i^\alpha}(X)$, that is, $\varphi_\alpha(X) = \prod_{i=1}^{n} \varphi_{p_i^\alpha}(X_i)$, where p_i^α $(i = 1, ..., n)$ is a multi-index vector. The optimal choice of the univariate polynomial basis function is closely related to the probability density functions $\rho_i(X_i)$ (Xiu & Karniadakis, 2002). For instance, Legendre polynomials serve as an optimal basis function for uniform distributions. The Polynomial Chaos Expansion coefficients b_α can be computed in a non-intrusive and affordable way using a regression approach. A data set D is composed of N input vectors $X_D = (x_D^{(1)}, x_D^{(2)}, ..., x_D^{(N)})^T$ sampled from the PDF ρ_x, and their corresponding responses are put in a vector $Y_D = (y_D^{(1)}, y_D^{(2)}, ..., y_D^{(N)})^T$, with $y_D^{(i)} = M(x_D^{(i)})$. The expansion coefficients with a regularization term can be obtained by

minimizing the error $\sum_{i=1}^{N}(y_D^{(i)} - \bar{Y}(x_D^{(i)}))^2 + \lambda_P b^T b$. Defining $\mathbf{\Phi}$ as the design matrix whose components are $\varphi_j(x_D^{(i)})(i = 1, ..., N; j = 1, ..., NP)$, the expansion coefficients vector is then given as the solution of the ordinary least-squares system:

$$b = (\Phi^T \Phi + \lambda_P I)^{-1} \Phi^T Y_D \tag{2.2}$$

where λ_P is a regularization parameter and I is the identity matrix. The number of sample points is defined as $N = \gamma\, NP$, with $\gamma \geq 1$ an oversampling parameter used to control the accuracy of the PCE (Hosder *et al.*, 2007; Abdedou & Soulaimani, 2019). The sample input vectors can be generated using efficient sampling algorithms, such as the Latin hypercube sampling algorithm (LHS) or the Sobol scheme (Dige & Diwekar, 2018; Burhenne *et al.*, 2011; Bratley & Fox, 1988). Once the expansion coefficients are computed, the polynomial expansion defined in Eq.2.1 can be used to predict the approximate response for any input variable (within the learning domain). For instance, the mean and the variance of the response can be computed using the basis function orthonormality property (Abdedou & Soulaimani, 2019). Their expressions are given by:

$$\mu_D = \int \bar{Y} \rho_x dX = \int (\sum_{\alpha=1}^{NP} b_\alpha \varphi_\alpha(X)) \rho_x dX = b_1 \tag{2.3}$$

and

$$\sigma_D^2 = \int (\bar{Y} - \mu_D)^2 \rho_x dX = \sum_{\alpha=2}^{NP} b_\alpha^2 \tag{2.4}$$

Remark: The inputs variables are assumed to be independent in the above approach. However, it is possible to use the Rosenblatt transformation (Lebrun & Dutfoy, 2009) to formulate the problem as a function of auxiliary independent variables.

2.2.1.2 Deep neural networks

Deep neural networks (DNN) are widely considered to be a powerful and general numerical approach to building a nonlinear mapping between a set of inputs (features) and their corresponding outputs (labels or targets). Deep neural networks are well-known in data science, with various

applications in science and engineering. In the PCE approach, the surrogate model comprises linear combinations of fixed basis functions. Such models have useful practical applications, but they may be limited by the curse of dimensionality for large data sets. It should be mentioned that much effort has been invested in reducing the severity of the curse of dimensionality by using sparse expansions (Papaioannou, Ehre & Straub, 2019). Furthermore, in order to apply such models to large-scale problems, the basis functions must be adapted to the data. There is a large body of literature on deep networks (Goodfellow *et al.*, 2016; Bishop, 2006; Hsieh, 2009), and a brief description is given next. Deep neural networks use parametric forms for basis functions, in which parameter values are adapted during training. Moreover, with respect to these parameters, the model is nonlinear, as it uses nonlinear activation functions. Fig.2.1 illustrates a DNN with one hidden layer. The input data are mapped to the hidden layer (1) to compute

$$h_j^{(1)} = f(\sum_{i=1}^{n} W_{ji}^{(1)} x_i + a_j^{(1)}) \tag{2.5}$$

which are then fed to the output layer (o) to compute the response

$$y_k = g(\sum_{j=1} W_{kj}^{(0)} h_j^{(1)} + a_k^{(0)}) \tag{2.6}$$

where f and g are activation functions, $W_{ji}^{(1)}, W_{kj}^{(0)}$ are the weight parameters and $a_j^{(1)}, a_k^{(0)}$ are the bias parameters. The number of neurons in the input layer is the number of input features n, and m is the dimension of the neural network response vector Y_{NN}. The number of hidden layers in a deep neural network and the number of neurons in each hidden layer are hyperparameters optimized by experimentation guided by monitoring validation and test errors. The network is trained on the data set to determine the weights and bias parameters by minimizing the loss (error) function. As described earlier, a data set D is composed of N input vectors $X_D = (x_D^{(1)}, x_D^{(2)}, ..., x_D^{(N)})^T$, which are sampled from the PDF, and of the corresponding targets, which are put in a vector $Y_D = (y_D^{(1)}, y_D^{(2)}, ..., y_D^{(N)})^T$ with $y_D^{(i)} = M(x_D^{(i)})$. In regression problems, the mean square error (MSE), also called the loss function, between the model outputs

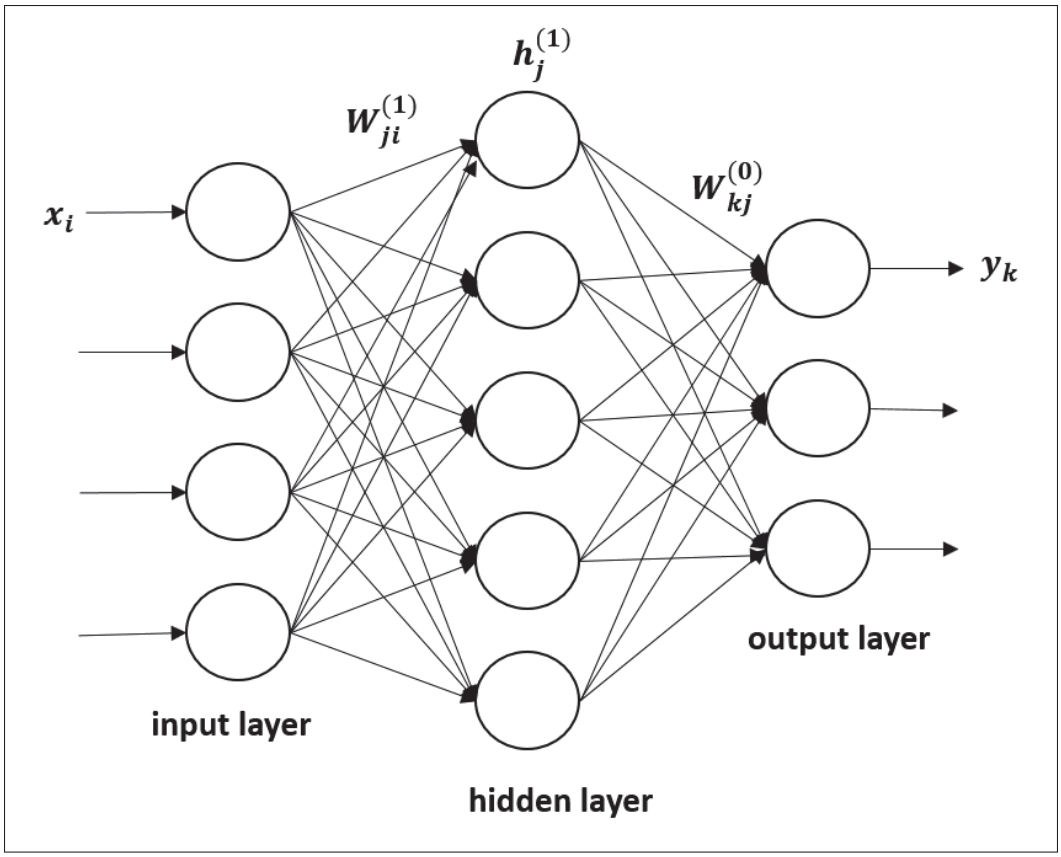

Figure 2.1 One-layer neural network

and the labels (targets) is used, along with a regularization term:

$$J = \frac{1}{N}\sum_{i=1}^{N}\left\{\frac{1}{2}\sum_{k=1}^{m}\left[y_k^{(i)} - y_{D,k}^{(i)}\right]^2\right\} + \lambda\sum_{l,\alpha,\beta}(W_{\alpha\beta}^{(l)})^2 \tag{2.7}$$

where λ is a regularization hyperparameter. An iterative approach based on the back-propagation algorithm is used to minimize the loss function. The activation function f is usually the sigmoid or the rectified linear unit, while g is the identity function for our regression problem. An example of a deep network is presented in Fig.2.2, where five hidden layers are used; the input layer has $n = 5$ input parameters, and the output layer has $m = 64$ responses ($Y_{NN} = (y_1, y_2, ..., y_{64})^T$). It can be shown that minimizing the error function E_D in Eq.2.8 is equivalent to minimizing the negative log of the likelihood function, under an assumed Gaussian distribution noise in the

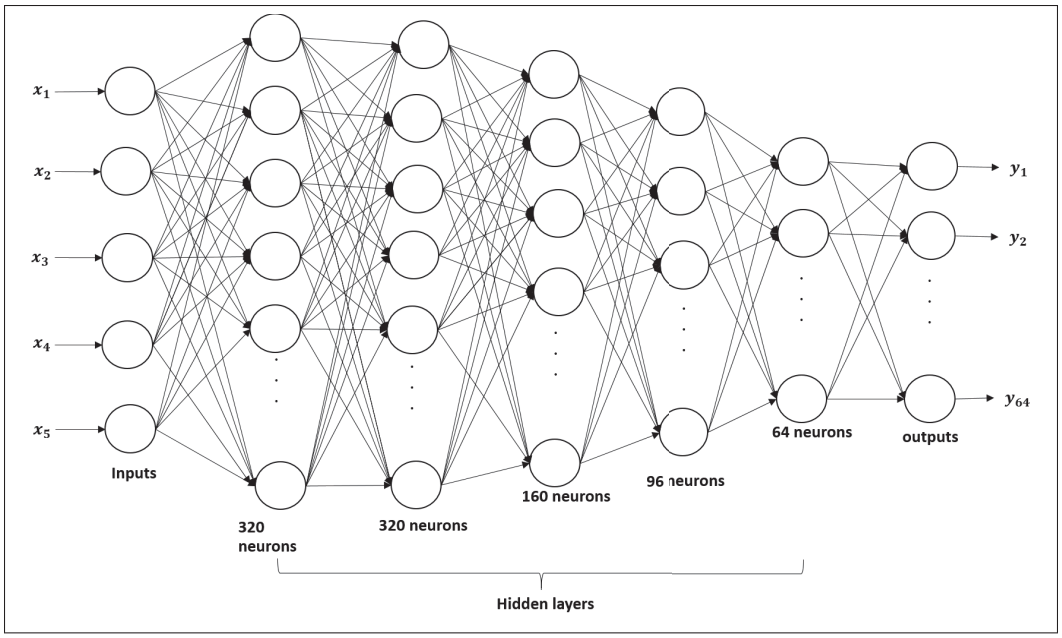

Figure 2.2 Five-layer Deep neural network

targets, with an assumed constant variance σ_D^2.

$$E_D = \frac{1}{N}\sum_{i=1}^{N}\left\{\frac{1}{2}\sum_{k=1}^{m}\left[y_k^{(i)} - y_{D,k}^{(i)}\right]^2\right\} = \frac{1}{2N}\sum_{i=1}^{N}(Y_D - Y_{NN})^2 \tag{2.8}$$

Moreover, maximizing the log-likelihood with respect to the noise variance gives the solution $\sigma_{D,ML}^2 = \frac{1}{N}\sum_{i=1}^{N}(Y_D - Y_{NN})^2$. Therefore, the prediction of the network for a given input parameter vector X is given by a Gaussian probability distribution with a mean $\bar{Y}(X) = Y_{NN}$ and a variance $\sigma_{D,ML}^2$, which represents the noise in the data. There are many public domain implementations of (standard) Deep neural networks, such as the TensorFlow library (Abadi *et al.*, 2016). In this work, the Matlab deep learning neural toolbox is used (Beale, Hagan & Demuth, 2019).

2.2.1.3 Ensemble of models

In machine learning, ensembling is a technique used to improve the predictive performance and reduce the generalization error by training several models separately, and subsequently combining their solutions (Breiman, 1996; Goodfellow *et al.*, 2016; Bishop, 2006; Hsieh, 2009).

The idea here is that the ensemble (i.e., averaged solution) will perform at least as well as any of its members. Given a data set, different neural network solutions can be obtained by varying the number of layers, the number of neurons for each layer, the training algorithm, the hyperparameters, etc. A simple and efficient approach is to use several random initializations of the weights. This option has been proven efficient enough to generate an ensemble with partially independent members (Jacquier, Abdedou, Delmas & Soulaïmani, 2021). Given a mixture of K trained neural networks, each member outputs a solution with a mean $Y_{NN}^{(k)}$ and a variance $\sigma_{D,ML}^{(k)}$, an averaged single normal mean distribution can be defined with a mean $\bar{Y}(X) = Y_{NN}^{ens}$ where:

$$Y_{NN}^{ens} = \frac{1}{K}\sum_{k=1}^{K} Y_{NN}^{(k)} \tag{2.9}$$

and a variance given by:

$$\sigma_{ens}^2 = \frac{1}{K}\sum_{k=1}^{K}\left\{(\sigma_{D,ML}^{(k)})^2 + (Y_{NN}^{(k)})^2\right\} - (Y_{NN}^{ens})^2 \tag{2.10}$$

K is typically taken between 5 and 12 (in the following numerical results, it is assumed to be equal to 10). Therefore, the numerical prediction of the network is represented by a Gaussian with the mean $\bar{Y}(X)$ and the variance σ_{ens}^2, which represents uncertainties in both the data and in the weights.

2.2.2 Global sensitivity analysis

Sensitivity analysis provides a means of determining the effects of variations of input parameters on the outputs of a model. If a small change in input parameters results in a relatively significant difference in the output, then the parameter is considered significant for the model. In a global sensitivity analysis, all the inputs are varied simultaneously over their range and are usually considered independent. The fundamental steps constituting the global sensitivity analysis technique are: i) specification of the computational model, ii) determination of relevant inputs and their bounds, iii) input sample generation by a sampling design method, iv) evaluation

utilizing the generated input parameters; and v) uncertainty analysis and calculation of the relative importance of each input through a sensitivity estimator. For more mathematical details, see (Das & Soulaïmani, 2019) and references therein. The code described in (Das & Soulaïmani, 2019) is also used for the present case study.

2.3 Case Study: Application to Romaine-2 Dam

A real rockfill dam was selected for a case study in order to illustrate the application of the surrogate modelling methodology for global sensitivity analysis and uncertainty analysis. Fig.2.3 illustrates a 2D cross-section of the Romaine-2 dam built in Quebec (Canada) (Smith, 2015; Vannobel *et al.*, 2013). The dam is 112 m high, and has an asphalt core and is grouted on a rock foundation. The asphalt core is surrounded by crushed stones having a maximum size of 80 mm, which act as supports. The transition zone (N) lies next to the support region (M), composed of crushed stones having a maximum size of 200 mm. Moreover, the particles with a maximum size of 600 mm are used in the inner shell zone (O) and in the outer region (P) composed of rocks with a maximum size of 1200 mm. Two vertical inclinometers named $INV1$ and $INV2$ are installed at two different positions (see Fig.2.3(a)) to measure the vertical displacements considered as the measured data in this study. Using the plane strain hypothesis, a finite element of the dam structure was built using the commercial code Plaxis (Plaxis, 2017). A mesh of (2187) triangular elements with 15 nodes each is presented in Fig.2.3(b), where the different soil sub-domains are meshed accordingly, and more refinement is used around the asphalt core. A mesh convergence study (Akbari Hamed, 2017) showed that the mesh is fine enough. To simplify the study, the Mohr-Coulomb (MC) constitutive law was used, given that the dam was heavily compacted during construction (Smith, 2015). Indeed, a detailed numerical study (Akbari Hamed, 2017) showed that the discrepancies between the MC results and those obtained with the more sophisticated Hardening-Soil model (Schanz *et al.*, 1999) for this rockfill dam are not significant. Several types of distributions could be utilized if more data are available to generate the sample set of soil parameters. A datasets D was built using Sobol's sampling algorithm to generate N sets of $n = 5$ physical parameters related to the

sub-domain (P). The parameters are the: cohesion(C), specific weight (ρ), shear modulus (G_{ref}), Poisson coefficient (ν), and friction angle (ϕ). For a sample (i), the input vector is then $x_D^{(i)} = (C^{(i)}, \rho^{(i)}, G_{ref}^{(i)}, \nu^{(i)}, \phi^{(i)})^T$. The parameters are supposed to follow a uniform distribution. The dilatancy angle is set relative to the friction angle as $\psi = \phi - 30$ (in degrees). Only the parameter variations in zone (P) are considered in this study, as this domain covers the maximum portion of the dam. Ideally, all sub-domain parameters could be included, but for the sake of illustration, only zone (P) is considered, as it is the most significant. The displacement fields corresponding to N sets of inputs $x_D^{(i)}$ are obtained by running Plaxis (Plaxis, 2017). The displacements on a number of points (32 in this case) on each inclinometer are extracted, yielding a response vector $Y_D^{(i)}$ of dimension $m = 64$. Table.2.1 presents the parameter interval

Table 2.1 Soil parameter values or intervals of variations for zones P, N, O, and M

Soil parameters	**Units**	**P**		**N**	**O**	**M**
		LB	**UB**			
Cohesion (C)	KNm^{-2}	10^{-3}	0	0	0	0
Specific weights (ρ)	KNm^{-3}	21.375	23.625	23.7	22.5	24.5
Shear modulus (G_ref)	KNm^{-2}	25000	35000	64000	45000	110000
Poisson coefficient (ν)	$--$	0.234	0.3465	0.33	0.22	0.33
Friction angle (ϕ)	$degree$	40.85	45.15	47	45	47

of variations of zone P and parameter values of zones N, O and M. The parameter estimates in Table.2.1 are based on a previous study conducted in (Smith, 2015; Akbari Hamed, 2017).

2.3.1 Sample size convergence study

The Sobol sampling technique (Joe & Kuo, 2008) was used to generate the samples by varying their size N ($N = 12, 48, 96, 156, 204, 252, 300, 348, 392, 444, 496, 512, 600, 720, 840, 900, 1080, 1500$ and 3000). The corresponding numerical simulations were performed using Plaxis, which required 587 CPU hours on an Intel-i7 PC, for $N = 3000$. To build confidence in the generated database, a convergence study with respect to N was performed for the standard deviation of the vertical displacement at the 64 measurement points on the inclinometers. To check the convergence for this statistical study, standard deviation plots were built for the sample size

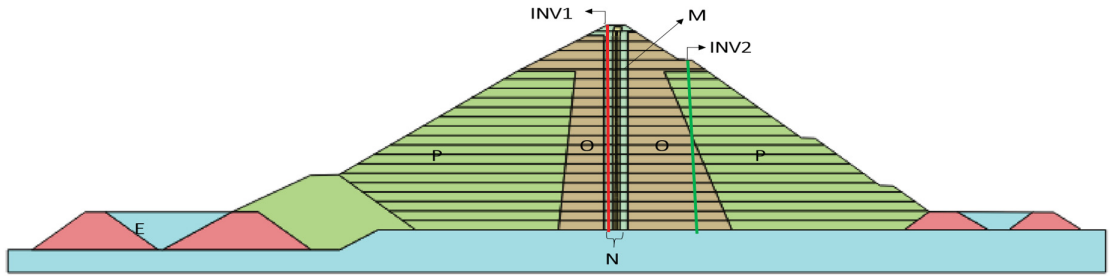

a) Cross-section of the Romaine-2 dam in Plaxis. Different zones of the dam are highlighted in alphabet. The vertical inclinometers are denoted by INV1 and INV2

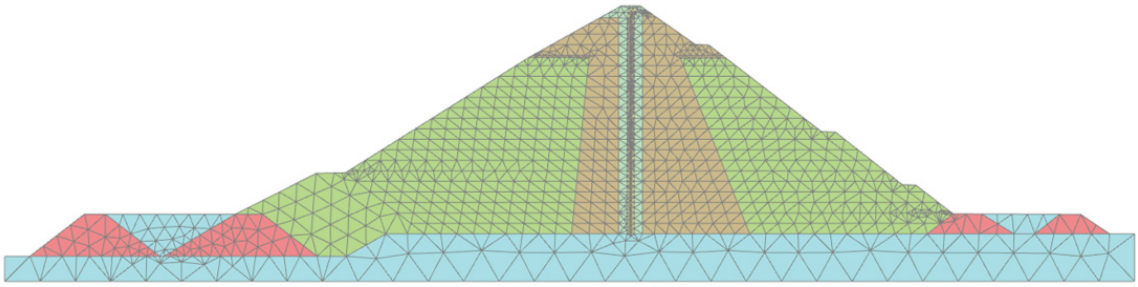

b) Mesh used for the computational domain

Figure 2.3 Romaine-2 dam

at three positions on each inclinometer: at the top, middle and bottom (see Fig.2.4). The standard deviations show some fluctuations as the sample size is increased up to 1080; however, between sample sizes 1080 and 3000, the standard deviation is close to constant (up to 1% of variation), which implies that sample size 1080 is sufficient for subsequent sensitivity studies. The confidence intervals for the displacements (mean ±2 standard deviation) obtained by using this classical statistical analysis (which is a Monte Carlo simulation (MCS)) are shown in Fig.2.5. The measured data for each inclinometer are also represented in this Fig., revealing fluctuations that can be attributed to some external effects such as the installation process, calibrations, temperature variations, and human factors, which may have influenced some probes in the inclinometers. At the bottom, where the displacements should be zero, there is instead a 2.5 cm displacement. Therefore, the uncertainty in the measured displacement is estimated to be at least ±2.5 cm. Fig.2.5 shows that, considering the uncertainties, the measured data are mostly within the predicted numerical confidence intervals, especially when the displacements are more

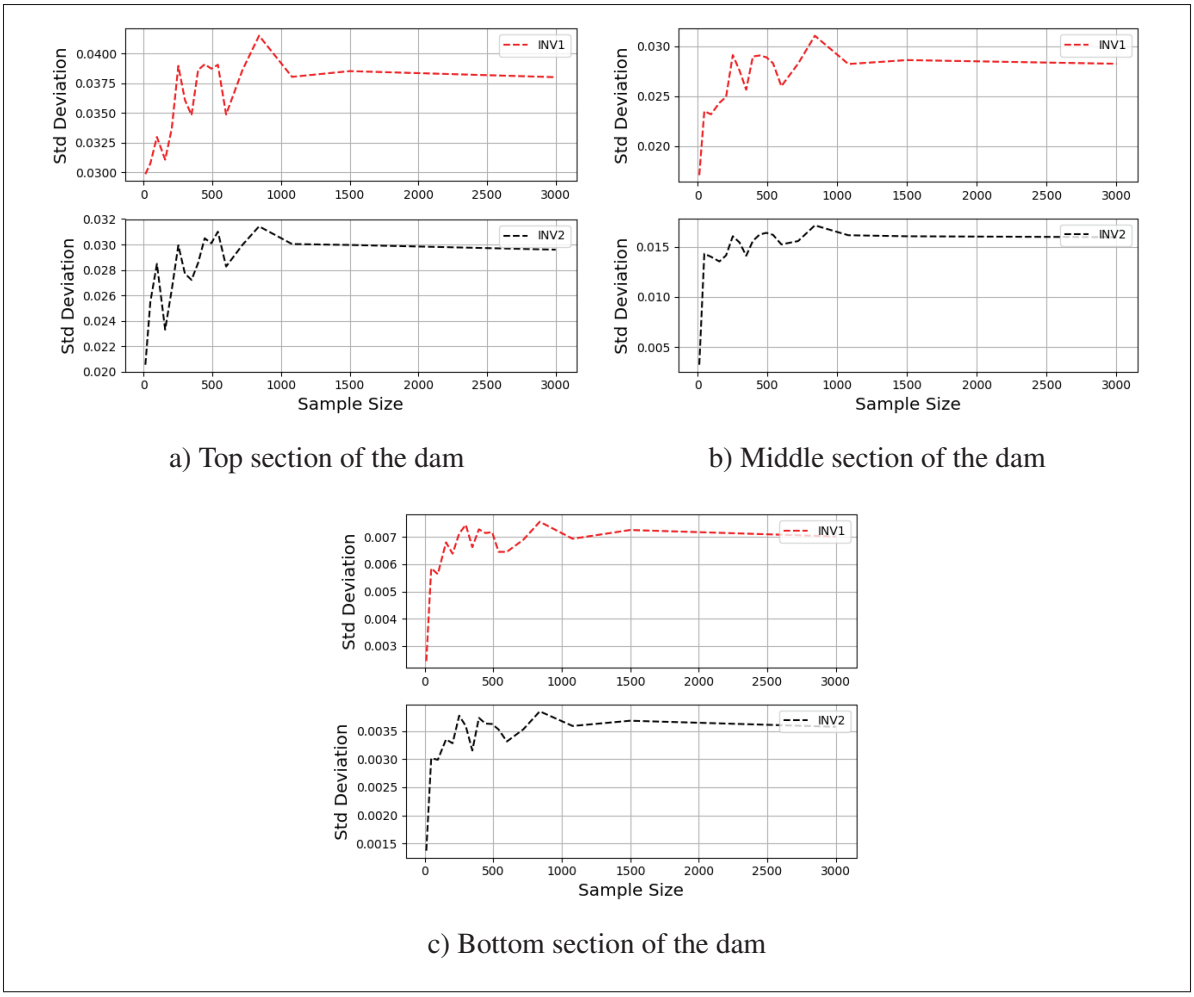

Figure 2.4 Variations of standard deviation (of the vertical displacement) with respect to the sample size for each inclinometer. The plots are built for the nodes close to the top, middle, and bottom sections of the dam

significant. The statistical confidence intervals could be enlarged by changing the distribution intervals of the input parameters. Indeed, we used a priori uniform distributions on estimated input intervals (Smith, 2015).

2.3.2 Sobol indices

A Sobol index is defined as the ratio of partial variances to the total variance, and reflects the relative importance of each input parameter (Li *et al.*, 2010), as shown in Fig.2.6 for points

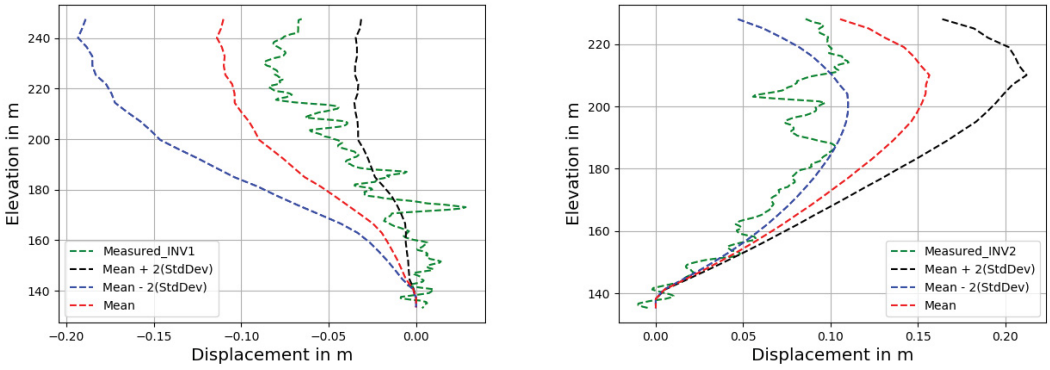

a) Vertical displacements for inclinometer INV1 b) Vertical displacements for inclinometer INV2

Figure 2.5 Confidence intervals for numerical vertical displacements

located at the top, middle, and bottom of the inclinometers. The indices here range from 0 to 1. It is evident from Fig.2.6 that the shear modulus is the dominant parameter, with a contribution of 44% to 71% in the top sections of the dam, and that it diminishes gradually with the depth. The Poisson's coefficient is the second most significant parameter, with a smaller effect (24%) on top, and a high impact (84%) close to the foundation. At 140m, there is the foundation (made up of grouted rocks) of the dam, therefore the impact of soil parameters is abrupt in the bottom. The first-order indices are calculated along the inclinometers, as shown in Fig.2.7. As stated earlier, for both inclinometers, the shear modulus is dominant in the upper section of the dam. The Poisson's coefficient is another crucial parameter influencing the dam's behaviour. While it is less influential at the top section, its impact increases as we head towards the bottom part. The specific weight only affects the lower section. Thus, the shear modulus and Poisson coefficients are the most significant parameters, although their contributions vary with the elevation.

2.3.3 Surrogate Modeling

Surrogate modelling is an approach aimed at generating an approximate numerical model to reduce the computing time, especially when a large number of simulations are required, as is the case in uncertainty and sensitivity analysis. Instead of using the 'full-order' original

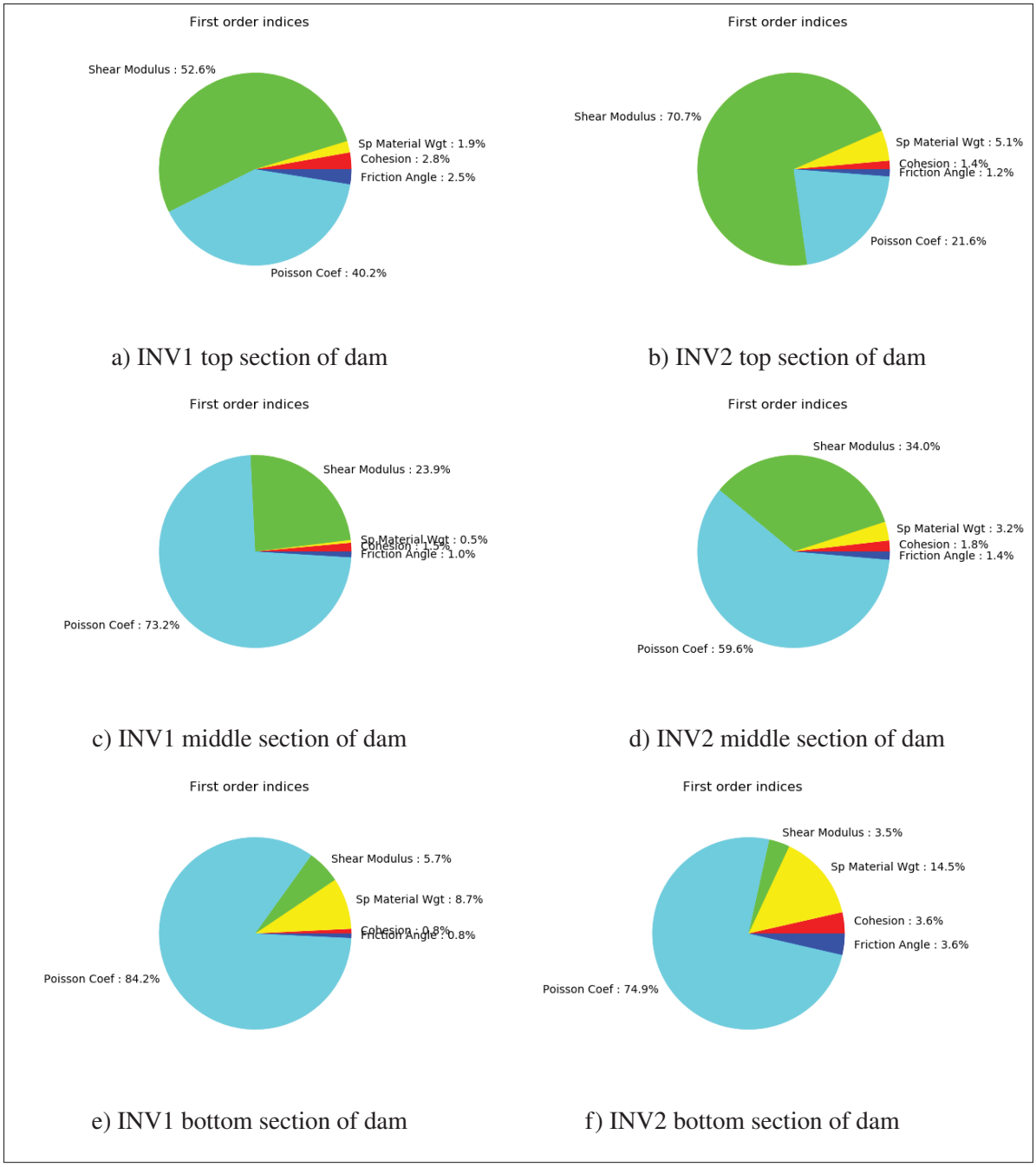

a) INV1 top section of dam

b) INV2 top section of dam

c) INV1 middle section of dam

d) INV2 middle section of dam

e) INV1 bottom section of dam

f) INV2 bottom section of dam

Figure 2.6 The pie charts show the sensitivity indices for INV1 and INV2 vertical displacements, respectively

finite element model, an approximate one called a 'surrogate model' (or surface response) is built using the input-output database. Many techniques could be used, but here we consider Polynomial Chaos Expansions and Deep neural networks. Based on the convergence study in

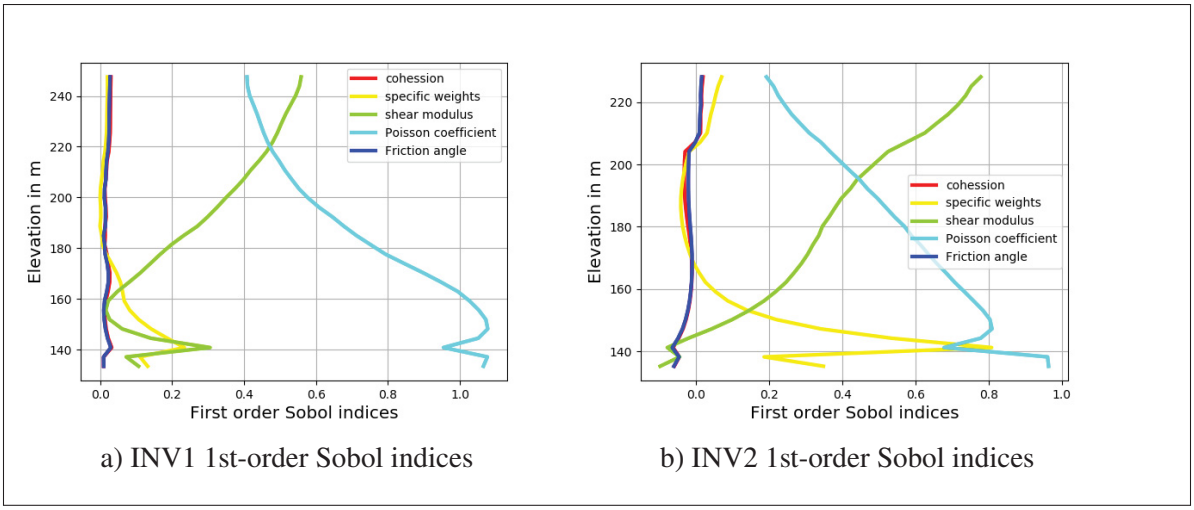

a) INV1 1st-order Sobol indices

b) INV2 1st-order Sobol indices

Figure 2.7 First Sobol variations with respect to the elevation

Section.2.3.1, the $N = 1080$ datasets are accurate enough to build the surrogate models. To assess the accuracy of these models, we examine the residual errors (the root mean square error (RMSE) and the coefficient of determination (R^2)).

2.3.3.1 Polynomial Chaos Expansion (PCE)

A Polynomial Chaos Expansion-based method (Wiener, 1938) is a probabilistic technique that can be used to build an accurate surrogate model. The degree of the polynomials and the regularization parameters are tuned for the best results. The PCE degree is varied from 2 to 6, and the regularization parameter λ_P is taken as 0.001, 0.01 and 0.1 respectively. The mean and standard deviation are calculated using the surrogate model obtained by running a simple Monte Carlo method on the PCE. The evaluation of the absolute mean error with respect to the polynomial order and the regularization parameter for an output response is shown in Fig.2.8, and is defined as:

$$E_1 = \frac{1}{m}\sum_{i=1}^{m}\|Y_{mp}^i - Y_{ms}^i\| \tag{2.11}$$

where m is the number of nodes and Y_{mp} denotes the mean of predicted displacement at the same node as Y_{ms}, the simulated displacements. Ideally, λ_P is selected as the smallest value,

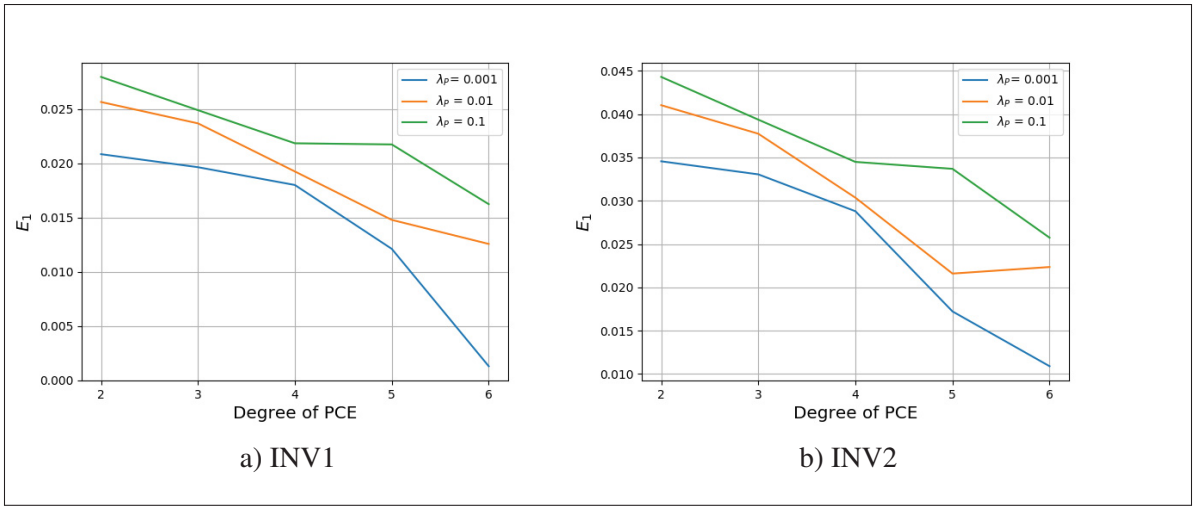

Figure 2.8 Absolute mean error for degree and regularization parameters

avoiding overfitting. Fig.2.8 shows that for 0.001, 0.01 and 0.1, the value E_1 decreases with the polynomial degree for both inclinometers. Therefore, the results for $P = 6$ and $\lambda_P = 0.001$ are considered as the most reliable.

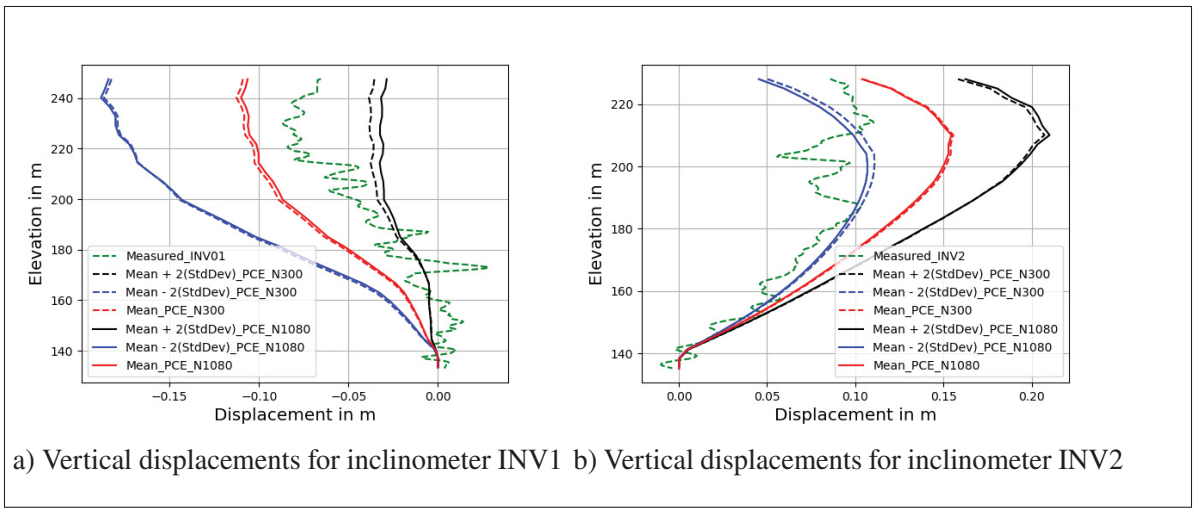

Figure 2.9 Confidence intervals using Polynomial Chaos Expansion-based surrogate model

Fig.2.9 shows that the measured and predicted displacements obtained using PCE trained for data sets N=300 and N=1080 are in better agreement. Moreover, when considering the

measurements along with their uncertainties, we see that they are mostly within the predicted numerical confidence intervals of PCE, especially when the displacements are more significant. The first-order indices along the inclinometers by using PCE are shown in Fig.2.10. As stated earlier, for both inclinometers, the shear modulus is dominant in the upper section of the dam. The Poisson's coefficient is another crucial parameter influencing the dam behavior. While it is less influential at the top section, its impact increases as we head towards the bottom part. The specific weight only affects the lower section. Thus, the shear modulus and Poisson coefficients are the most significant parameters, although their contributions vary with the elevation. The Sobol indices at the top, middle and bottom of the dam are also recomputed based on the PCE surrogate model, as shown in Fig.2.10 and Fig.2.11 , which illustrates almost the same information and conclusions as those shown in Fig.2.6 and Fig.2.7.

The shear modulus is the dominant parameter, with a contribution of 50 to 70% in the top sections of the dam, and whose influence diminishes gradually with the depth. The Poisson coefficient is the second most significant parameter, with a smaller effect (18%) on top and a high impact (90%) close to the foundation.

2.3.3.2 Deep neural network results

In order to fit the data, a MATLAB function 'Neural Net Fitting' is used with a five-layer feedforward network, as shown in Fig.2.2. A scaled conjugate gradient algorithm was used for the training. The (N = 1080 and N = 300) datasets were divided into training, validation, and testing subsets, at the following proportion: 70%, 15%, and 15% respectively. An ensemble of 10 trained networks was created by randomly initializing the weights in the training, and the outputs were predicted individually and averaged to get an ensemble output solution. An example of plots for data sets N = 300 and N = 1080, showing the fitness variation with respect to the training iterations (epochs) is presented in Fig.2.12.

The mean and standard deviation are calculated using the surrogate model obtained by running a simple Monte Carlo method on the ensemble neural network model. The mean and variance for

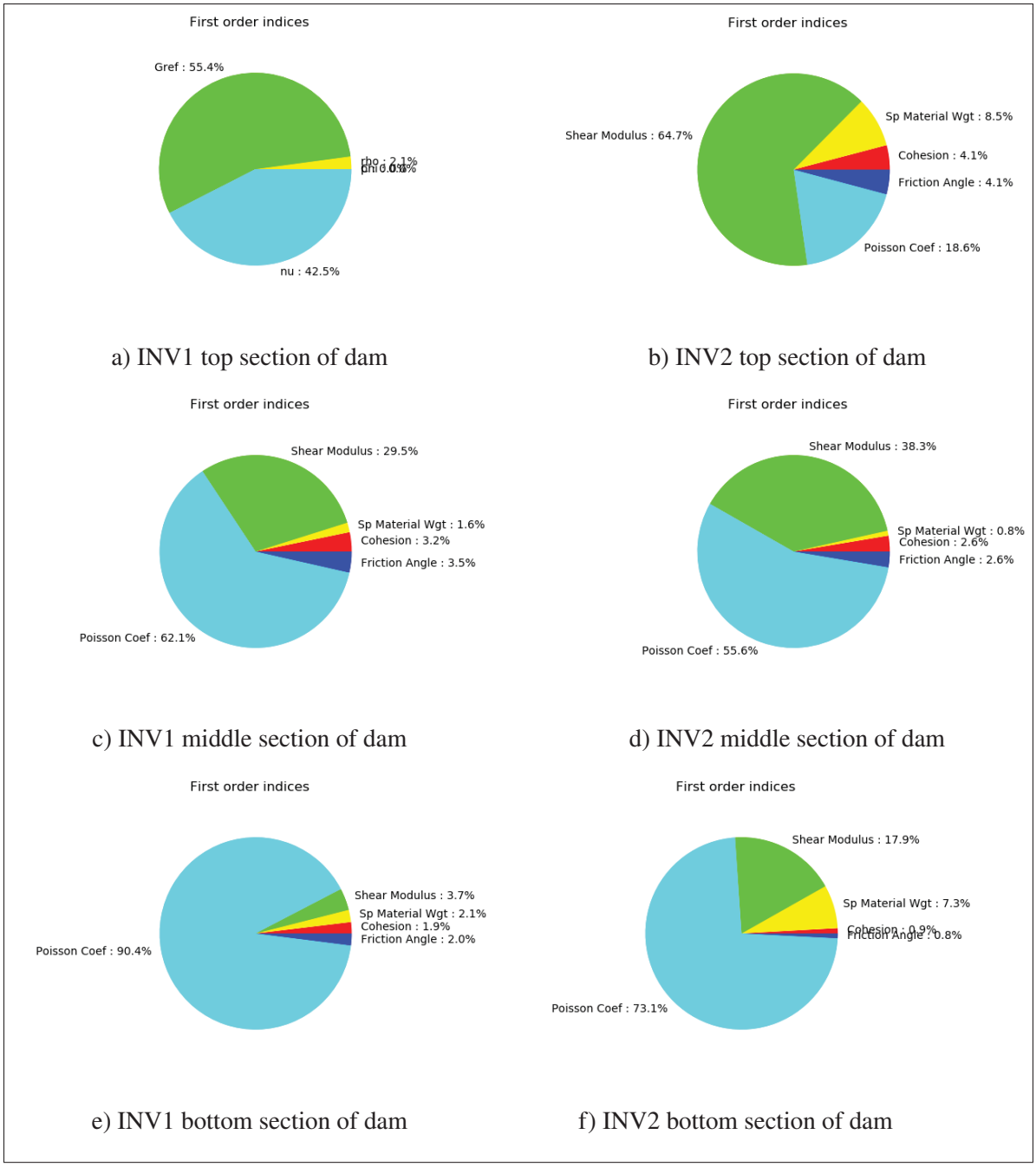

Figure 2.10 The pie charts show the sensitivity indices based on PCE for INV1 and INV2 vertical displacements, respectively

the ensemble model are computed by Eq.2.9 and Eq.2.10.

The displacements obtained with the ensemble neural network are shown in Fig.2.13, and are very similar to those obtained with the statistical approach Fig.2.5, and are the pie charts and the

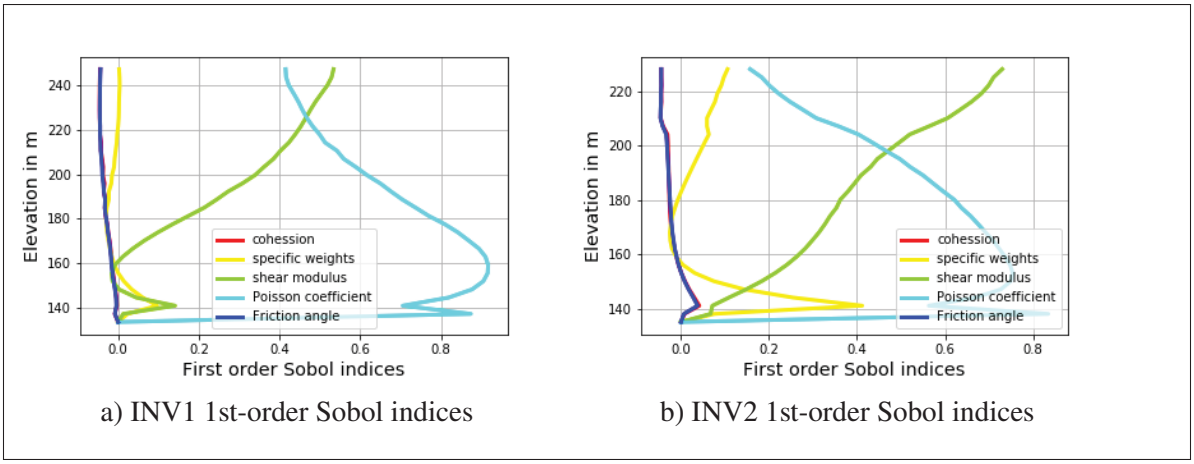

a) INV1 1st-order Sobol indices

b) INV2 1st-order Sobol indices

Figure 2.11 First Sobol index results obtained using PCE surrogate model

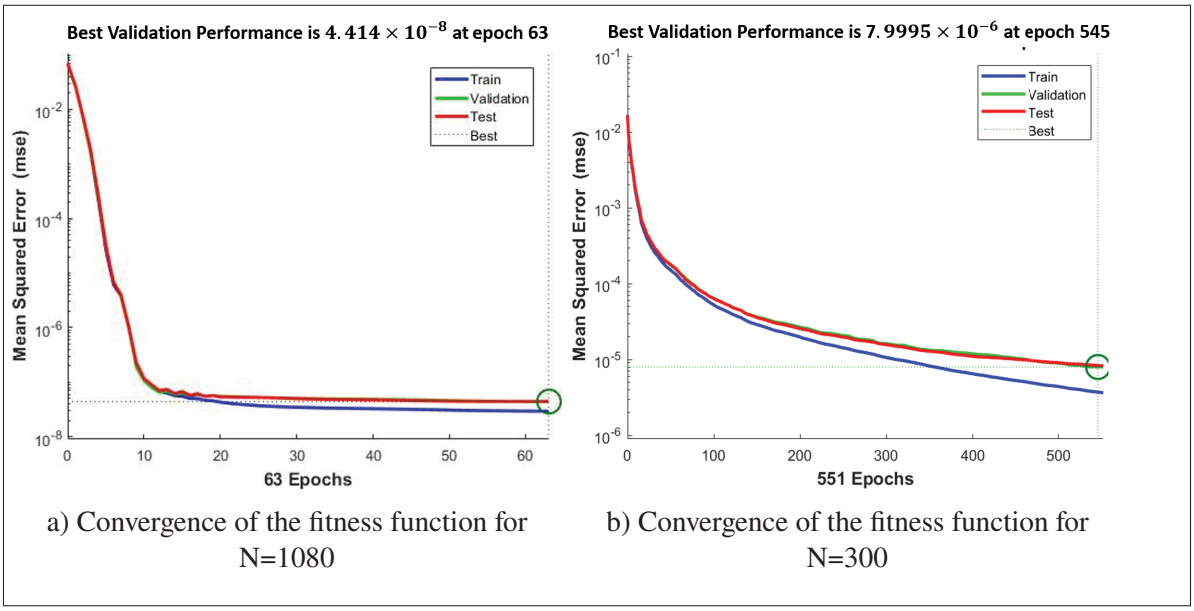

a) Convergence of the fitness function for N=1080

b) Convergence of the fitness function for N=300

Figure 2.12 Performance of NN

indices as shown in Fig.2.14 and Fig.2.15 respectively. The displacement standard deviations calculated on the inclinometers using the statistical approach (MCS) and the PCE surrogate models and DNN models are reported in Table.2.2, with a maximum standard deviation for all methods close to 4 centimeters. Moreover, near the foundation of the dam the displacements are almost zero. Fig.2.16 shows the computational efficiency for the CPU for one plaxis realizations

Table 2.2 Comparative study of standard deviation in m by numerical simulations and surrogate models for top, middle and bottom sections of the dam

Inclinoimeters	**INV1**			**INV2**		
Approach	**Top**	**Middle**	**Bottom**	**Top**	**Middle**	**Bottom**
Statistical approach (MCS)	0.0388	0.0282	0.0043	0.0292	0.0161	0.0028
Polynomial Chaos Expansion(PCE)	0.0364	0.0291	0.0084	0.0313	0.0238	0.0079
Ensemble of Deep neural networks	0.0387	0.0311	0.00121	0.0285	0.0189	0.0042

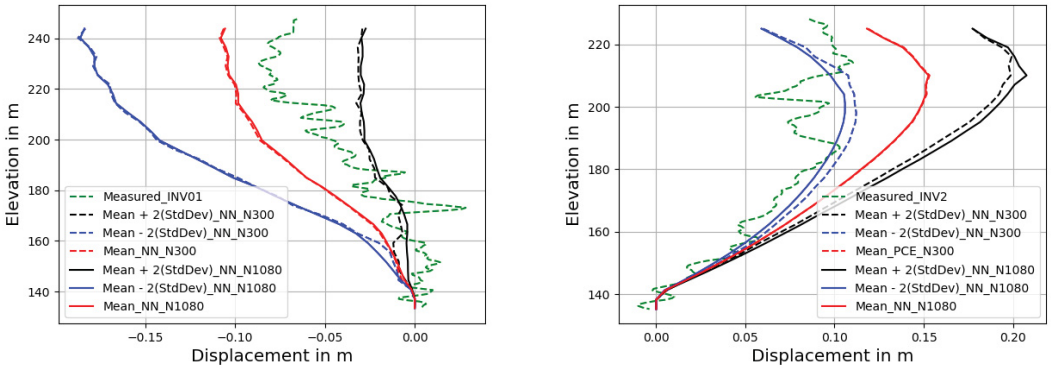

a) Vertical displacements for inclinometer INV1 b) Vertical displacements for inclinometer INV2

Figure 2.13 Confidence intervals using an ensemble of neural networks-based

and for the surrogate models with respect to the number of samples for soil parameters. It can be observed that the surrogate models are more efficient to predict the results as compared to getting the simulations by the FEM model. Noteworthy, this result will be helpful for an upcoming study that consists of the identification of soil parameters by inverse analysis. In the inverse analysis, the optimization algorithm makes hundreds of calls to obtain the numerical solutions (Das & Soulaimani, 2021). Therefore, the surrogate models will be used instead of the full-order original finite element model for computational efficiency. The outcome of this study is that indeed NN requires much fewer samples to realize a sensitivity or identification analysis compared to the full-order model.

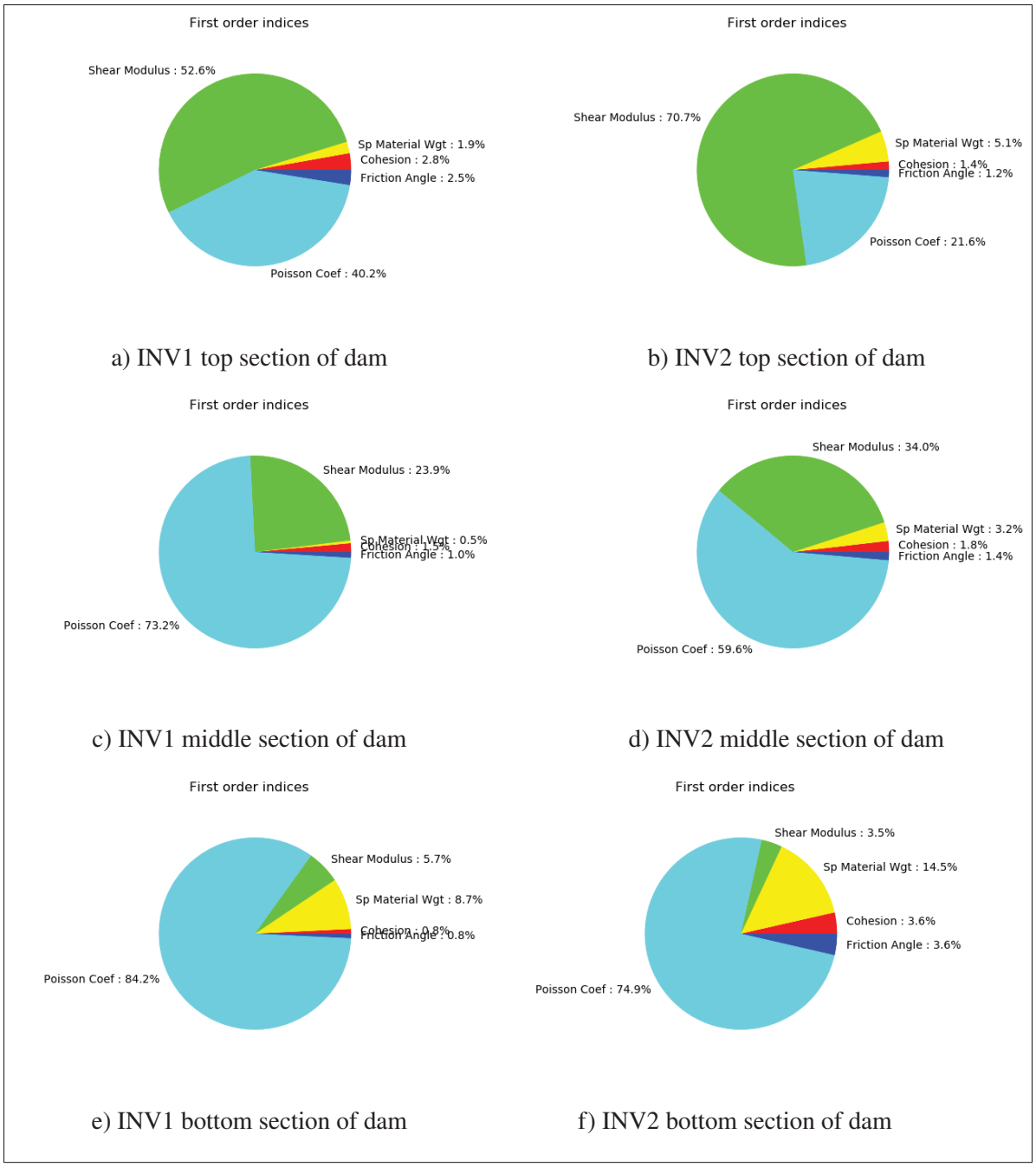

a) INV1 top section of dam

b) INV2 top section of dam

c) INV1 middle section of dam

d) INV2 middle section of dam

e) INV1 bottom section of dam

f) INV2 bottom section of dam

Figure 2.14 The pie charts show the sensitivity indices based on DNN for INV1 and INV2 vertical displacements, respectively

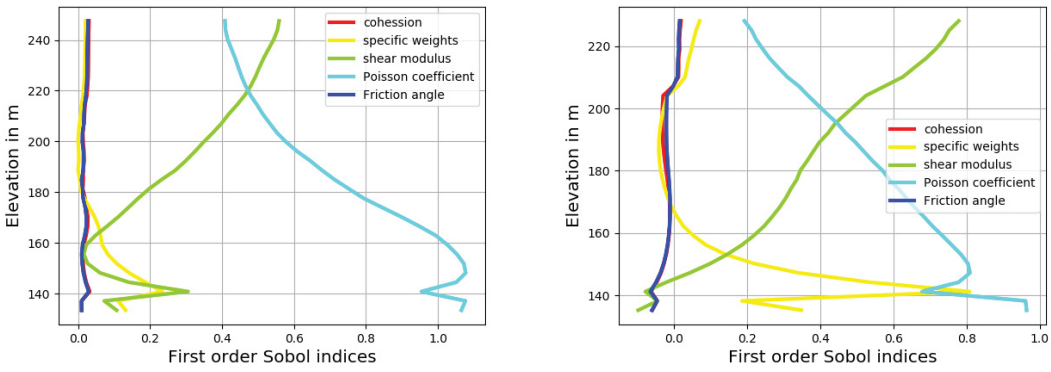

a) INV1 1st-order Sobol indices

b) INV2 1st-order Sobol indices

Figure 2.15 First Sobol variations with respect to the elevation

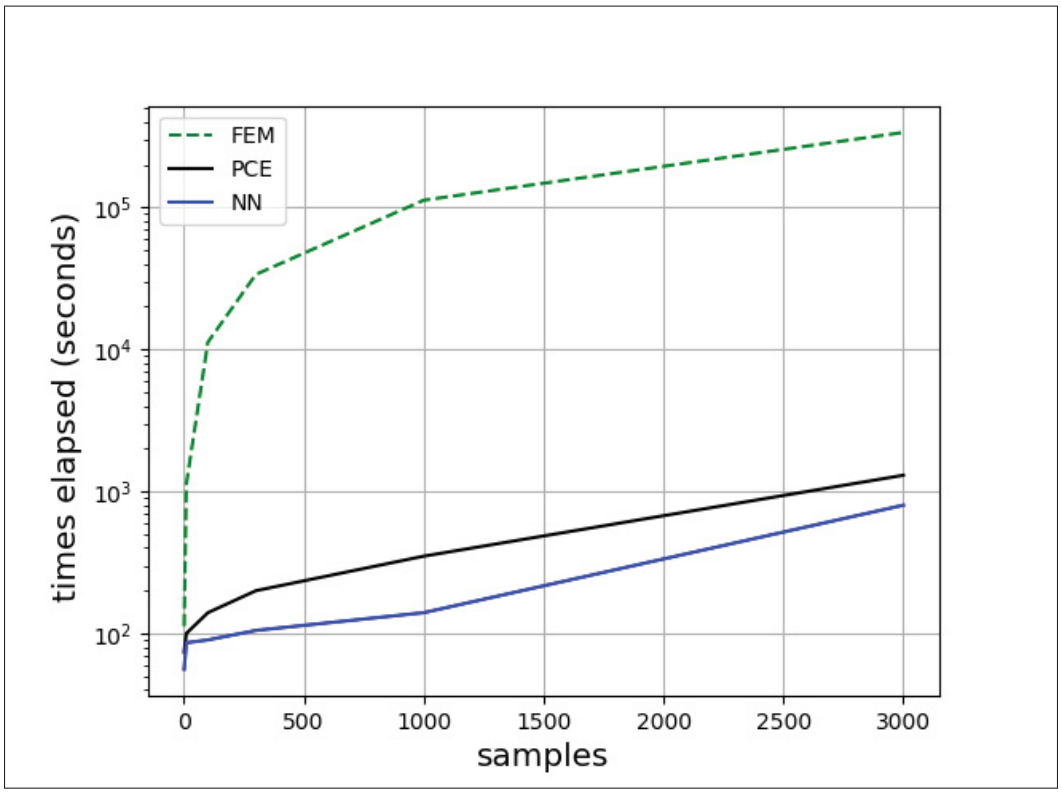

Figure 2.16 Computational Efficiency for the displacements obtained by FEM, PCE and NN

2.4 Conclusion

This paper contributes to rockfill dams' sensitivity and uncertainty analysis using the surrogate modelling approach. The approach was applied to an actual rockfill dam with an asphalt core. Two surrogate models were developed, namely, a Polynomial Chaos Expansion (PCE) model and a Deep Neural Network (DNN), by training for two data sets, N=300 and N=1080. Their results were compared to those obtained with Monte Carlo simulations. The variance-based sensitivity analysis reinforces that the shear modulus and the Poisson coefficient are the parameters that play the most significant role in the dam's behaviour. Therefore, when considering all material sub-domains, these two parameters may be kept as the only significant uncertain parameters, thereby significantly reducing the total number of uncertain inputs. A second analysis was conducted by sampling the input parameters using a uniform probability distribution. The statistical mean displacements, on two inclinometers, obtained with the PCE surrogate model, were more consistent with the mean of the measured data than those computed with the DNN model. Overall, this study shows that building surrogate models reduces the computational cost of numerical models when a large number of simulations are required, as in sensitivity and uncertainty analysis.

CHAPTER 3

DEEP NEURAL NETWORK-BASED INVERSE ANALYSIS WITH APPLICATION TO A ROCKFILL DAM

Gullnaz Shahzadi[1] , Azzeddine Soulaïmani[1]

[1] Department of Mechanical Engineering, Ecole de Technologie Supérieure, 1100 Notre-Dame W., Montreal (QC), Canada H3C 1K3

This article has been Submitted in:
KSCE Journal of Civil Engineering, on 27 February 2023

Abstract

The availability of significant computational resources has played an essential role in developing advanced numerical models for the design and safety assessment of complex structures such as rockfill dams. Determining the geomechanical parameters is a crucial but challenging task for effective modelling. The general approach involves using laboratory or in situ tests or empirical relationships from the literature to estimate these parameters. However, such measures lack an accurate representation of the actual scenario. This paper proposes a data-driven approach using deep neural networks and non-deterministic optimization algorithms to identify the soil parameters leading to displacements that best approximate the measured data. The methodology is applied to a rockfill dam recently built in Quebec, for which some measurements of inclinometer displacements are available. A two-dimensional finite element model (FEM) generates the numerical solutions. A comparative study is performed to account for the heterogeneity of the materials by decomposing the computational domain into subdomains. Subsequently, the inverse analysis uses the surrogate model instead of the full FEM model for rapid computations. A suitable objective function is defined to account for large oscillations in the measurement data. Non-intrusive stochastic optimization algorithms (Genetic algorithm (GA), Particle Swarm Optimization (PSO), and Differential evolution (DE)) are evaluated for the minimization problem. Finally, the case study confirms the capability of the proposed methodology to identify the relevant dam parameters and provides insights into the performance of the three optimization algorithms.

keywords

Deep neural networks, inverse analysis, uncertainty analysis, optimization algorithms, rockfill dam.

3.1 Introduction

To overcome new challenges, engineers face the demand for innovative computational methods in geotechnical engineering. These methods are essential in the design process and dam safety assessments. A dam that relies on rocks compacted in layers or dumped in lifts is known as a rockfill dam (Asthana & Khare, 2022). Rockfill dams are increasing in geotechnical water conservation projects due to their low cost and short construction period. In the early nineteens, to prevent seepage through rockfill, impervious membranes of asphaltic concrete or cement concrete were used on the upstream face of the dam. However, geotechnical engineers face significant challenges in designing rockfill dams due to the uncertainties in the material properties used in their complex structures (Akbari Hamed, 2017). The finite element method (FEM) combined with the appropriate soil constitutive laws is considered the most powerful approach for dam modeling and design (Pietruszczak, 2010). However, the lack of information on soil properties limits each constitutive model from representing the actual dam behavior. Different materials are used for each zone in dam construction; therefore, identifying the material parameters for each zone will help to improve the modelling. In this context, the inverse analysis provides an easy and efficient way to identify the soil parameters when appropriate measurement data is available (Yin *et al.*, 2018; Carbonari, Dezi, Arezzo & Gara, 2022). Inverse analysis tries to minimize a norm that defines the difference between the numerical solutions and the measurements. However, this procedure may become time-consuming if a large-scale FEM model is used during the iterative optimization process. Several methods have been developed to improve efficiency by replacing the time-consuming FEM calculations for inverse analysis. For instance, the finite element method can be replaced for parametric studies and calibration by numerical methods based on suitable orthogonal decomposition in conjunction with radial basis interpolation (Bolzon & Buljak, 2011).

Geotechnical problems are characterized by significant uncertainties and involve various factors that engineers cannot determine directly. Due to the inherent complexity of geotechnical materials, researchers replace tedious theoretical solutions with flexible computational methods to solve various geotechnical design and evaluation problems, a practice which has led to the rapid popularity of machine learning (ML) methods (Zhang *et al.*, 2021a; Zhang & Phoon, 2022). The popularity of ML and deep neural network (DNN) models in complex engineering problems has also encouraged researchers in the field of geotechnics to apply these techniques (Shahriari, Pardo, Moser & Sobieczky, 2020).

In the last decade, the use of surrogate modeling in geotechnical applications based on machine learning (ML) methods has increased in popularity(Phoon & Zhang, 2022; Salazar & Hariri-Ardebili, 2022; Kang, Liu, Li & Li, 2022). However, limited studies have been conducted on actual data-based ML. Deep neural networks require less human guidance and vast amounts of data compared to other ML methods to explore the complex, heterogeneous, and inherent relationships hidden in the data (Zhang *et al.*, 2022). Most ML algorithms build a surrogate model and then optimize the objective function (or loss function) via optimization algorithms to find the best model with the best performance. To improve the accuracy of establishing a surrogate model in ML, ensemble learning trains multiple algorithms to gain complementary advantages and achieve better prediction results than a single algorithm. The state-of-the-art approach uses a regression model based on DNNs to approximate the original FEM model (Shahzadi & Soulaïmani, 2021; He, Wang, Li & Sheng, 2022), due to its efficiency compared to purely sampling methods.

Several constitutive models exist, and each involves different soil parameters. In addition, a dam is constructed of several material zones; consequently, different soil parameter values must be employed, which requires automatic calibration of soil parameters. However, several factors affect the calibration process, such as the number of parameters and the smoothness of the data. In recent research, optimization techniques have been widely used in inverse analysis to reduce the computational cost and improve accuracy (Zhao & Yin, 2016; Das & Soulaimani, 2021; Zhang *et al.*, 2022).

An inverse analysis based on the multi-output least-squares support vector regression machine (MLSSVR) and improved differential evolution algorithm (IDE) is proposed in (Bao, Li, Lu & Gu, 2020) to map the relationship between numerical displacements of the dam and related soil parameters. However, the above methods require establishing many inversion models with different sample sizes for sufficient accuracy. A hybrid fireworks algorithm (FWA) with a surrogate model based on radial basis functions was proposed in (Dou, Li & Kang, 2019) to identify the elastic modulus of concrete dams. The radial basis function neural network (RBFNN) model based on brainstorm optimization and genetic algorithm was developed to predict slope stability(Shang *et al.*, 2022). Although the surrogate models based on RBF improve the efficiency and accuracy, those improvements have only been validated for pseudo experiments, i.e., without using any measured data from real dams. Therefore, this technique needs more verification for engineering practice.

Inverse analysis based on optimization techniques has been utilized in various applications of geotechnical engineering (Hashash *et al.*, 2010a; Kim & Finno, 2019; Levasseur *et al.*, 2010; Vahdati, Levasseur, Mattsson & Knutsson, 2014). The most common optimization techniques to identify the optimal parameters are the Genetic Algorithm (GA) (Zhou *et al.*, 2016; Deng-gang, Ying-xi & Shou-ju, 2000; Vahdati *et al.*, 2013), Particle swarm optimization (Kennedy & Eberhart, 1995; Jia & Chi, 2015; Dou *et al.*, 2017), and the Differential evolutionary method (DE) and its modified forms (Yin *et al.*, 2018). Moreover, the precise formulation of the objective function according to the problem requirement is crucial to achieving the optimum, particularly when the measurement data on the inclinometers present large oscillations. Hence, there is a need to formulate an appropriate objective function that can be used as a prepossessing phase in parameter identification (Hokes, Kral, Krnavek & Husek, 2017). (Eykhoff, 1974) presents several methods used to define an objective function.

This paper proposes a data-driven approach using deep neural networks and non-deterministic optimization algorithms to identify the best parameters to fit non-smooth measurements. The methodology is applied to a rockfill dam recently built in Quebec, for which some measurements of inclinometer displacements are available. A set of FEM numerical solutions is computed

by sampling the input parameters using Sobol's sampling technique (Sobol, 1993). A deep neural network (DNN) with five layers is used to build a surrogate model of the FEM of the dam. Consequently, a multi-objective function for the displacements of four inclinometers is incorporated into a single error function by using the weighted sum method (Gunantara, 2018).

Non-intrusive optimization algorithms are then used to identify the soil parameters by minimizing an error function measuring the difference between the numerical predictions (obtained online using the surrogate model) and the measured data. As a benchmark, we consider the case of a rockfill dam called Romaine-2 (Smith, 2015). More specifically, a two-dimensional plane-strain finite element model is used in the geotechnical software Plaxis (Plaxis, 2017) to compute the numerical displacements for two separate cross-sections of the dam where data are available. The Mohr-Coulomb elastoplasticity model(MC) (Labuz & Zang, 2012) is employed to model the nonlinearities. The Romaine-2 dam is composed of five different material zones.

The rest of this paper is organized as follows: the next section presents the methodology for inverse analysis, including surrogate modelling, objective function formulation, and a brief presentation of optimization algorithms. A case study of the Romaine-2 dam is then described in the third section. Finally, the relevant dam parameters estimated by the analysis are presented along with insights into the performance of the three procedures to solve the inverse problem. The conclusion also proposes an avenue to explore to expand this approach.

3.2 Methodology

The parameters of the constitutive soil models used in the modelling of complex continuum media are often associated with high degrees of uncertainty. The inverse analysis provides a way to identify these parameters. The procedure involves using real measured or synthetic data (stemming from multiple runs of a high-fidelity numerical model). Using optimization methods and a reduced-order model for the system, it is possible to determine the values of the parameters by minimizing the difference between simulated and observed results. As an actual application, we consider the measured data from an actual rockfill dam in Quebec and

propose a surrogate-assisted non-deterministic framework for the inverse analysis. The parameter identification process is composed of three main steps: 1) a surrogate model is built by using numerical simulations data sets to predict the numerical displacements; 2) the formulation of an objective function, which measures the difference between the measured and the predicted variables; and 3) the use of a robust optimization algorithm to minimize the objective function. Fig.3.1 illustrates the flow chart of the methodology.

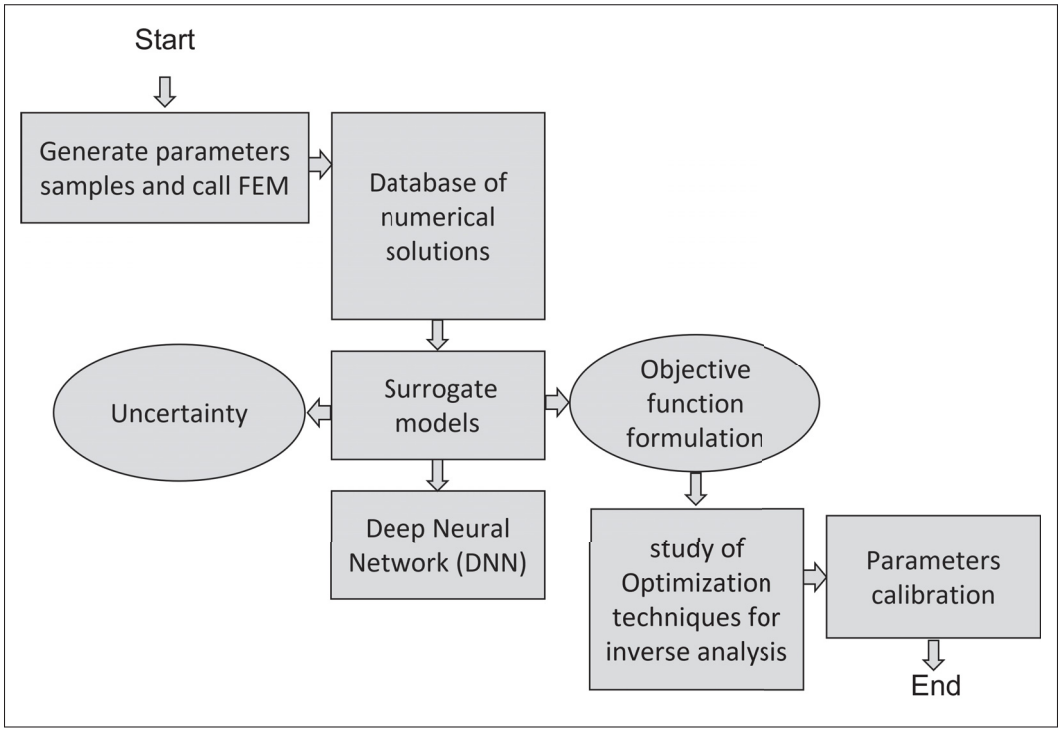

Figure 3.1 The flowchart of the proposed Methodology

3.2.1 Surrogate Modeling

Most continuum mechanical problems are described by parameterized nonlinear partial differential equations (PDEs). The finite element and finite volume methods are among the most popular approaches to discretizing these equations. When they are solved over fine spatial meshes and for a high number of parameters, PDE discretizations lead to the so-called high-fidelity numerical models. Furthermore, in the context of uncertainty or inverse analyses,

the overwhelming demand for computational resources makes these high-fidelity computations too expensive to allow repeated solutions for various parameters. Reduced-order modelling has been considered a promising approach for learning and representing high-fidelity models through a reduced-dimension manifold (or surrogate model). We adopt the non-intrusive paradigm, in which a surrogate model is trained using existing data which works in a black-box manner without requiring access to the source codes. This data-driven approach has been attracting increased attention in various engineering fields, stimulated by the explosive development of machine learning.

3.2.1.1 Deep neural networks

In modern research, deep neural networks (DNN) are widely used as a powerful and common numerical approach to creating a non-linear mapping between inputs (features) and their corresponding outputs (labels or targets). Deep neural networks are structured with nodes; a node collects the inputs, sums the weights, and applies the activation functions to produce the outputs. Nodes are arranged in several layers. The nodes in one layer are connected to the nodes of the subsequent layer. However, the nodes in each layer are not interconnected. The parametric forms for basis functions are used in deep neural networks, in which parameter values are adapted during training. Moreover, the model is nonlinear, as it uses nonlinear activation functions. Fig.3.2 illustrates a DNN with one hidden layer. The input data are mapped to the hidden layer (1) to compute

$$h_j^{(1)} = f(\sum_{i=1}^{n} W_{ji}^{(1)} x_i + a_j^{(1)}) \tag{3.1}$$

which are then delivered to the output layer (o) to compute the response

$$y_k = g(\sum_{j=1} W_{kj}^{(0)} h_j^{(1)} + a_k^{(0)}) \tag{3.2}$$

where f and g represent the activation functions, and where $W_{ji}^{(1)}, W_{kj}^{(0)}$ are the weight parameters and $a_j^{(1)}, a_k^{(0)}$ are the bias parameters.

An iterative technique based on the back propagation algorithm is used to minimize the error

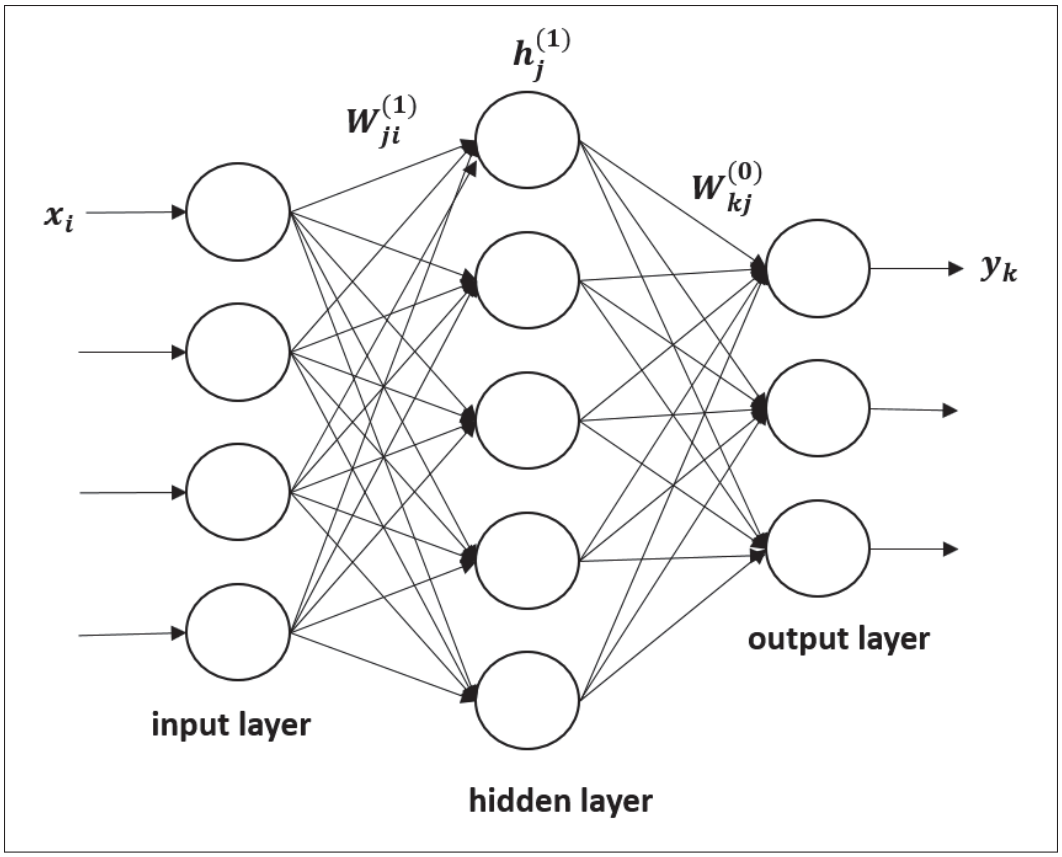

Figure 3.2 One-layer neural network

function J. Generally, the activation function f is the sigmoid or the rectified linear unit; however g is the identity function for our regression problem. Fig.3.3 presents an example of a deep network, where five hidden layers are used; the input layer has the dimension $n = 5$ and the output layer has $m = 128$ nodes. There are many public domain implementations of a (standard) deep neural network, such as the TensorFlow library, PyTorch and Keras. The Matlab deep learning neural toolbox is used (Beale *et al.*, 2019) in this study.

3.2.1.2 Ensemble of models

An ensemble learning technique is used in machine learning to improve the predictive performance and reduce the model uncertainty, training various models separately and combining their

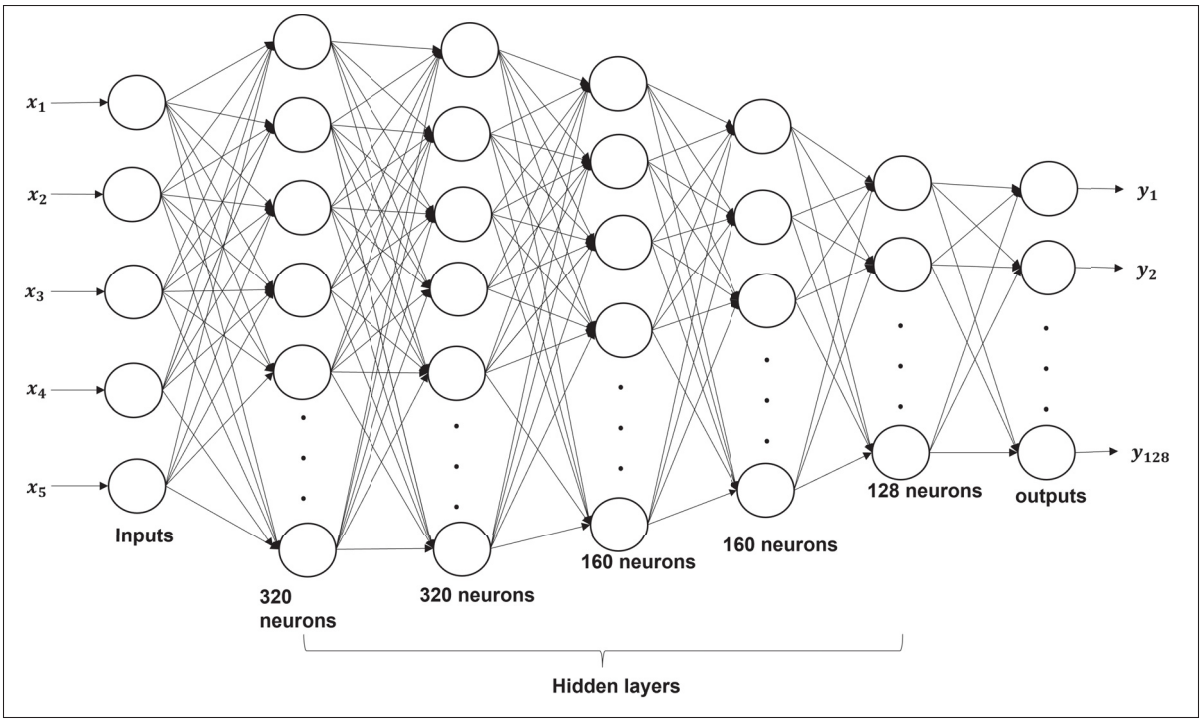

Figure 3.3 A five-layer Deep neural network

solutions (Goodfellow *et al.*, 2016; Bishop, 2006; Hsieh, 2009). The idea here is to obtain different neural network solutions by varying the number of neurons in hidden layers, the training algorithms and the hyper-parameters, etc. An efficient approach uses the random initialization of weights, effectively generating an ensemble with partially independent members (Jacquier *et al.*, 2021). Given the combination of K-trained neural networks, each member develops a solution with a mean $Y_{NN}^{(k)}$ and a variance $(\sigma_{D,ML}^{(k)})^2$; an average single normal average distribution can be defined with a mean Y_{NN}^{ens}, where:

$$Y_{NN}^{ens} = \frac{1}{K}\sum_{k=1}^{K} Y_{NN}^{(k)} \tag{3.3}$$

and variance is given by:

$$\sigma_{ens}^2 = \frac{1}{K}\sum_{k=1}^{K}\left\{(\sigma_{D,ML}^{(k)})^2 + (Y_{NN}^{(k)})^2\right\} - (Y_{NN}^{ens})^2 \tag{3.4}$$

K is usually taken between 5 and 12 (in the following numerical results, it is assumed to equal 10). Therefore, the numerical prediction of the network is represented by a Gaussian with the mean Y_{NN}^{ens} and the variance σ_{ens}^2, which represents uncertainties in both the data and the weights.

3.2.2 Formulation of the objective function for calibration

For rockfill dams, the constitutive soil parameters are the variables to be identified. In general, the reliability of the identification process is a function of the quantity and the quality of the measured data set. In the present work, some displacement measurements made by inclinometers in a rockfill dam are available. The most straightforward method to define an objective function is to use the mean square error:

$$J_{obj} = \frac{1}{N_m} \sum_{i=1}^{N_m} (Y_i - \bar{Y}_i)^2 \tag{3.5}$$

where N_m is the number of measurement points, Y_i is the measured data, and $\bar{Y}_i$ is the numerical prediction. A generalization of the above equation that considers additional weights C_i is given by:

$$J_{obj} = \frac{1}{N_m} \sum_{i=1}^{N_m} C_i (Y_i - \bar{Y}_i)^2 \tag{3.6}$$

More weight could thus be given to the more reliable measurements, as uncertainties are unavoidable due to several factors that affect the performance of inclinometers. These uncertainties may be reflected in large fluctuations displayed in the measured displacement plots. Such fluctuations may make the optimization iterative process difficult to converge or cause it to converge to an unreliable solution. Therefore, the weights C_i are formulated here as:

$$C_i = \tanh(\frac{1}{\delta_i}) \tag{3.7}$$

$$\delta_i = \beta(\frac{Y_i - \bar{Y}_m}{\sigma_m + \varepsilon})^2 \tag{3.8}$$

where $\bar{Y}_m$ is the mean of the measured displacements along the inclinometers, σ_m is their standard deviation, β is an empirical parameter ($\beta = 3$ is a typical value), and ε is a small numerical value to avoid a division by zero. A large value of δ_i indicates a large uncertainty affecting the ith measured data, and when it is present, C_i will tend to zero. However, for small δ_i, indicating less uncertainty, C_i will be close to 1. To calibrate the soil parameters more accurately, the objective functions corresponding to each inclinometer needs to be minimized simultaneously. For a multi-objective problem, the weighted sum method can incorporate multi-error functions into a single composite function (Murata & Ishibuchi, 1995). The greater the weight, the higher the priority of the function compared to an objective function associated with a lower weight (Gunantara, 2018). Several approaches are used to determine weights; in this study, we chose a similar weights approach.

3.2.3 Selection of a robust optimization algorithm

A robust algorithm is required to obtain the global minimum for the objective function, considering the data fluctuations. Previously, deterministic techniques were widely used in the application of geotechnics for inverse problems due to their fast convergence (Nocedal & Wright, 2006). However, these methods are insufficient to deal with nonlinear geotechnical applications. To avoid the pitfalls of solution divergence or of a solution trapped in local minima, non-deterministic or stochastic optimization techniques are preferred (Coello, Lamont, Van Veldhuizen *et al.*, 2007).

A variety of non-deterministic optimizers are available, such as Genetic Algorithms (GAs), Particle Swarm Optimization (PSO), and Differential Evolution (DE), and have been applied in several geotechnical applications (Yin *et al.*, 2018; Boumezerane, 2022). These techniques are briefly described in the following subsection. The algorithms are implemented in Matlab's optimization toolbox (MATLAB, 2016), which is used in this study.

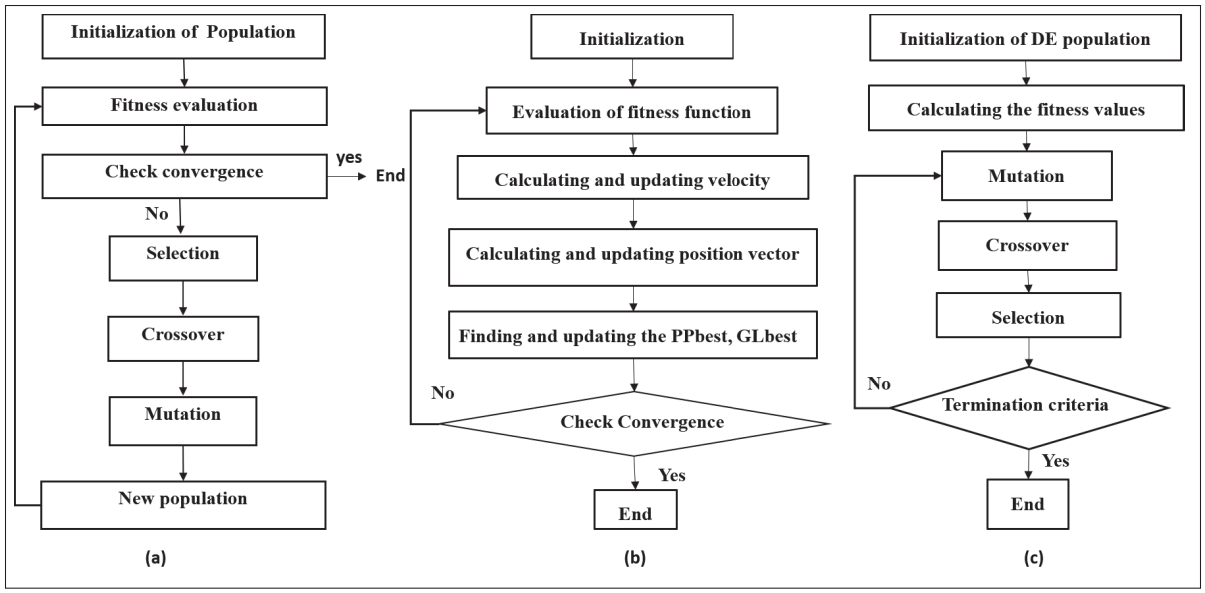

Figure 3.4 Flow diagrams of the GA, PSO and DE algorithms representing the different steps associated with the three non-deterministic algorithms

3.2.3.1 Genetic Algorithm(GA)

The Genetic algorithm (GA), initially developed by (Holland *et al.*, 1992), is defined as a search procedure based on the mechanism of natural evolution and involves selection and genetics (Darwin, 2007). Unlike gradient-based methods, the optimal solution of a GA is not a function of the initial solutions, giving it a robustness that is the main reason for its popularity. However, robustness is often associated with a higher computational cost than conventional optimization procedures. The genetic algorithm flow chart is shown in Fig.3.4(a). It consists of four crucial steps: initialization, evaluation, selection, and combination. An initial population set of possible solutions is generated randomly by considering the specific bounds of each parameter in the first step. Next, each individual's fitness is evaluated to meet convergence criteria based on stochastic principles. The chromosomes with the lowest functional values are selected as parents for the next set of operations, where a crossover probability combines them to create offspring. The idea is to imitate what occurs in nature, where the best chromosomes are passed onto new offspring to secure an improved next generation. This study applies a single-point crossover

approach with a 0.6 probability ratio. The mutation probability is defined as 0.1 to achieve the global optimum. The pseudo-code for GA is summarized in Algorithm 3.1:

Algorithm 3.1 An algorithm of GA

```
1 Create the initial population
2 Evaluate the fitness function for each individual
3 while Termination is not met do
4 |   Selection
5 |   Crossover with a 0.6 probability ratio
6 |   Mutation (Probability ratio = 0.1)
7 |   Evaluate fitness
8 end while
```

3.2.3.2 Particle Swarm Optimization(PSO)

Particle Swarm is a nonlinear global optimization technique for continuous functions introduced by (Kennedy & Eberhart, 1995), based on the theory of bird flocking, swarming, and fish schooling. In PSO, various search points are explored together in each iteration. The design variables in PSO can take any value based on their actual position in the search space and in the velocity vector, compared to GA (binary encoding). Moreover, PSO is ideal for asynchronous parallel implementation as it contains no evolution operators (mutation or crossover). Although both GA and PSO have the same function in investigating the solution, the particle swarm optimization algorithm is directed by the individual and global fitness of the particles and their current position to obtain their following post in the search space. Individuals explore the search space to achieve their target, and if any particle finds the source to reach the target, it starts to chirp louder and louder, and as a result, the other birds/particles circle the area. If any particle from the circle comes closer to the target, it chirps even louder, and the others veer towards it. This tightening pattern continues until one of the birds/particles locates the food/target. The algorithm keeps track of three global variables: 1) The Target value or condition, 2) The Global best value indicating which particle's data is currently closest to the Target, and 3) The Stopping value, which indicates when the algorithm should stop if the Target is not found.

The PSO algorithm generally seeks the global optimum among individuals by utilizing their shared information and collaboration. The PSO algorithm works in the directions given by the optimal position ($PPbest$) of each particle and the global best position ($GLbest$) of the whole population. The movement of the particles indicates the next position in the search space. The position vector and velocity of a j particle are denoted by x_j and V_j, respectively, and updated for the kth iteration using the following formulas (Arora, 2015):

$$V_j^k = w_1 V_j^{k-1} + c_1 r_1 (PPbest - x_j^{k-1}) + c_2 r_2 (GLbest - x_j^{k-1}) \tag{3.9}$$

and

$$x_j^k = x_j^{k-1} + V_j^k \tag{3.10}$$

where r_1 and $r_2 \epsilon [0, 1]$ are random numbers, whereas c_1, c_2 and w_1 are algorithmic tuning parameters. In this study, the tuning parameters c_1, c_2 are set equal to 2 and w_1 is 0.9. The pseudo code for PSO is as follows:

Algorithm 3.2 An algorithm of PSO

```
Initialization of position and velocity of the particle
while Termination is not met do
    For each particle
    Evaluate the fitness function
    Select the particle with the best fitness value
    Compute velocity and position of particle by Eq.3.9 and 3.10
end while
```

3.2.3.3 Differential Evolution(DE)

The differential evolution (DE) algorithm is based on an evolutionary approach introduced by (Storn & Price, 1997). DE is useful for non-differentiable, nonlinear, discontinuous functions, and have many local minima. Several new differential evolution methods were introduced over the past decade (Eltaeib & Mahmood, 2018). Recent studies (An, Kang, Kim & Song, 2019;

An *et al.*, 2020; Yang *et al.*, 2019) have elevated the DE, making it a top-ranked optimization technique. The differential mutation strategy of DE distinguishes it from other evolutionary techniques; the technique applies to all individuals and explores the space based on other individual solutions. The selection method and control parameters are the two main factors that enhance the performance of DE. The DE strategy consists of mutation, crossover and selection operators that are used for each iteration to find the global optimum. The population size, scaling factor and the crossover rate are the control parameter components used in DE. Various studies have aimed to improve DE by introducing some variations in the mutation or crossover parameters (Yagiz, Yazitova & Karahan, 2020). The main steps of DE are presented in the flow chart in Fig.3.4(c). Initially a population set is created randomly, and then three random vectors are sampled to generate the mutant vector by equation

$$M_j^k = x_j^1 + F * (x_j^2 - x_j^3) \tag{3.11}$$

Subsequently, the crossover in equation 3.11 is selected as a trial vector; either a mutant vector or a parent vector based on the crossover rate.

$$U_j^k = \begin{cases} M_j^k, if rand(0,1) \leq C_r \\ x_j, otherwise \end{cases} \tag{3.12}$$

In the selection process, the parent value is replaced by the trial vector if the fitness value for the trial vector is less than the fitness value of the parent vector. The mutation, crossover and selection processes, followed by the random initialization of the DE population, are repeated until the termination criteria are met. This method includes several parameters, which must be tuned to ensure it performs well. The control parameters' crossover and scaling factor are assigned the values of 0.7 and 0.6 in this study, which uses the trial and error approach. The Pseudo code is summarized as follows:

Algorithm 3.3 An algorithm of DE

```
Randomly initialize the population
Evaluate the fitness function
while Termination is not met do
    Select any three random vectors from the population
    Determine the mutant vector by Eq.3.11 and 3.12 Evaluate the fitness values
    If the parents' fitness value is less than the individual fitness
    Replace the parent vector with the individual in the next iteration
end while
```

3.3 Application to a rockfill dam

A rockfill dam called Romaine-2 (Smith, 2015; Vannobel *et al.*, 2013) was selected as a case study to demonstrate the application of the surrogate model-based inverse analysis. A 2D cross-section of the Romaine-2 dam is illustrated in Fig.3.5. The dam is built on a rock foundation of 112 meters and has an asphaltic core. The core is surrounded by crushed stones with a maximum size of 80 mm, which serve as its support. The transition region (N) adjoins the support zone (M), comprised of crushed stones with a maximum size of 200 mm. In addition, particles with a maximum length of 600 mm are used in the inner shell region (O), and the outer area (P) is composed of rocks with a maximum size of 1200 mm.

Two vertical inclinometers named INV1 and INV2 are located at two different positions in Fig.3.5(a) to measure the horizontal displacements, and inclinometers INH1 and INH2 are installed horizontally on another cross-section to measure the vertical displacements, as shown in Fig.3.5(b). The Plaxis code (Plaxis, 2017) is utilized to build the 2D finite element models, in tandem with the plane strain hypothesis. A two-dimensional mesh of triangular elements with 15 nodes is considered for both cross-sections. The different soil sub-domains are meshed accordingly, and more refinement is used around the asphaltic core. A mesh convergence study (Akbari Hamed, 2017) shows that this mesh is fine enough for these objectives. The dam was strongly compressed during construction (Smith, 2015), so the Mohr-Coulomb (MC) constitutive law is used to simplify the study. Previous numerical studies (Akbari Hamed, 2017)

have shown that the discrepancies between the MC results and the results obtained with the hardening soil model (Schanz *et al.*, 1999) are not significant. Different zones of the dam are highlighted by letters (O, P, N, and M). Two different cases are discussed in this study: case 1 considers five uncertain parameters (cohesion(C), specific weight (ρ), shear modulus (G_{ref}), Poisson coefficient (ν), and friction angle (ϕ)) for the subdomain P of the dam, while case 2 contains twelve uncertain soil parameters (the specific weight (ρ_P, ρ_N, ρ_O), shear modulus ($G_{ref,P}, G_{ref,N}, G_{ref,O}$), Poisson coefficient ($\nu_P, \nu_N, \nu_O$), and friction angle ($\phi_P, \phi_N, \phi_O$)) of subdomains P, N and O. The samples of input parameters are generated by Sobol's sampling method (Dige & Diwekar, 2018). Subsequently, the soil parameters are assigned to the numerical model, and the computed displacements are extracted for each inclinometer. Once the data set of inputs and their corresponding outputs are produced, the deep neural network methodology is used to build the surrogate model for each case (Goodfellow *et al.*, 2016; Kang *et al.*, 2022). After establishing the response surface, the multi objective optimization techniques are applied in order to get the optimal parameters.

3.3.1 Case I

Only the parameter variations in zone P are considered in this case since this domain covers the maximum portion of the dam. Based on the convergence study in (Shahzadi & Soulaïmani, 2021), a data set of 300 samples is used to build the surrogate models. The parameter estimates in Table.3.1 are based on a previous study conducted in (Smith, 2015), (Akbari Hamed, 2017). The input vector is $x_D^{(i)} = (C^{(i)}, \rho^{(i)}, G_{ref}^{(i)}, \nu^{(i)}, \phi^{(i)})^T$, for a sample (i). The parameters are assumed to follow a uniform distribution. The dilatancy angle is set relative to the friction angle as $\psi = \phi - 30$ (in degrees). The numerical displacement fields are obtained by running Plaxis (Plaxis, 2017). Next, the displacements are extracted at a number of points on each inclinometer, yielding a response vector $Y_D^{(i)}$ of dimension $m = 128$. Consequently, a DNN model was established using a data set of 300 input parameters and their corresponding displacements. Moreover, several models were built to increase the response surface's reliability by initializing

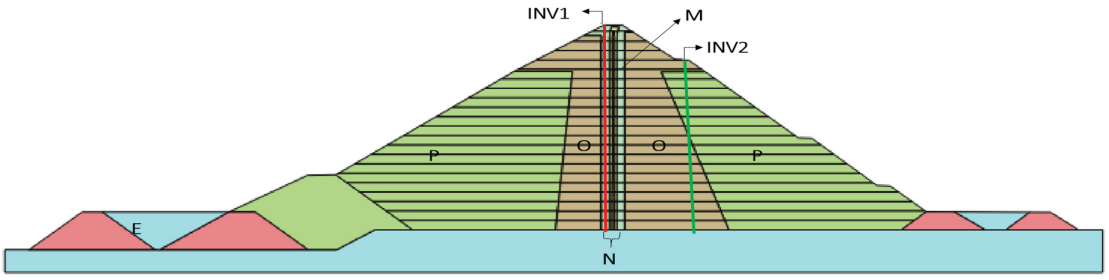

a) Cross-section of the Romaine-2 dam. Different zones of the dam are highlighted in alphabets. The vertical inclinometers are denoted by INV1 and INV2

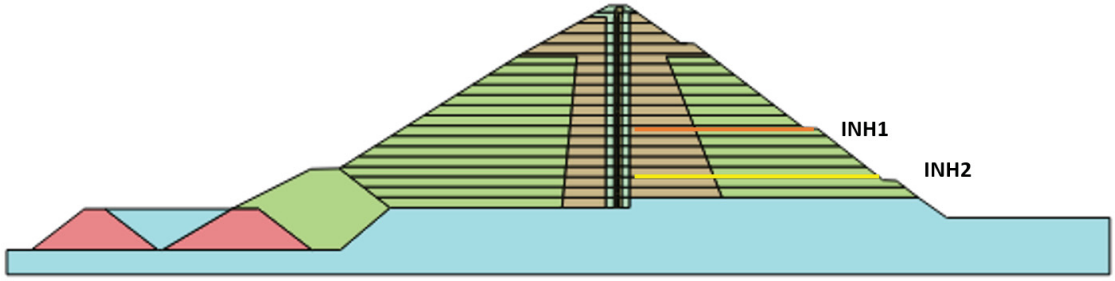

b) Cross-section of the Romaine-2 dam. The horizontal inclinometers are denoted by INH1 and INH2

Figure 3.5 Romaine-2 dam

Table 3.1 Soil parameter values or intervals of variations for zones P, N, O, and M

Soil parameters	**Units**	**P**		**N**	**O**	**M**
		LB	**UB**			
Cohesion (C)	KNm^{-2}	10^{-3}	0	0	0	0
Specific weights (ρ)	KNm^{-3}	21.375	23.625	23.7	22.5	24.5
Shear modulus (G_ref)	KNm^{-2}	25000	35000	64000	45000	110000
Poisson coefficient (ν)	$--$	0.234	0.3465	0.33	0.22	0.33
Friction angle (ϕ)	$degree$	40.85	45.15	47	45	47

different weights. The performance of the DNN model is presented in Fig.3.6, showing almost zero fitness variation with respect to the training iterations (epochs).

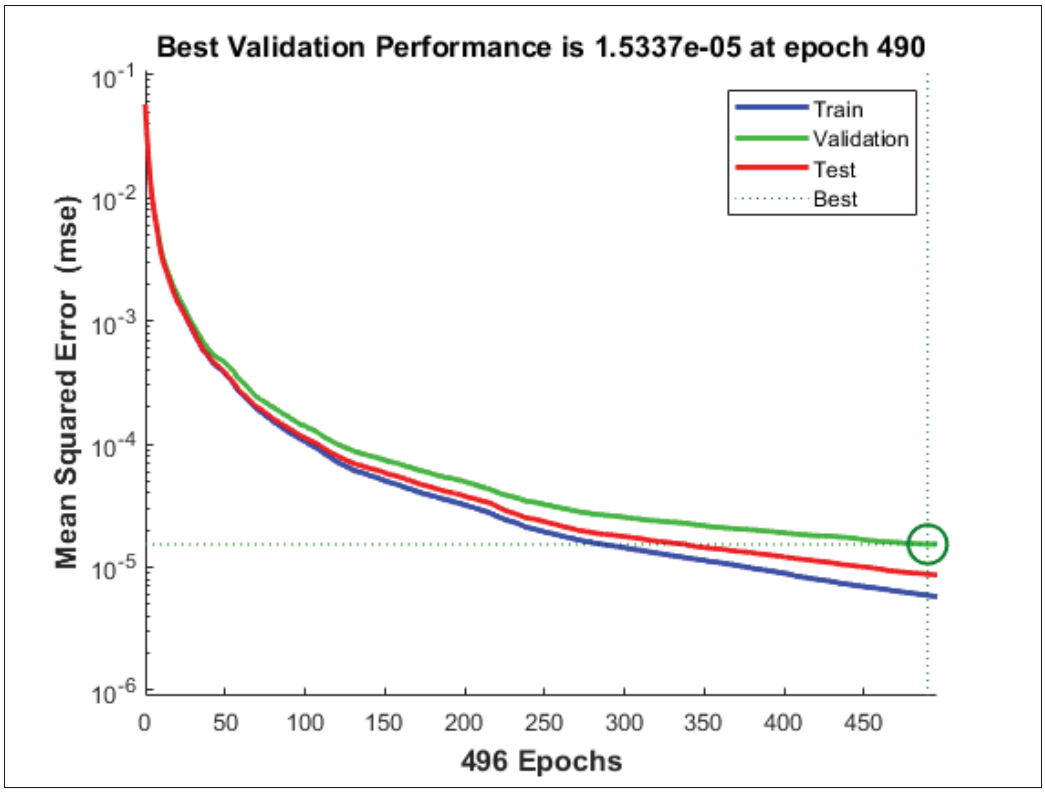

Figure 3.6 The performance of DNN

3.3.1.1 Results and discussion

Inverse analysis was performed for the Romaine-2 dam using the data measured by inclinometers INV1, INV2, INH1 and INH2 installed in two different cross-sections as shown in Fig.3.5(a) and Fig.3.5(b). The confidence intervals for the displacements (mean ±2 standard deviation), obtained by using classical statistical analysis (a Monte Carlo simulation (MCS)) are represented in Fig.3.7 and Fig.3.8. The behaviours of the numerical horizontal displacements and the measured values in Fig.3.7 are similar, with the measured data showing large fluctuations. This may be due to external effects such as the installation process, calibration, temperature changes, and human factors, which may have affected some probes on the inclinometers. Nevertheless, Fig.3.7 and Fig.3.8 show that considering their uncertainties, the measured data for all inclinometers are mostly within the predicted numerical confidence intervals. An inverse analysis is then used to identify the optimal physical parameters. The PSO, GA, and DE algorithms are used to minimize

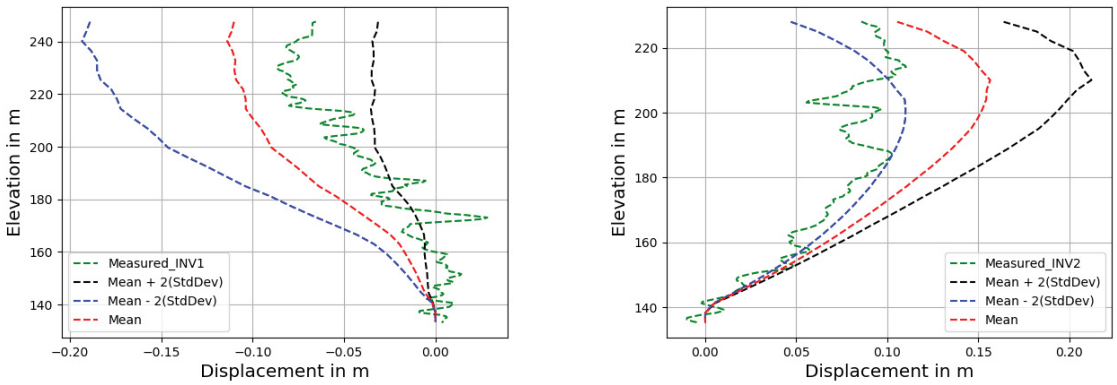

a) Horizontal displacements for INV1 b) Horizontal displacements for INV2

Figure 3.7 Confidence intervals for numerical horizontal displacements of vertical inclinometers

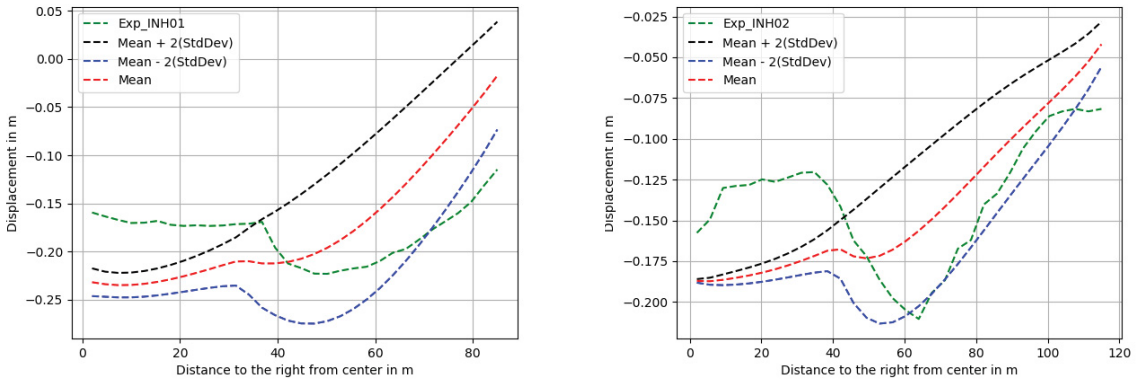

a) Vertical displacements for INH1 b) Vertical displacements for INH2

Figure 3.8 Confidence intervals of numerical vertical displacements for horizontal inclinometers

the objective function described by Eq.3.6. By employing the surrogate model, this analysis allows computing the numerical displacements rapidly. Initially, a trial and error approach was performed to estimate the parameters for each algorithm. The population size and the number of iterations were varied to analyze the convergence. Once determined, the population size and

iteration counts were set to 100 for all the selected techniques. The crossover and mutation probabilities for GA and DE were set at 0.6 and 0.1, respectively, while for PSO, the learning factors $c1$ and $c2$ were assumed as 2. The argument here is to have an iteration count in all techniques, beyond which there is no significant improvement in convergence and a population that achieves this goal without compromising performance or accuracy. Since these algorithms are essentially stochastic, the computer codes were executed several times for each algorithm (using an Intel-i7 processor compute machine with 32 GB RAM) to ascertain that there was not a significant deviation in the results. The obtained optimal parameters and the time elapsed for each algorithm are summarized in Table.3.2. It is clear that the PSO converges to the minimum fitness in less time than the GA and DE. Moreover, the optimal parameter values obtained are almost the same for all three algorithms, leading to similar predicted displacements for the deep neural network surrogate model, as shown in Fig. 3.9. Overall, all the results demonstrate that the PSO algorithm performs the best in identifying the parameters.

Table 3.2 Optimal parameters and minimum fitness values obtained using different optimization algorithms and the deep neural network surrogate model

Parameters	C	ρ	G_{ref}	ν	ϕ	**Fitness Value**	**time elapsed**
Units	KNm^{-2}	KNm^{-3}	KNm^{-2}	$--$	$degree$	m^2	seconds
GA	$6.3E{-}09$	22.06	$3.07E{+}04$	0.33	45.14	$5.89E{-}05$	446
DE	$5.5E{-}07$	22.03	$3.05E{+}04$	0.33	45.14	$5.83E{-}05$	1572
PSO	$4.6E{-}08$	21.8	$3.02E{+}04$	0.33	44.09	$5.85E{-}05$	191

3.3.2 Case II

The motivation for the present analysis is to increase the accuracy by considering parameter variations in zones P, N, and O. Sobol's sampling technique is used to build a data set D of the soil parameters (the specific weight (ρ), shear modulus (G_{ref}), Poisson coefficient (ν), and the friction angle (ϕ)) for each sub-domain P, N and O. The size of the data set is 1508 for 12 physical parameters; each parameter has a value within the interval specified in Table. 3.3. Each sample of inputs $x_D^{(i)}$ is assigned to Plaxis to obtain the geomechanical displacements. The

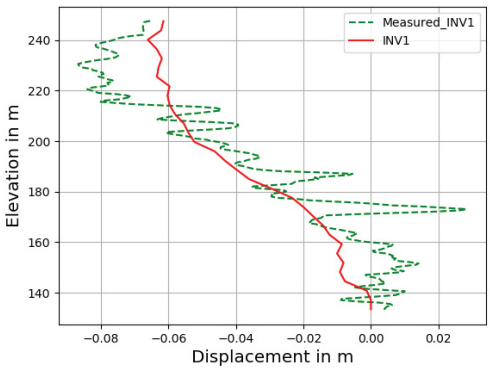

a) Plots of measured and predicted displacements for optimal values (INV1)

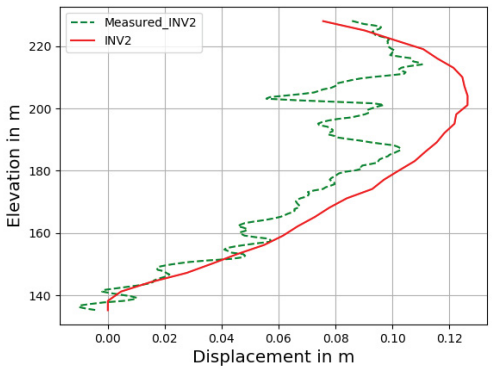

b) Plots of measured and predicted displacements for optimal values (INV2)

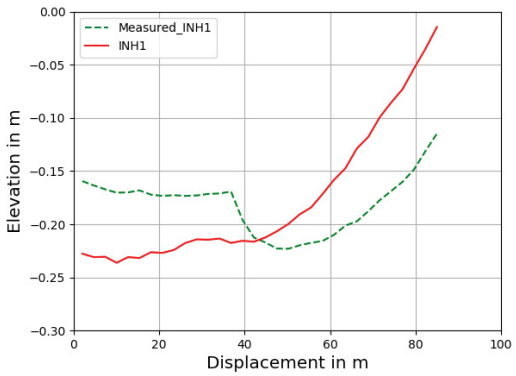

c) Plots of measured and predicted displacements for optimal values (INH1)

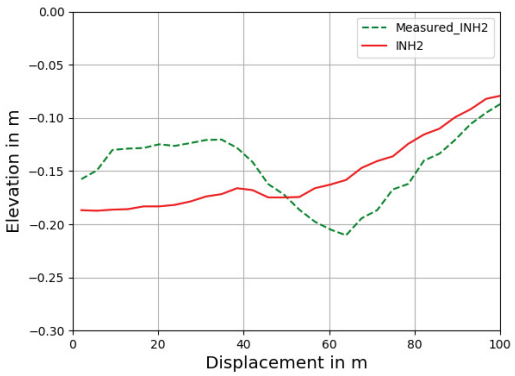

d) Plots of measured and predicted displacements for optimal values (INH2)

Figure 3.9 Displacements measured and predicted by surrogate models for optimal parameter values are displayed by dotted and solid lines, respectively

displacements along the measurement lines (32 points in this case) are then extracted, yielding a response vector $Y_D^{(i)}$ of dimension $m = 128$. A DNN model is created for the date set of 1508 input vectors and the corresponding displacements of each inclinometer. The data set was split into training, validation, and testing subsets. The best validation performance of DNN model is presented in Fig.3.10, showing the convergence of the error function with respect to the training iterations (epochs). The random initialization of weights trained ten different networks, and the outputs were predicted for each network. Next, the mean and standard deviation are

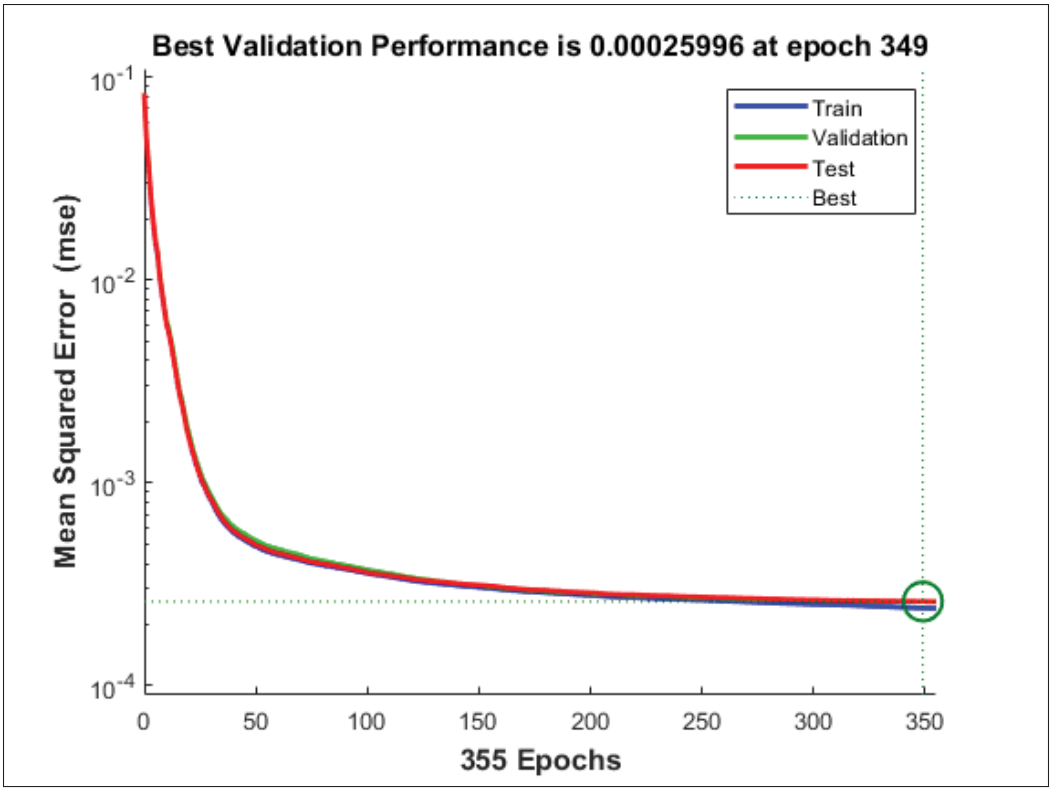

Figure 3.10 The performance of DNN

calculated by employing a simple Monte Carlo method on the ensemble neural network model. The mean and variance for the ensemble model are computed by Eq.3.3 and Eq.3.4. Finally, the soil parameters are identified by minimizing the difference between the measured and the numerically simulated displacements for each inclinometer.

Table 3.3 Soil parameter values or intervals of variations for zones P, N, O, and M

Soil parameters	**Units**	**P**		**N**		**O**		**M**
		LB	**UB**	**LB**	**UB**	**LB**	**UB**	
Specific weights	KNm^{-3}	21.375	23.625	22.51	24.88	21.37	23.62	24.5
Shear modulus	KNm^{-2}	25000	35000	55000	74000	39000	52000	11000
Poisson coefficient	$--$	0.234	0.3465	0.212	0.345	0.227	0.253	0.33
Friction angle	$degree$	40.85	45.15	44.65	49.35	42.75	47.25	47

3.3.2.1 Results and discussion

For uncertainty analysis, the confidence intervals (mean±2 standard deviation) are obtained using the surrogate model and shown in Fig.3.11 for inclinometers INV1 and INV2, and the results for horizontal inclinometers INH1 and INH2 are represented in Fig.3.12. While Fig.3.11 shows that the confidence intervals for the displacements measured on INV1 and INV2 are quantitatively reasonable, the measured and the predicted numerical displacements in Fig.3.12 are not in good agreement. This could be attributed to the FEM modelling or various factors affecting the measurement accuracy, such as changes in temperature, the inclinometers' installation process, etc. The soil parameters are calibrated by minimizing the multi-objective function. The

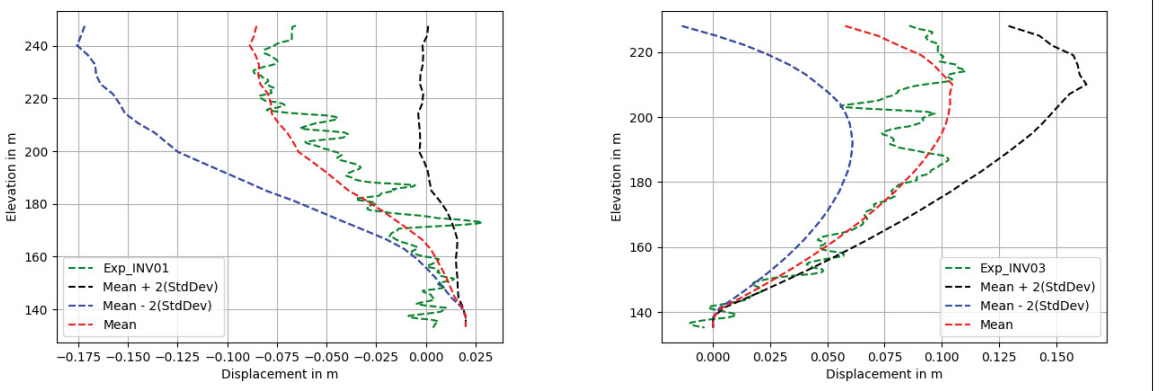

a) Horizontal displacements for INV1

b) Horizontal displacements for INV2

Figure 3.11 Confidence intervals of numerical horizontal displacements for vertical inclinometers

population size and iteration count are set at 100 for all selected techniques. The crossover and mutation probabilities for GA and DE were set at 0.6 and 0.1, respectively; and for PSO, the learning factors $c1$ and $c2$ were assumed as 2. The search domains in all three algorithms are presented in Table. 3.3. Each non-deterministic optimization algorithm was then executed approximately ten times to get convergence. The optimal parameters and time elapsed for each algorithm are presented in Tab.3.4.

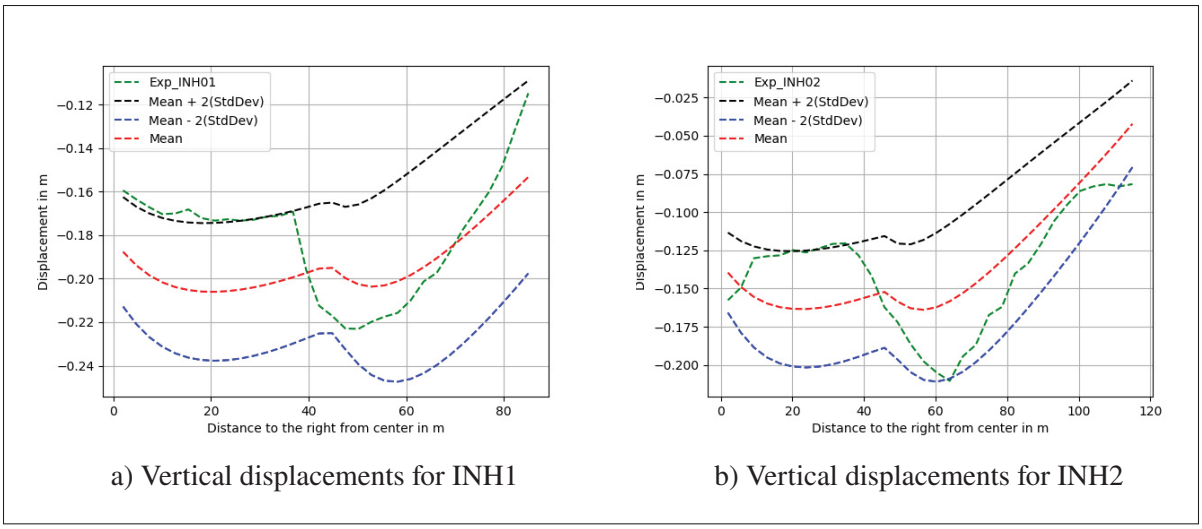

a) Vertical displacements for INH1 b) Vertical displacements for INH2

Figure 3.12 Confidence intervals of numerical vertical displacements for horizontal inclinometers

Table 3.4 Optimal parameters and minimum fitness values obtained using different optimization algorithms and the deep neural network surrogate model

Soil Parameters	**Optimization Techniques**		
Sub-domains P,N and O	GA	PSO	DE
ρ(P)	23.08	22.98	23.12
G_{ref}(P)	2.9484E+04	2.8962E+04	2.886E+04
ν(P)	0.32	0.32	0.32
ϕ(P)	42.60	42.30	41.90
ρ(N)	22.61	23.18	23.23
G_{ref}(N)	6.262E+04	6.14482E+04	6.1941E+04
ν(N)	0.27	0.28	0.27
ϕ(N)	49.22	48.98	49.14
ρ(O)	22.13	22.30	22.62
G_{ref}(O)	4.7899E+04	4.6742E+04	4.7171E+04
ν(O)	0.23	0.243	0.22
ϕ(O)	46.32	45.74	46.75
Fitness value	5.66E-05	4.9155E-05	4.87.9162E-05
Time elapsed(sec)	2340	669	5489

The results in 3.4 show that the PSO attained the minimum fitness in less time compared to GA and DE. However, more parameters are tuned for PSO compared to the GA and DE, which only

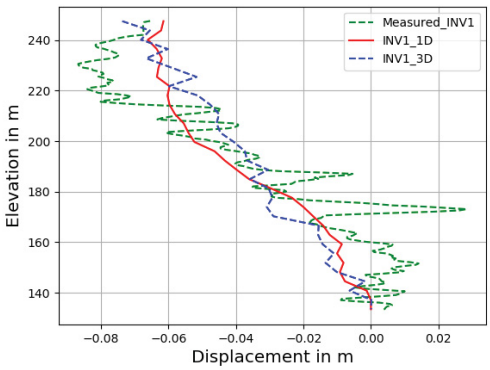

a) Plots of measured and predicted displacements for optimal values (INV1)

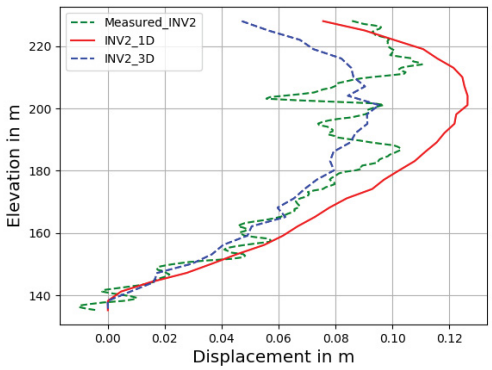

b) Plots of measured and predicted displacements for optimal values (INV2)

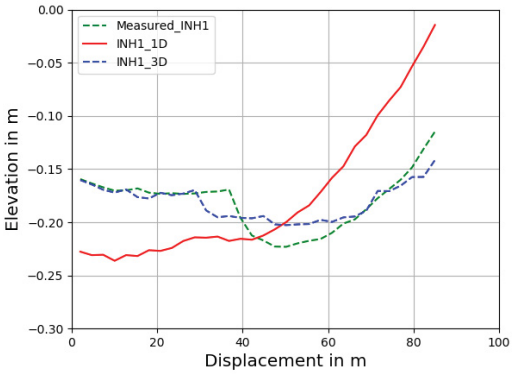

c) Plots of measured and predicted displacements for optimal values (INH1)

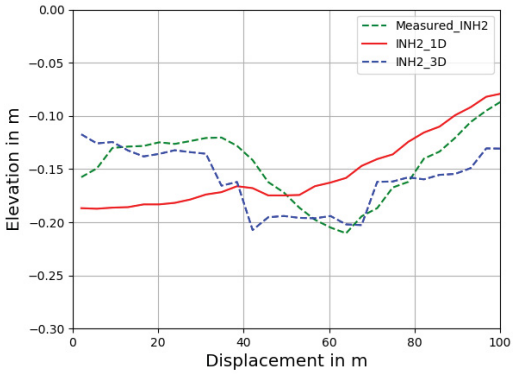

d) Plots of measured and predicted displacements for optimal values (INH2)

Figure 3.13 Displacements measured and predicted for the optimal parameters values are displayed in dotted and solid lines, respectively

have two parameters to adjust. Fig.3.13 presents the measured and predicted displacements of the optimal parameters for both cases (case1: the optimal parameters of subdomain P, denoted by 1D; and case2: the optimal parameters of subdomains P, N and O, signified by 3D). The results of case 2 are in better agreement for all inclinometers, providing better modelling of the dam.

3.4 Conclusion

This paper contributes to the inverse analyses for rockfill dams using the surrogate modelling approach. The approach was applied to identify the physical parameters of an actual rockfill dam with an asphaltic core. Deep neural networks are used in place of the full-scale finite element model to speed up the computations for the optimization process. A comparative study of three non-intrusive optimization algorithms (GA, PSO, and DE) was conducted to identify the constitutive soil parameters. Since the measured displacements show strong fluctuations along the inclinometers, an objective function was developed to smooth out the oscillations and improve the algorithms' convergence. The optimal parameter values obtained by each algorithm were almost identical, leading to similarly predicted displacements for both cases. The PSO algorithm proved to be the most efficient approach in this study. While the measurement data set is not very large, as is usually the case in machine learning studies, the results demonstrate that the combination of deep neural networks and non-deterministic optimization algorithms constitute valuable computational tools in this inverse analysis.

In future work, a comparative study will be done by considering the Hardening Soil model, as the present study was limited to the Mohr-Coulomb model.

CHAPTER 4

IDENTIFICATION OF CONSTITUTIVE SOIL PARAMETERS USING MULTI-OBJECTIVE OPTIMIZATION WITH DEEP NEURAL NETWORKS: APPLICATION TO A ROCKFILL DAM

Gullnaz Shahzadi[1] , Azzeddine Soulaïmani[1]

[1] Department of Mechanical Engineering, Ecole de Technologie Supérieure, 1100 Notre-Dame W., Montreal (QC), Canada H3C 1K3

This article has been Submitted in:
Structures (Elsevier), on 17 April 2023

Abstract

The inherent uncertainty of the material properties of rockfill dams makes computational predictions of their structural behaviour particularly challenging. Inverse analysis may be a practical solution for such problems. This paper presents a surrogate-assisted multi-objective hybrid optimization approach, a novel parameter identification technique that can help to improve safety and stability analyses. First, a deep neural network (DNN) surrogate model that reflects a nonlinear mapping between the displacements of a dam and the soil parameters is established. Second, a multi-objective function is framed as a weighted norm of the difference between the predicted and the measured displacements. Next, a hybrid Particle Swarm-Genetic Algorithm (PSOGA) is applied to the surrogate model proposed to identify the soil parameters; the PSOGA combines the benefit of the lower computational expense of surrogate models and the prompt convergence of search algorithms. The methodology is applied to a recently built rockfill dam (Romaine-2) in Quebec, Canada. In two different cross-sections of the dam, four inclinometers were installed vertically and horizontally in different locations to simultaneously collect measured data. A comparative study of constitutive soil models, the Mohr-Coulomb (MC) and Hardening Soil (HS) model, is also conducted. It is found that the MC model displacement predictions do not match the actual displacements. In contrast, the HS model analysis results are the closest displacements to the values measured onsite. Finally, this research presents the optimal set of

parameters of the Romaine-2 dam assessed by the proposed analysis and offers insight into the performance of DNNs and hybrid optimization to solve inverse problems.

keywords

Mohr-Coulomb (MC), Hardening soil models (HS), Deep learning, Inverse analysis, Hybrid Optimization techniques, Rockfill dams

4.1 Introduction

As one type of high dam, rockfill dams are characterized by the fact that they have low technical requirements, low construction costs, limited environmental effects, and the ability to self-operate. However, dams undergo various structural and material changes throughout their lifetimes, significantly impacting their performance. Based on the nature and position of the watertight element, rockfill dams can be divided into two main types: (i) those containing relatively impervious earth cores, either thick or thin; and (ii) those with concrete or asphalt cores. In cases where suitable soil is unavailable, asphalt or concrete cores can be utilized. Asphalt cores are generally narrow and almost one-meter wide (Asthana & Khare, 2022; Höeg, 1993). It is well known that deformation can occur in rockfill dams during construction and due to reservoir impoundment. Therefore, several techniques have been applied to control dam deformation, such as structure design, foundation treatment, and material properties (Han, Jiankang, Shengwei, Yazi & Beijia, 2016). However, the inherent uncertainties in the material properties used in their complex structure make the design of rockfill dams a challenging task (Akbari Hamed, 2017). To ensure the safety of dam operation, it is crucial to estimate soil parameters correctly. Parameter identification is thus vital in the design stage for monitoring structural health and damage detection in rockfill dams(Wang, Höeg & Zhang, 2010; Pramthawee *et al.*, 2011).

Parameter identification in rockfill dams is particularly complicated, as different rock sizes are used in their construction, with aggregates collected from various sources. In addition, the rate of aging or deterioration varies at other dam locations due to external effects, such as

temperature, stress state, humidity, etc. These factors lead to non-uniform conditions, resulting in nonhomogeneous structures in which the material properties cannot be quantified or exemplified correctly with limited samples. Identifying unknown parameters in a numerical dam model is a relatively cost-effective method for solving this problem. An adequate approach to designing a numerical model would be an effective solution for parameter identification.

The finite element method (FEM), combined with the appropriate soil constitutive laws, is widely used to deal with nonlinear and complex dam structures. The FEM is already considered the most powerful approach for dam modelling and design (Pietruszczak, 2010; Amouzou & Soulaïmani, 2021). Several finite element software approaches exist for geotechnical numerical modelling, such as Plaxis (Plaxis, 2017) and Zsoil (Obrzud, Truty, Podles, Commend & Zimmermann, 2018), which offer a library of different constitutive models that can be utilized for various soils. Starting from the linear elastic model, several advanced constitutive models are implemented. Using a constitutive model suitable for a specific soil type and a set of loading conditions depends on the availability of experimental data. The Mohr-Coulomb (MC) is one of the simplest constitutive soil model that incorporates the nonlinear plastic deformation of rocks and is commonly operated in geotechnical structures (Labuz & Zang, 2012). In spite of this, it is widely known that the hardening soil (HS) constitutive model has overcome many of the issues associated with the MC soil model (Pietruszczak, 2010). Bhutto et al. (Bhutto *et al.*, 2019) predicted the settlement of an embankment dam using the Mohr-Coulomb and Hardening Soil Model. Also, Kim et al. (Kim & Jung, 2022) employed the Mohr-Coulomb (MC), hardening soil (HS), and hardening soil with small strains (HSS) models for the inverse analysis of deep excavation and compared the responses of each model.

A numerical analysis is carried out to conduct the simulations using both constitutive soil models, Mohr-Coulomb (MC) and Hardening Soil (HS) of a rockfill dam. Regardless, formulating a finite element model requires simplifying the physical model. Moreover, the lack of information on soil properties and external factors, such as climate conditions, limits any constitutive model from accurately representing dam behaviour. In such cases, the inverse analysis can help estimate

the most reliable and relevant parameters when some measurements are available, thereby improving the design or monitoring of the considered dam (Yin *et al.*, 2018; Xu & Wu, 2022).

Inverse analyses have been used for decades to solve geotechnical problems (Hashash *et al.*, 2010a; Hashemi & Rahmani, 2018; Vahdati *et al.*, 2014; Levasseur *et al.*, 2010). The inverse analysis involves two main components: an optimization algorithm that minimizes the error function (a norm of the difference between the numerical solutions and the measurements) and a numerical solver. It is very challenging to find global minima using classical gradient-based algorithms if a function is highly irregular. Therefore, many stochastic optimization techniques such as the Genetic algorithm (GA) (Deng-gang *et al.*, 2000), Particle swarm optimization (PSO) (Kennedy & Eberhart, 1995), the Differential evolutionary method (DE), the gravitational search algorithm and their modified forms are widely used in inverse problems (Vahdati *et al.*, 2013; Levasseur *et al.*, 2008). Su et al. (Su, Li & Wu, 2007) calibrated the soil parameters of a dam and its foundation using the genetic simulated annealing optimization technique, and the results confirmed the robustness and efficiency of the method. Bao et al. (Bao *et al.*, 2020) implemented a multi-output least-squares SVR machine incorporated with an upgraded differential evolution algorithm to evaluate several parameters of the Jinping-I arch dam. Four different methods were compared, and the proposed algorithm outperformed them all. Displacement inverse analysis is widely used in geotechnics to verify and identify structural parameters (Sharifzadeh, Tarifard & Moridi, 2013; Lin *et al.*, 2020). Das and Soulaimani (Das & Soulaimani, 2021) proposed a methodology to identify the parameters of the Mohr-coulomb constitutive soil model for a rockfill dam based on a polynomial regression model coupled with optimization techniques (GA, PSO and DE). In comparing particle swarm optimization and genetic algorithms, Kang et al. (Kang, Wu, Li & Li, 2021) presented a methodology based on the Kriging and Jaya algorithm for the rapid identification of the dynamic parameters of concrete dams. Kang et al. (Kang *et al.*, 2022) developed an accelerated Jaya algorithm that minimizes the objective function of dam material using a kernel extreme learning machine. Song et al. (Song, Liu, Jiang & Yao, 2022) identified the soil parameters of a constitutive model using the crossover real coded genetic

algorithm (RCGA) coupled with machine learning. The accuracy of their proposed algorithm is proven by comparing the optimal parameters with the real laboratory clay parameters.

Optimization algorithms are iterative processes that find optimal parameters where the numerical model requires access more often. Such a crude operation is intricate for nonlinear and large-scale structures such as rockfill dams. Therefore, a classical optimization algorithm may be inefficient if the high-fidelity numerical finite element model is time-consuming. In addition, while PSO is efficient in convergence, its population diversity decreases too quickly during searching, which, coupled with its inability to perform global searches, results in premature convergence and poor accuracy. The GA has a strong ability to perform global searches and cross-mutations, but its local search ability is weak, which causes low efficiency. To avoid these shortcomings, a hybrid optimization technique, the PSOGA, is utilized in this study, which combines the advantages of both algorithms and yields efficiency and effectiveness in its results. (Shi, Gong & Zhai, 2022; Li, Zhang, Xu & Zhong, 2019).

Surrogate modelling helps to reduce computational costs by replacing the FEM model with an inexpensive surrogate model. Surrogate models can therefore play an essential role in enhancing the efficiency if trained, tested and appropriately validated according to the model's dataset. Several methods have been developed to build surrogate models, such as Kriging (Gaussian process regression), polynomial chaos expansion (PCE), support vector regression (SVR) and deep learning(Shahzadi & Soulaïmani, 2021; Song *et al.*, 2022; Li, Hariri-Ardebili, Deng, Wei & Cao, 2023). Sun et al. (Sun, Jiang, Yin & Zhou, 2018) established the mapping between the soil parameters and the displacements through an artificial neural network to reduce the time consumption of FEM. Yang, Mei and Gange (Yang & Mei, 2022) proposed a physics-informed neural network-based deep learning approach for a numerical investigation of soil–water vertical infiltration and evaluated soil–water infiltration in different soil types. Shahzadi and Soulaimani (Shahzadi & Soulaïmani, 2021) built and compared deep neural network (DNN) and polynomial chaos expansion (PCE) based surrogate models. Their results proved that deep neural network-based surrogate models are more efficient and accurate than PCE-based models in representing nonlinear mappings (between input and output parameters).

This paper describes a deep neural network-based hybrid optimization approach for inverse analysis. A deep neural network with several hidden layers is used to build a surrogate model of a dam. A multi-objective function for the displacements of vertical and horizontal inclinometers is incorporated into a single error function using the weighted sum method (Gunantara, 2018). A hybrid particle swarm optimization-genetic algorithm (HPSOGA) is utilized to obtain the optimal soil parameters by minimizing the objective function. The methodology is applied to the Romaine-2 rockfill dam built in Quebec, (Smith, 2015), for which the displacements are measured on two vertical and two horizontal inclinometers installed in different locations. The Romaine-2 dam comprises five different material zones and is the tallest asphalt core structure in North, Central or South America. To build a surrogate model, a dataset of high-fidelity solutions is obtained using a finite element plane strain model of two cross sections where measurements were taken.

This paper is organized as follows: the next section presents the problem description and the methodology, including constitutive soil models, finite element modelling, surrogate modelling, cost function formulation, and a brief presentation of optimization algorithms. The uncertainty and optimal results for the MC and HS constitutive models are then compared and discussed in the third section. A promising avenue to expand this approach is presented as part of the conclusion.

4.2 Methodology

A rockfill dam called Romaine-2(Smith, 2015; Vannobel *et al.*, 2013) was chosen as a case study to demonstrate the application of the surrogate model-based inverse analysis. The cross-section of the Romaine-2 dam is illustrated in Fig.4.1. The dam, 112 meters in height, is built on a rock foundation with an asphalt core. A crushed stone layer with a maximum size of 80 mm surrounds the asphalt core, which serves as support. The transition region (N) adjoins the support zone (M), comprised of crushed stones nearly 200 mm in diameter. The inner shell region (O) contains particles that are 600 mm long, and the outer area (P) is formed of rocks of mixed sizes, up to 1200 mm in diameter.

The parameter identification process is composed of four steps: 1) finite element modelling and simulations to obtain a high-fidelity dataset of solutions; 2) construction of a surrogate model to predict the numerical displacements for the unseen values of input parameters; 3) the formulation of a multi-objective function, which measures the difference between the measured and the predicted results; and 4) the use of a hybrid optimization algorithm to identify the parameters by minimizing the objective function. Fig.4.2 illustrates the flow chart of the methodology.

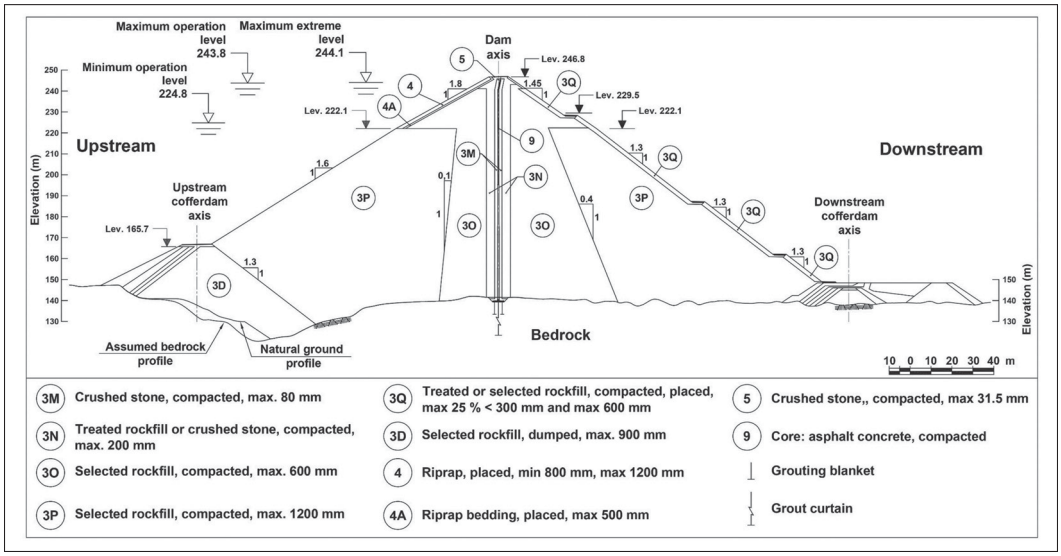

Figure 4.1 Cross section of Romaine-2 dam, taken from Lashin *et al.* (2022, p. 717)

4.2.1 Constitutive soil models

The choice of the structural model and soil parameters will significantly affect the analyzed results. The finite element method (FEM) can deal with nonlinear and complex geometries and offers high accuracy in solving governing equations. FEM-based software, including GTS, Zsoil, Flac and Plaxis, offer various constitutive models to simulate soil behaviour (Zukri & Nazir, 2018). It should be noted that each software platform differs in its abilities and limitations, so the user should be aware of their possible impact on the accuracy of the investigation. The following

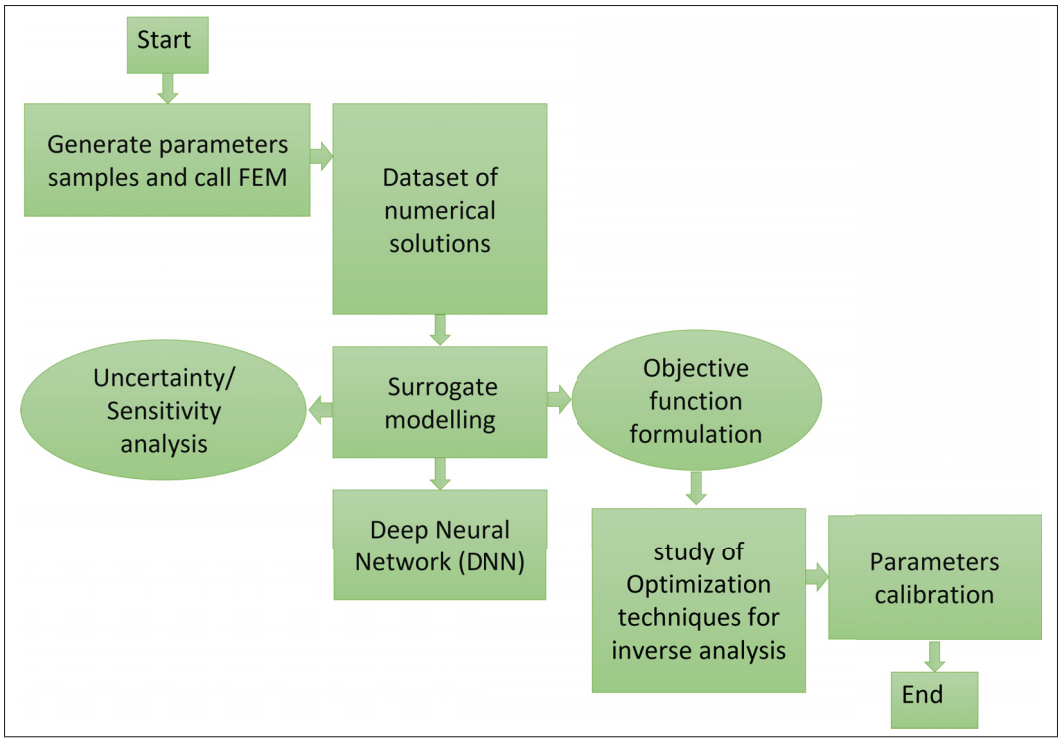

Figure 4.2 The flowchart of the proposed methodology

sections briefly describe two constitutive soil models, Mohr-Coulomb (MC) and Hardening soil (HS).

4.2.1.1 Mohr-Coulomb (MC) model

The Mohr-Coulomb model is a common and simple linear elastic perfectly plastic constitutive soil model in geotechnics (Owen & Hinton, 1980), (Pietruszczak, 2010). As soon as the linear elastic deformation reaches a certain point, Mohr-Coulomb's failure criteria predict the failure of the system. After the breaking point, the stress level remains unchanged since the deformation is assumed to be perfectly plastic. The input (soil) parameters for an MC model are the cohesion (C), shear modulus (G_{ref}), specific weight (ρ), Poisson coefficient (ν), and friction angle (ϕ). The shear modulus (G_{ref}) and Poisson coefficient (ν) parameters are related to Hook's law, whereas the friction angle (ϕ) and cohesion(C) are related to the Mohr-Coulomb criterion.

4.2.1.2 Hardening Soil (HS) model

The hardening soil model is an effective stress model developed within the elastoplasticity framework (Schanz *et al.*, 1999). It is an advanced model that differs from the MC model in several features, chiefly in its consideration of a hyperbolic stress-strain relationship (Duncan, 1996), the use of plasticity related to two types of isotropic hardening, and the implication of the unloading/reloading relationship assumed to be elastic. Two expandable yield surfaces are used to calculate the plastic strains. The plastic strains are included as three additional parameters called the stiffness moduli (E_{50}^{ref}, E_{ur}^{ref} and E_{oed}^{ref}), used in this model at a reference pressure of 100 KPa. Stiffness moduli E_{50} and E_{oed} control the plastic part of the model, which hyperbolically rely on stress by means of a power law. The types of hardening, cap-hardening (compression hardening) and cone-hardening (strain hardening) describe the plastic deformations amassed by primary compression loading and primary deviatoric stress, respectively. In contrast, cone hardness is dominated by E_{50}, and E_{oed} dominates the rigour of the course. As with the Mohr-Coulomb soil model, the failure surfaces are decided by the MC theory; the failure surfaces presented in the HS model respect these constraints. In this work, for the inverse analysis, E_{50}^{ref} is considered an imperative variable of the HS model, the parameters E_{ur}^{ref} and E_{oed}^{ref} are assumed to be in proportion to E_{50}^{ref}, as given by

$$E_{ur}^{ref} = 3 * E_{50}^{ref} \tag{4.1}$$

and

$$E_{oed}^{ref} = 0.8 * E_{50}^{ref} \tag{4.2}$$

Although these parameters should be mutually independent, the investigations in (Plaxis, 2017) found that E_{ur}^{ref} is three times the value of E_{50}^{ref}, and E_{oed}^{ref} is almost linearly proportional to E_{50}^{ref}, as in (4.1) and (4.2), and so these assumptions are adopted.

4.2.2 Finite element modeling and simulation

The finite element software (Plaxis2D) (Plaxis, 2017) is used to numerically solve the governing partial differential equations along with the constitutive relations and boundary conditions. Plaxis3D could be favoured instead of Plaxis 2D to enhance the accuracy (if more data are available), but the efficiency would be diminished to achieve that increased precision. Moreover, the 2D plane strain hypothesis is well-accepted for long structures.

Table 4.1 Mohr-Coulomb (MC) model parameter values and the bounds of variations for different zones.

Soil parameters	**Units**	**P**		**N**		**O**		**M**
		LB	**UB**	**LB**	**UB**	**LB**	**UB**	
Specific weights	KNm^{-3}	21.375	23.625	22.51	24.88	21.37	23.62	24.5
Shear modulus	KNm^{-2}	25000	35000	55000	74000	39000	52000	11000
Poisson coefficient	$--$	0.234	0.3465	0.212	0.345	0.227	0.253	0.33
Friction angle	$degree$	40.85	45.15	44.65	49.35	42.75	47.25	47

The vertical and horizontal inclinometers, named INV1, INV2, INH1 and INH2, are located at the positions indicated in Fig.4.3(a) and Fig.4.3(c) to measure the displacements. Different dam zones are indicated by letters (P, N, O and M). Three subdomains, P, N and O, are considered variation zones. Two meshes, of 2187 and 1891 triangular 15-node elements, are generated for both cross-sections, as illustrated in Fig.4.3(b) and Fig.4.3(d). All the subdomains of the different soils are meshed accordingly, and the surrounding asphalt core is well refined. The mesh convergence study in (Akbari Hamed, 2017) shows that such mesh densities are fine enough.

This study uses and compares the MC and HS constitutive laws. Table 4.1 presents the upper and lower bounds of soil parameters for the Mohr-Coulomb model (the specific weight ρ, shear modulus G_{ref}, Poisson coefficient ν, and friction angle ϕ), while the bounds of the Hardening soil model's parameters (the secant stiffness E_{50}^{ref}, friction angle ϕ, the exponent of the power law m, the specific weight ρ and dilation angle (ψ)) are presented in Table 4.2. The values of soil parameters in Table 4.1 and Table 4.2 are estimated based on the studies conducted in (Smith,

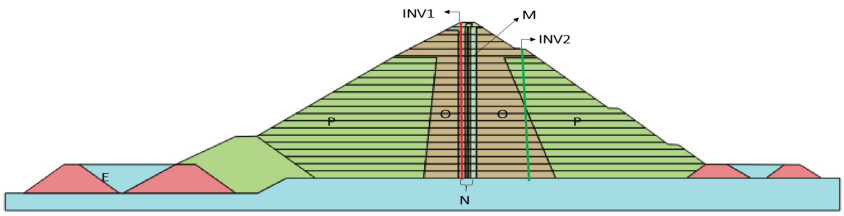

a) Finite element model of the Romaine-2 dam. Different zones of the dam are indicated by a letter code. INV1 and INV2 denote the vertical inclinometers

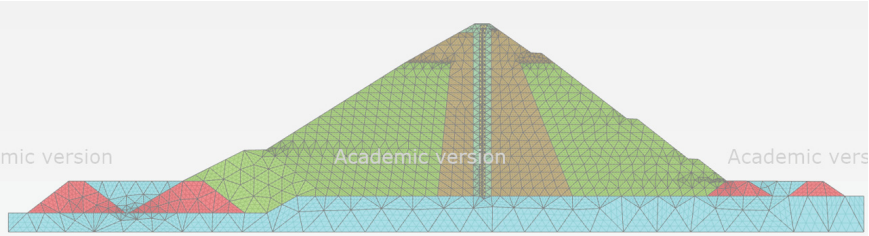

b) Finite element mesh for the cross-section containing vertical inclinometers

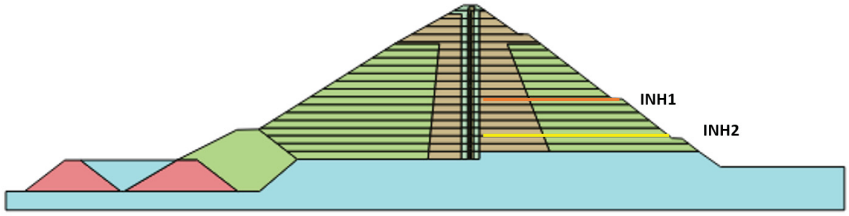

c) Finite element model of the Romaine-2 dam. INH1 and INH2 denote the horizontal inclinometers

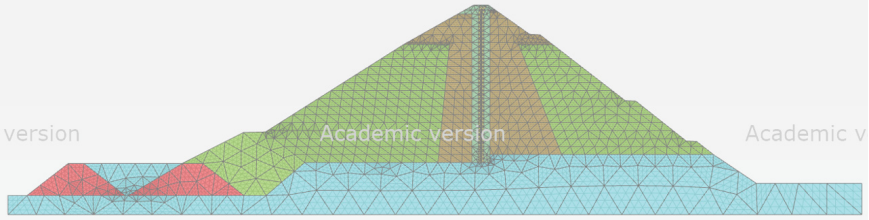

d) Finite element mesh for the cross-section containing horizontal inclinometers

Figure 4.3 Romaine-2 dam

2015; Akbari Hamed, 2017). The datasets are generated using Sobol's sampling algorithm (Joe & Kuo, 2008). The dataset sizes are $N = 1560$ and $N = 1664$ for the soil parameters of the

Table 4.2 Hardening soil (HS) model's soil parameter bounds for the P, N, O, and M zones

Soil	**Units**	**P**		**N**		**O**		**M**
Parameters		**LB**	**UB**	**LB**	**UB**	**LB**	**UB**	
Secant stiffness E_{50}^{ref}	KNm^{-2}	6.8E4	9.2E4	1.445E4	1.955E4	9.35E4	1.265E4	2.8E4
Friction angleϕ	$degree$	40.85	45.15	45.15	49.15	42.85	47.15	47
Power m	$--$	0.35	0.7	0.20	0.26	0.35	0.7	0.18
Specific weightsρ	KNm^{-3}	21.375	23.625	22.55	24.85	21.37	23.63	23.6
dilation angleψ	$degree$	8.5	11.5	12.75	17.25	8.5	11.5	15

MC and HS models, respectively. Based on the convergence study in (Shahzadi & Soulaïmani, 2021), these sizes are considered reliable for building surrogate models. Each soil parameter has a value within a specified interval for both constitutive models.

Next, the soil parameters for both constitutive models are assigned to their corresponding numerical models, and the computed displacements are extracted for each inclinometer. Once the inputs and their corresponding outputs are produced, the deep neural network methodology is used to build the surrogate model for each case (Goodfellow *et al.*, 2016; Kang *et al.*, 2022). After establishing the response surface, a comparative inverse analysis study is performed for both constitutive soil models.

4.2.3 The Deep Neural network (DNN)

In machine learning, neural networks are widely used to solve complex regression and classification problems (Goodfellow *et al.*, 2016; Georgevici & Terblanche, 2019). To more effectively manage information, deep neural network (DNN)-based models consist of multiple interconnected layers that contain several nonlinear neurons. A DNN can capture a complicated input-output relationship without knowing the precise mathematical expressions by extracting

hidden underlying regularity from an array of training samples. Nodes are the building blocks of deep neural networks. A node collects inputs, computes weights, and applies activation functions to generate outputs. There are several layers of nodes; all nodes in one layer are connected to nodes in the next layer, but the nodes in each layer are not interconnected. Deep neural networks learn parameter values during training based on the parametric form of basis functions. The model uses nonlinear activation functions, making it nonlinear. Fig.4.4 illustrates a typical feed-forward neural network model consisting of three layers: an input layer, a hidden layer and an output layer. The response vectors are computed by,

$$y_k = g(\sum_{j=1} W_{kj}^{(0)} h_j^{(1)} + b_k^{(0)}) \tag{4.3}$$

where $h_j^{(1)}$ is a hidden layer (1), which is used to compute the output from the input data, as shown in:

$$h_j^{(1)} = f(\sum_{i=1}^{n} W_{ji}^{(1)} x_i + b_j^{(1)}) \tag{4.4}$$

where $W_{ji}^{(1)}, W_{kj}^{(0)}$ are the weight parameters, and $b_j^{(1)}, b_k^{(0)}$ are the bias parameters. The activation functions are f and g. The N input vectors $X_D = (x_D^{(1)}, x_D^{(2)}, ..., x_D^{(N)})^T$, and their corresponding outputs $Y_D = (y_D^{(1)}, y_D^{(2)}, ..., y_D^{(N)})^T$ with $y_D^{(i)} = M(x_D^{(i)})$ constitute a dataset D. The error function is the mean square error (MSE), which is the difference between the outputs of the model and the labels, such as shown in Eq.4.5. The error function is minimized to determine the optimal weights and bias parameters. To avoid overfitting in the neural network model, a regularization parameter λ is added to the error function, as in Eq.4.6

$$E_D = \frac{1}{2N} \sum_{i=1}^{N} (Y_D - Y_{NN})^2 \tag{4.5}$$

$$E' = E_D + \lambda \sum_{l,\alpha,\beta} (W_{\alpha\beta}^{(l)})^2 \tag{4.6}$$

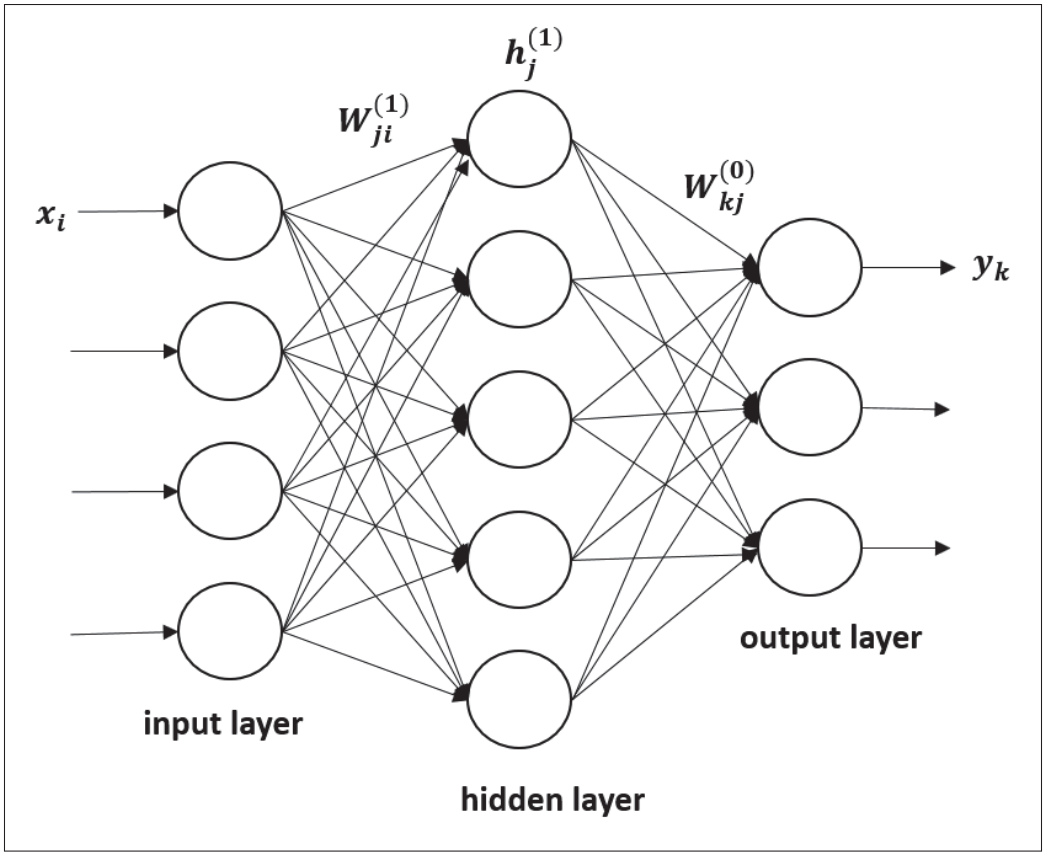

Figure 4.4 A single-layer deep neural network

An iterative backpropagation process minimizes the error function E'. In this regression problem, f is the Relu activation, and g is the identity function. As an example, a neural network of five hidden layers is presented in Fig.4.5 with five parameters in the input layer for each sample and the corresponding outputs are $m = 128$ in the output layer. There are many libraries for implementing DNNs, including TensorFlow, PyTorch and Keras. Matlab's Deep Learning Neural Toolbox is used in this study (Beale *et al.*, 2019).

4.2.4 Formulation of the cost function

The soil parameters of constitutive models to be identified are variables. The identification process reliability depends upon the quality of the measured dataset. The dataset of displacements, measured at different inclinometers installed at different locations of the rockfill dam, is available

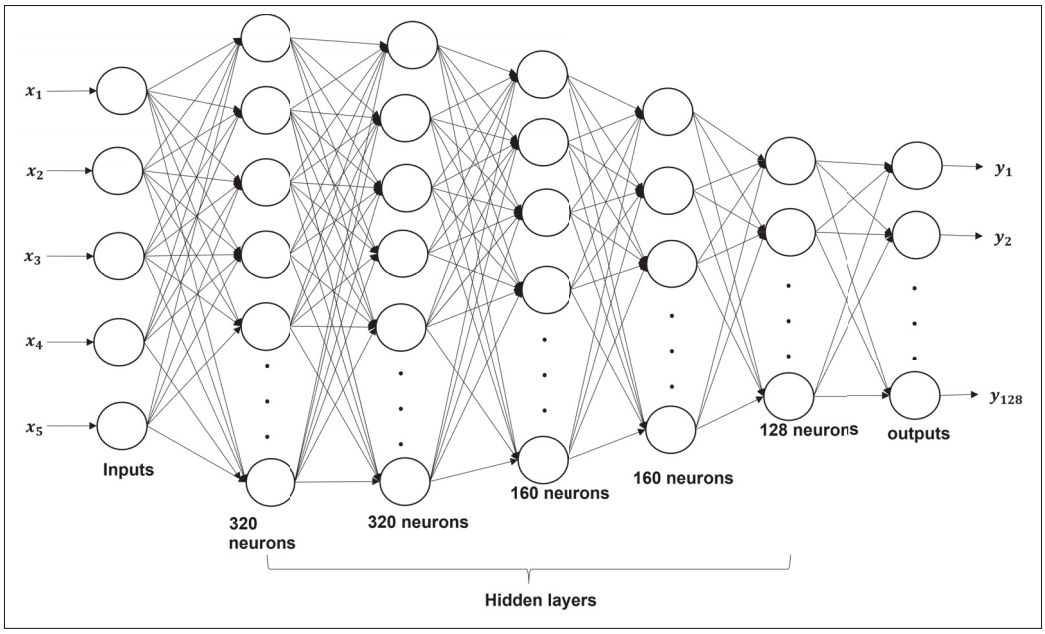

Figure 4.5 A five-layer deep neural network

for this study. The objective function can be defined as the mean square error:

$$J_{obj} = \frac{1}{N_m}\sum_{i=1}^{N_m}(Y_i - \bar{Y}_i)^2 \tag{4.7}$$

where N_m is the number of measurement points, and Y_i and $\bar{Y}_i$ are the measured and predicted displacements. The above equation can be generalized by adding some weights C_i, as given below:

$$J_{obj} = \frac{1}{N_m}\sum_{i=1}^{N_m}C_i(Y_i - \bar{Y}_i)^2 \tag{4.8}$$

It is thus possible to give more weight to more reliable measurements, as uncertainty occurs due to several factors that affect the performance of inclinometers. Measured displacement plots show large fluctuations as a result of this uncertainty. An iterative optimization process can become unreliable or difficult to converge with such fluctuations. Therefore, the weights C_i are formulated as:

$$C_i = \tanh(\frac{1}{\delta_i}) \tag{4.9}$$

$$\delta_i = \beta(\frac{Y_i - \bar{Y}_m}{\sigma_m + \varepsilon})^2 \tag{4.10}$$

where $\bar{Y}_m$ and σ_m are the mean and standard deviation of measured displacements along the inclinometer. β denotes the empirical parameter ($\beta = 3$ is a typical value), and $\varepsilon \rightarrow 0$. A value of δ_i increases with the increasing effect of uncertainty in the ith measured data; therefore, C_i will tend to zero if δ_i is large. However, C_i will be close to 1 for small δ_i, indicating less uncertainty. The accuracy in the calibration process can be improved by minimizing the objective functions simultaneously for each inclinometer. For a multi-objective problem, the weighted sum method can incorporate multi-error functions into a single composite function (Marler & Arora, 2010), defined in Eq.4.11.

$$J = \frac{1}{N_m * N_I} \sum_{i=1}^{N_I} w_i * J_{obj_i} \tag{4.11}$$

where N_I is the number of objective functions along each inclinometer and w_i is the weight associated with each objective function. The greater the weight, the higher the priority of a function compared to an objective function associated with a lower weight. Several approaches can be used to determine weights; in this study, we chose a scalarization method that incorporates the multi-objective function into a single function by assigning the weights to every function, as detailed in (Gunantara, 2018).

4.2.5 Optimization methods

Optimization techniques have been widely used to identify soil parameters in geotechnics (Nocedal & Wright, 2006). Several non-deterministic optimizers, such as Genetic Algorithms (GAs), Particle Swarm Optimization (PSO), and Differential Evolution (DE), have been applied in various geotechnical applications (Yin *et al.*, 2018; Boumezerane, 2022). However, these methods cannot address geotechnical applications involving nonlinearity. This paper aims to develop a hybrid optimization technique, PSOGA, which combines the advantages of PSO and GA algorithms to avoid the pitfalls of solution divergence and local minima. Local minima are a problem in PSO due to the lack of crossover and mutation operators, and so GA operators are

integrated into a PSO algorithm in the PSOGA. These techniques are briefly described in the following subsection.

4.2.5.1 Particle Swarm Optimization (PSO)

Particle Swarm Optimization is a nonlinear global optimization technique for continuous functions introduced by (Kennedy & Eberhart, 1995), inspired by bird flocking, swarming and other bird behaviours. It is common practice for birds to share their locations with the flock during collective feeding. This information-sharing mechanism enabled the flock to find large amounts of food quickly. Although this algorithm has the flaw of going into local optimal solutions when solving discrete optimization problems, it still works well in most optimization scenarios and has been widely used in several fields. PSO is based on velocity and position models, which use the velocity of particles to update particle positions, and it uses particle positions to represent possible solutions in the search bounds. The fitness function determines the adaptation value of each particle. A particle also keeps track of its previous best position and the global best position found by the entire particle population. Initially, the particle positions and velocities are randomly distributed within prescribed search bounds. The position vector and velocity of a j particle are denoted by x_j and V_j, respectively, and updated for the kth iteration using the following formulas (Arora, 2015):

$$V_j^k = w_1 V_j^{k-1} + c_1 r_1 (PPbest - x_j^{k-1}) + c_2 r_2 (GLbest - x_j^{k-1}) \tag{4.12}$$

and

$$x_j^k = x_j^{k-1} + V_j^k \tag{4.13}$$

where r_1 and $r_2 \epsilon [0, 1]$ are random numbers, whereas c_1, c_2 and w_1 are algorithmic tuning parameters.

4.2.5.2 Genetic Algorithm (GA)

The Genetic algorithm (GA), originally developed by (Holland *et al.*, 1992), is a search procedure based on natural evolution that combines selection and genetics (Darwin, 2007). In contrast to gradient-based methods, a GA does not determine the optimal solution based on initial solutions, giving it a robustness that is a significant reason for its popularity. A GA consists of initialization, evaluation, selection, and combination steps. In the first step, a set of possible solutions are generated randomly based on the bounds of each parameter. The individual's fitness is then evaluated according to stochastic convergence criteria (Marappan & Sethumadhavan, 2020) $10^{-}6$. In the next set of operations, the chromosomes with the lowest functional values are selected as parents, and then a crossover probability combines them to form offspring. The process is intended to mimic nature, where the best chromosomes are passed on to new offspring to ensure an improved next generation. An intermediate or heuristic crossover approach was used, which arrived at a 0.8 probability ratio and a mutation probability set to 0.1 to achieve the global optimum.

4.2.5.3 Hybrid PSOGA

A hybrid PSOGA optimization algorithm combines a particle swarm optimization (PSO) and a genetic algorithm (GA) to capture each algorithm's best properties and overcomes its drawbacks. Its high convergence performance and ability to avoid being trapped in locally-optimal solutions are attributable to the PSO and GA approaches. This hybrid approach thus provides a better way to find the optimal solution (Li *et al.*, 2019). In this study, the hybrid PSOGA technique is based on a PSO in which GA is incorporated by crossover and mutation. This optimization technique is realized through the following steps:

1) PSO is utilized as the first step due to its high convergence efficiency. Equ 4.12 updates the position vector and velocity of every particle and 4.13 in each iteration. The tuning parameters $c_1 and c_2$ are both set to 2, and w_1 is 0.9.

2) To incorporate the GA into a PSO, a crossover and mutation of GA genes are introduced into

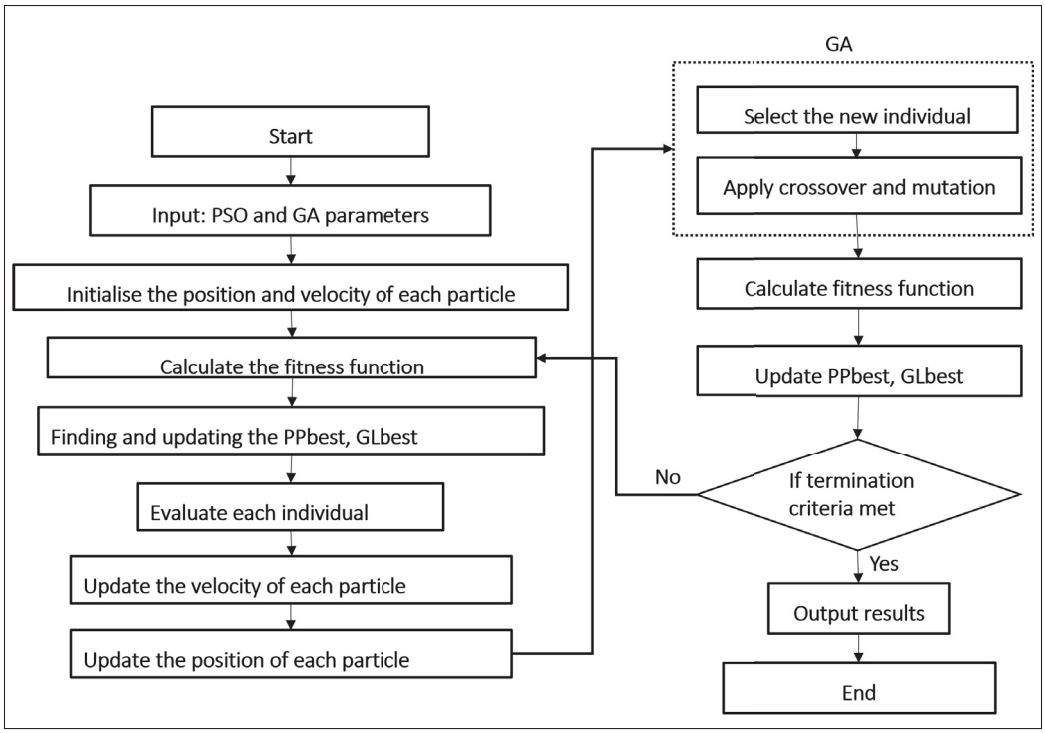

Figure 4.6 Flowchart of a PSOGA algorithm

the PSO in each iteration to increase population diversity and prevent the PSO from falling into a local optimum solution too quickly.

The flow chart illustrates the basic concept of a hybrid PSOGA presented in Fig.1.10.
The proposed PSO-GA algorithm is inspired by (Shi *et al.*, 2022); however, the crossover and mutation operators are modified to adapt it to this problem. The original hybrid optimization PSOGA has proven its ability to achieve global optimum solutions in a shorter time than either optimizer on its own (Shi *et al.*, 2022; Torkashvand, Neshat, Javadi & Pradhan, 2021).

4.3 Parameter identification, results and discussion

This section presents a comparative study of the MC and HS constitutive models. The input datasets D_1 and D_2 for the MC ($N = 1560$) and HS ($N = 1664$) models, respectively, are built using Sobol's sampling algorithm (Joe & Kuo, 2008). The input vectors for the MC model are $x_{D_1}^{(i)} = (C^{(i)}, \rho^{(i)}, G_{ref}^{(i)}, \nu^{(i)}, \phi^{(i)})^T$, and for the HS model they are $x_{D_2}^{(i)} =$

Algorithm 4.1 A PSOGA algorithm

```
Initialization of the position and velocity of the particle
while Termination is not met do
    Estimate the fitness function of each particle.
    Select the particle with the best position by comparing the fitness value of each
    particle. Compare the fitness value of each particle with the one that presents the
    best global position.
    Upgrade the velocity and position of each particle by Eq.4.12 and 4.13
    Apply the crossover operator to all particles and produce the offspring.
    Mutate the particles and evaluate their fitness
    Update the best particle position and the best global position
end while
```

$(E_{50}^{ref\,(i)}, \phi^{(i)}, \mathrm{m}^{(i)}, \rho^{(i)}, \psi^{(i)})^T$ for a sample (i) of each sub-domain P, N and O. It is assumed that the parameters are distributed uniformly. The numerical displacements corresponding to the N and M set of inputs $x_{D_1}^{(i)}$ and $x_{D_2}^{(i)}$ are obtained by running Plaxis2D (Plaxis, 2017). The displacements are then extracted along the measurements' line (32 points) for each inclinometer (INV1, INV2, INH1 and INH2), yielding response vectors $Y_{D_1}^{(i)}$ and $Y_{D_2}^{(i)}$ of dimension $m_1, m_2 = 128$ for both constitutive soil models.

The datasets are divided into three subsets, training, validation, and testing, in proportions of 70%, 15% and 15%, respectively. Several DNN architectures were tested by varying the number of layers and nodes. The 5-layer architecture shown in Fig.4.5 provided good results; the mean square error decreased by a factor of at least$5e-3$ from its initial value, as shown in Fig.4.7, which was the best validation performance of the DNN model and indicated the convergence of the error function with the iterations (epochs).

In order to better assess the response surface, several models were constructed and then initialized with random weight parameters. Fig.4.8 shows that the predicted and targeted datasets have a reasonable correlation, which indicates a good response surface between the numerical simulations and the DNN predictions. Indeed, the correlation coefficient R is 0.99 for both

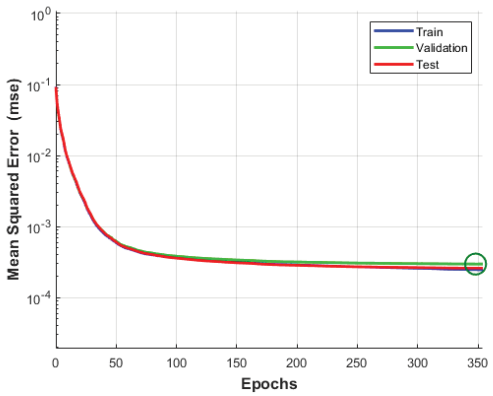

a) Training, validation and test errors for the MC model

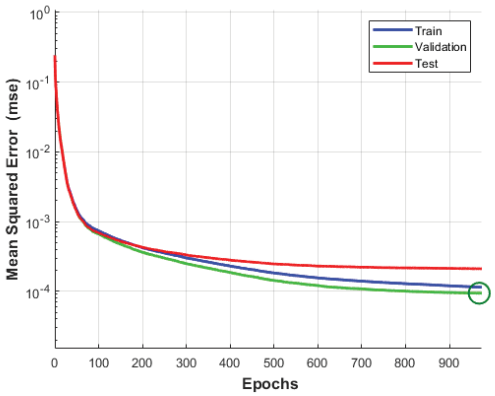

b) Training, validation and test errors for the HS model

Figure 4.7 Performance of deep neural network models

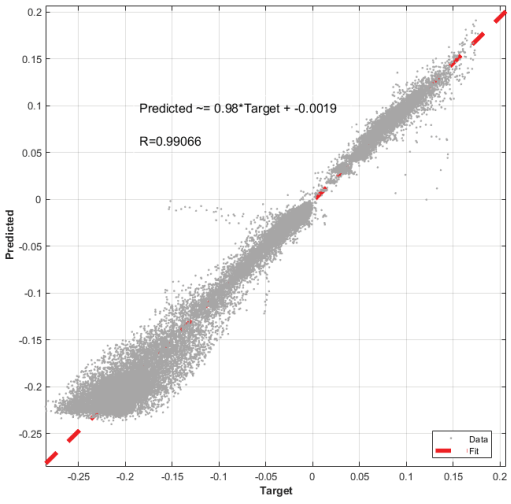

a) Fitted line plot for the MC soil model dataset

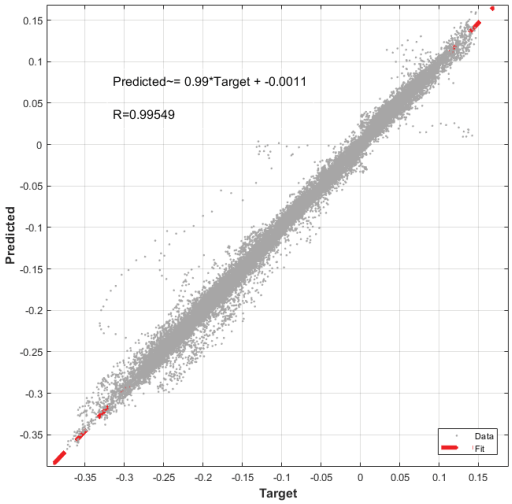

b) Fitted line plot for the HS model dataset

Figure 4.8 Correlation between the targeted and predicted test data for the MC and HS models

constitutive models. The DNN model is highly accurate, as the relative errors between the predicted and observed outputs are only 10^{-4} and 10^{-5} for the MC and HS models, respectively.

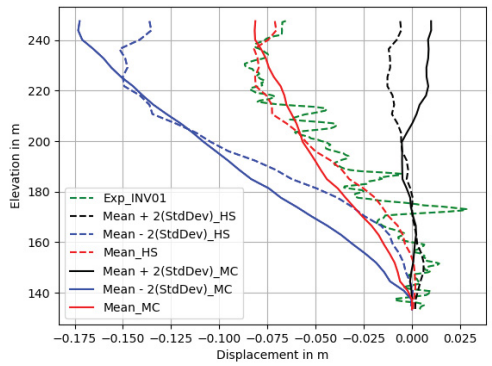

a) Horizontal displacements for inclinometer INV1

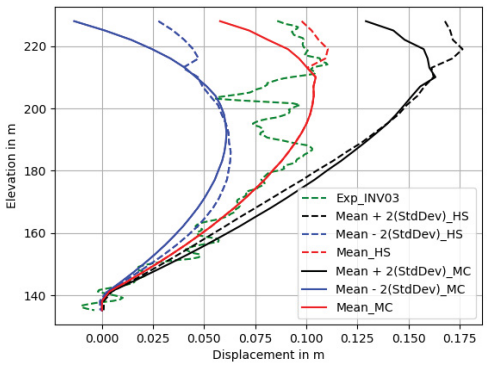

b) Horizontal displacements for inclinometer INV2

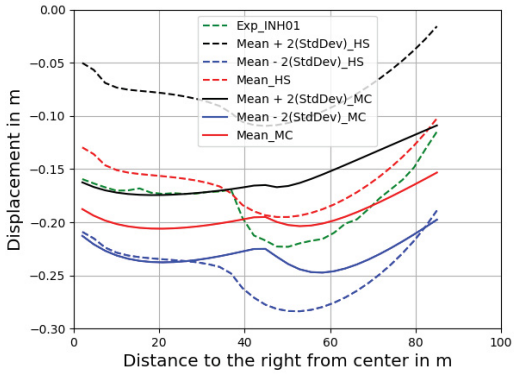

c) Vertical displacements for inclinometer INH1

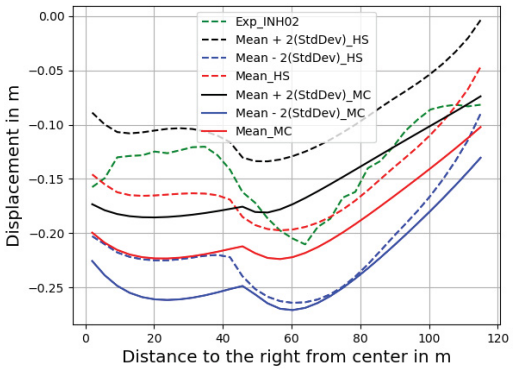

d) Vertical displacements for inclinometer INH2

Figure 4.9 A comparison of the confidence intervals of numerical displacements for MC and HS constitutive models

Uncertainty is inevitable due to a lack of knowledge or inherent noise in the measurements. The uncertainty analysis quantifies the output uncertainty due to aleatoric variations in the input parameters and can be performed using the Monte Carlo method if the sample size is large enough. The confidence intervals for the displacements of the inclinometers for the MC and HS soil models are shown in Fig.4.9.

While the numerical and measured displacements for the INV1 and INV2 (vertical) inclinometers are within the predicted confidence intervals (mean ±2 standard deviation), the measured

Table 4.3 Optimal parameters of the MC model and the minimum fitness values obtained using different optimization algorithms

Soil Parameters	**Optimization Techniques**		
Sub-domains P,N and O	PSO	GA	PSOGA
ρ(P)	22.98	23.08	23.12
G_{ref}(P)	2.8962E+04	2.9484E+04	2.886E+04
ν(P)	0.32	0.32	0.32
ϕ(P)	42.30	42.60	41.90
ρ(N)	23.18	22.61	23.23
G_{ref}(N)	6.14482E+04	6.262E+04	6.1941E+04
ν(N)	0.28	0.27	0.27
ϕ(N)	48.98	49.22	49.14
ρ(O)	22.30	22.13	22.62
G_{ref}(O)	4.6742E+04	4.7899E+04	4.7171E+04
ν(O)	0.243	0.23	0.22
ϕ(O)	45.74	46.32	46.75
Fitness value	1.59E-04	1.733E-04	1.177E-04
Time elapsed(sec)	569	996	1190

Table 4.4 Optimal parameters of HS model and the minimum fitness values obtained using different optimization algorithms

Soil Parameters	**Optimization Techniques**		
Sub-domains P,N and O	PSO	GA	PSOGA
E_{50}^{ref}(P)	8.849E+04	8.239E+04	7.3429E+04
ϕ(P)	43.24	44.20	44.37
m(P)	0.43	0.47	0.57
ρ(P)	23.30	22.49	23.16
ψ(P)	10.09	10.75	8.50
E_{50}^{ref}(N)	1.633E+04	1.541E+04	1.445E+04
ϕ(N)	48.41	47.09	49.14
m(N)	0.20	0.21	0.22
ρ(N)	23.35	22.75	23.18
ψ(N)	16.82	15.41	12.75
E_{50}^{ref}(O)	1.256E+04	1.2083E+04	1.265E+04
ϕ(O)	44.83	43.96	42.85
m(O)	0.435	0.46	0.462
ρ(O)	21.41	21.68	21.37
ψ(O)	10.89	10.83	8.5
Fitness value	1.8759E-04	1.9046E-04	1.138E-04
Time elapsed(sec)	662.6	932	1070

and numerical displacements of the horizontal inclinometers INH1 and INH2 show some discrepancies. Nevertheless, the measured data for all inclinometers are mainly within the predicted numerical confidence intervals.

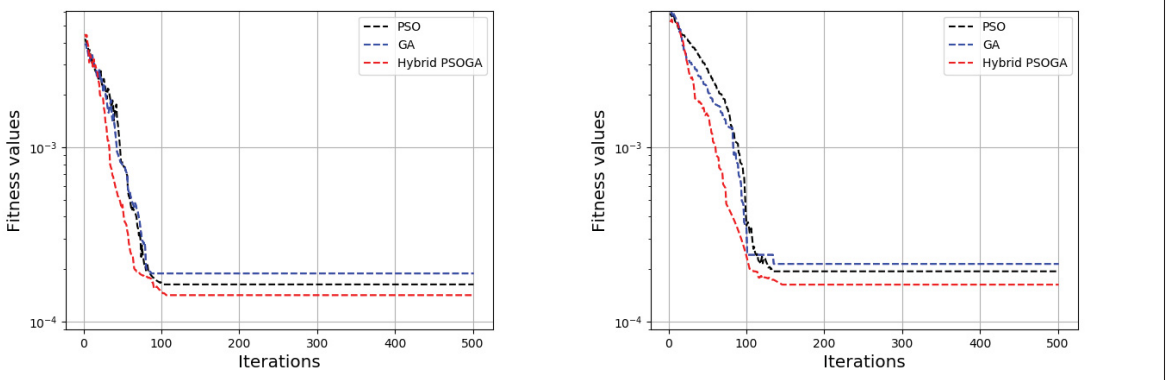

a) Evaluation of fitness function versus iterations for the MC model

b) Evaluation of fitness function versus iterations for the HS model

Figure 4.10 A comparative study of convergence observed during the analysis of optimization algorithms

The PSO, GA, and hybrid PSOGA algorithms are applied to identify soil parameters. Initially, the parameters for each algorithm are tuned by a trial and error approach. In the present study, the population sizes and the number of iterations are varied to analyze their optimal convergence. Once determined, the population size and iteration count are set at 100 for all optimization techniques. The crossover and mutation probabilities for the GA are set at 0.6 and 0.1, respectively; however, for PSO, the learning factors $c1$ and $c2$ are both assumed to be 2. The objectives here are to have an iteration count in all techniques, beyond which there is no significant improvement in convergence, and to assure the existence of a population that accomplishes this terminus without compromising performance or accuracy. Computer programs are executed several times with an Intel-i7 processor with 32 GB RAM to verify that the results have no significant differences.

The fitness functions are evaluated with respect to each iteration in PSO, GA and hybrid PSOGA for both constitutive soil models and the convergence trend is presented in Fig. 4.10. It is evident

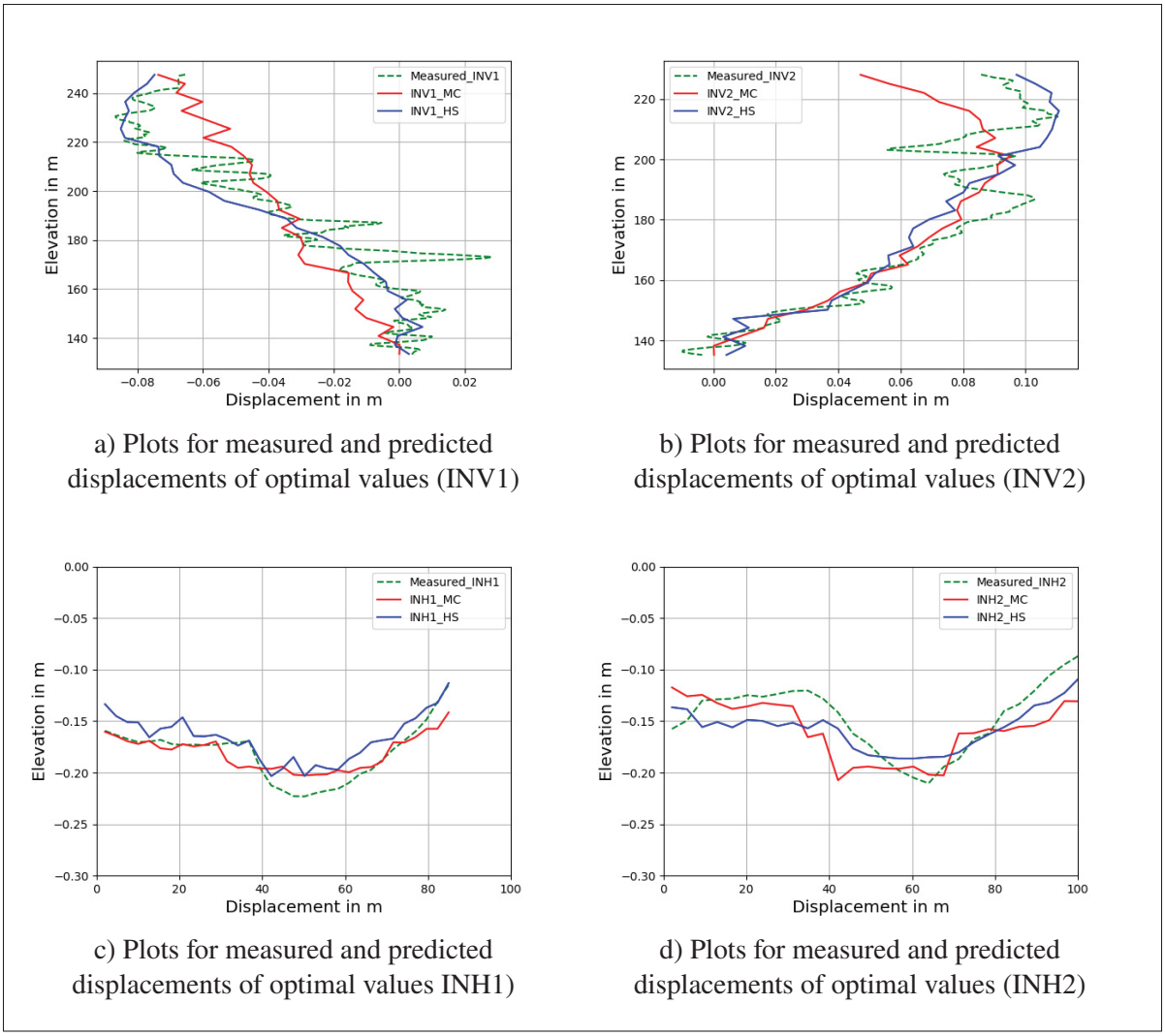

a) Plots for measured and predicted displacements of optimal values (INV1)

b) Plots for measured and predicted displacements of optimal values (INV2)

c) Plots for measured and predicted displacements of optimal values INH1)

d) Plots for measured and predicted displacements of optimal values (INH2)

Figure 4.11 Measured and predicted displacements for optimal parameter values of MC and HS models: displayed in dotted and bold lines, respectively

from the above results that the hybrid PSOGA offers the best performance, as it reaches the smallest fitness values first, followed by PSO and then GA.

The optimal parameters of MC and HS constitutive soil models, with minimum fitness values and the time elapsed for each algorithm, are summarized in Table4.3 and Table4.4, respectively. It can be seen that PSO converges in less time than the GA and hybrid PSOGA., but the hybrid PSOGA attains the minimum fitness value before the other two approaches. Fig. 4.11 shows that the predicted displacements for optimal parameters of the HS model best match the measured

displacements. Moreover, the optimal parameter values obtained for both soil models are almost the same for all algorithms, leading to similar behaviour of predicted displacements by the deep neural network surrogate model, as shown in Fig. 4.11. Overall, the results demonstrate that the HS model offers the best parameters to fit the oscillatory measurements, especially when combined with hybrid PSOGA.

4.4 Conclusion

This research aimed to present a framework to calibrate the parameters of different constitutive soil models for rockfill dams. The computational burden of numerical analysis is the major obstacle to the rapid determination of these parameters. Therefore, a DNN surrogate model is fine tuned and utilized to reduce the computational cost. Moreover, an objective function is formulated to smooth out the oscillations, as measured displacements show strong fluctuation among the inclinometers. To increase efficiency and accuracy, non-intrusive optimization algorithms (PSO, GA and hybrid PSOGA) are employed to minimize the error of the objective function and attain the optimal parameters. The hybrid PSOGA leads the optimization process to a global solution by maintaining the balance between PSO's exploration and exploitation capacity by adding GA operators. The method is applied to the calibration problem of Quebec's large rockfill dam, Romaine-2, which has an asphalt core. Two constitutive material models, Mohr-Coulomb (MC) and Hardening Soil (HS), are employed, and their responses are compared. The predicted displacements for the optimal parameters determined by the HS model are in better agreement with the measured displacements than those of the MC model. Overall, the results demonstrate that making use of the DNN surrogate model and the hybrid PSOGA optimization algorithm constitutes an efficient tool in inverse analysis.

CONCLUSION AND RECOMMENDATIONS

This thesis mainly examined the parametric uncertainties, sensitivity, and parameter identification of rockfill dams. It is important to note that the quality of sensitivity analysis, parameter calibration, and uncertainty analysis can significantly impact the dam's modelling. However, several limitations to different methods can make it challenging to achieve satisfactory results, especially when dealing with various sources of uncertainty.

The dam (Romaine-2) structure was initially numerically modelled using the plane strain hypothesis with a finite element approach using the simple Mohr-Coulomb constitutive soil parameters. The model consisted of triangular elements meshed to different soil sub-domains, with additional refinement around the asphalt core. Chapter 2 used a classical uncertainty propagation technique such as Monte Carlo on a numerical model describing dam behaviour. Only one subdomain in the dam was considered in this study; therefore, only five soil parameters were assumed as input parameters. A careful convergence study was conducted to determine the optimal sample size to ensure acceptable convergence and precision. Although the Monte Carlo approach is effective and easy to implement, its usefulness is limited when dealing with problems that require extensive simulation time. The fact remains that this approach is widely used as a reference solution with which all other methods have been tested and validated.

Additionally, the extensive need for computational resources renders high-fidelity computations cost-prohibitive for multiple parameter solutions when conducting sensitivity or uncertainty analyses. To address this challenge, surrogate modelling has emerged as a promising technique for learning and representing high-fidelity models. Polynomial chaos expansion (PCE) and deep neural network (DNN) methods were trained to overcome the limitations of sampling methods and a surrogate model was developed to reduce the computational cost of numerical models. Indeed, these techniques make it possible to efficiently approximate the variability of the output responses of numerical models with a considerably reduced number of sampling points.

Comparing results obtained from $N = 300$ and $N = 1080$ datasets to Monte Carlo simulations, the statistical mean displacements on two inclinometers obtained with the PCE surrogate model were more consistent with measured data than those computed with the DNN model. However, DNN was proven to be efficient in predicting the numerical solution for any input data set.

Overall, this study showed that surrogate models can be used to reduce computational costs when a large number of simulations are required. Moreover, variance-based sensitivity analysis identified that the shear modulus and Poisson coefficient parameters of the Mohr-coulomb constitutive soil model have the most significant impact on the dam's behaviour.

In order to understand how constitutive soil models affect the behaviour of a structure, an inverse analysis was conducted to examine its properties and parameters. The main priority was identifying the parameters that accurately correspond to the physical system. This was accomplished by minimizing discrepancies between the gathered measurements and numerical data. In the instance of the Romaine-2 dam, the measurements were taken through four inclinometers installed at different locations across the dam's cross-sections. The computational domain was decomposed into three subdomains to conduct a comparative study that accounted for the heterogeneity of the materials, so the input parameters were increased to twelve. Due to the high efficiency of deep neural networks, the surrogate model was built for input parameters and corresponding displacements simulated through the finite element model to speed up identification. A comparative study of three non-intrusive optimization algorithms (Genetic algorithm (GA), Particle Swarm Optimization (PSO), and Differential evolution (DE)) were conducted to determine the constitutive soil parameters. The measured displacements showed significant fluctuations along the inclinometers, so an objective function was developed to smooth out the oscillations and improve the algorithms' convergence. The optimal parameter values obtained by each algorithm were almost identical, resulting in similar predicted displacements for both cases. Although the measurement data set was not very large, as is typical in machine

learning studies, the findings demonstrate that combining deep neural networks and non-deterministic optimization algorithms were valuable computational tools in this inverse analysis. All the results are discussed in detail in Chapter 3. While this study found particle swarm optimization (PSO) to be the most effective method, it's essential to be aware of its limitations. One significant concern is that PSO can become trapped in a local optimum when working with high-dimensional spaces. Moreover, the convergence rate of the algorithm during iterative processes is often below average. However, this issue was resolved using a hybrid method that perfectly balances robustness and efficiency. A hybrid optimization technique that merges particle swarm optimization (PSO) with a genetic algorithm (GA) incorporated by crossover and mutation was developed. This innovative approach captured the best features of each algorithm, thereby overcoming their limitations.

The high computational load of numerical analysis posed a significant challenge in updating every particle's position vector and velocity in each iteration. To alleviate this issue, a DNN surrogate model was fine-tuned for the soil parameters of each constitutive model. A comparative study of constitutive soil models Mohr-Coulomb (MC) and hardening soil (HS) models, was considered to understand how the optimized parameter changes along the dam. In addition, a multi-objective function was developed by combining the objective functions along each inclinometer. To optimize efficiency and accuracy, non-intrusive optimization algorithms such as PSO, GA, and hybrid PSOGA were employed to minimize the multi-objective function error and obtain optimal parameters for each constitutive soil model. The hybrid PSOGA algorithm effectively achieved a global solution by balancing PSO's exploration and exploitation capabilities with GA operators. The predicted displacements for the optimal parameters determined by the HS model were in better agreement with the measured displacements than those of the MC model. The results demonstrated that utilizing DNN surrogate models and hybrid PSOGA optimization algorithms was an efficient tool in inverse analysis. The study's objective was to devise a framework for the calibration problem of Quebec's Romaine-2 rockfill dam, which has an asphalt core.

The methodology presented in this thesis for inverse analysis considering MC and HS models was highly adaptable and efficient, allowing customization to suit specific problem requirements. However, there are some limitations. The success of this adaptability is mainly dependent on the numerical model, formulation of objective functions and optimization methods utilized for the given problem. Sometimes, a robust algorithm can lead to unnecessary computational costs, while other times, highly efficient ones may not be able to handle complex problems. However, the main objective of this thesis is to define a methodology that can be applied to numerous geotechnical problems. Therefore, while differential evolution (DE) has weaknesses in terms of efficiency, it is essential to focus on improving it. Additionally, a 2D finite element model was used throughout the study. Three dimensional modelling (provided that additional measurement data are available) would help better understand dam behaviour. In order to improve the reliability and adaptability of data-driven approaches for the Romaine-2 Dam and related projects, one of the main future plans is to implement real-time monitoring systems. This involves continuously collecting data from sensors and monitoring devices to update surrogate models and calibrated parameters over time. Long-term monitoring will ensure that the approach takes into account the actual behaviour and performance of the dam. Additionally, real-time validation of manual measurements will allow any errors to be immediately identified and corrected by the technicians on-site before making the final record. This will help to eliminate errors resulting from human error or defects in measuring devices. Identifying potential failure scenarios based on monitoring data would also be valuable.

BIBLIOGRAPHY

Abadi, M., Agarwal, A., Barham, P., Brevdo, E., Chen, Z., Citro, C., Corrado, G. S., Davis, A., Dean, J., Devin, M. et al. (2016). Tensorflow: Large-scale machine learning on heterogeneous distributed systems. *Computer Science*, 1-19.

Abdedou, A. & Soulaimani, A. (2019). A non-intrusive B-splines Bézier elements-based method for uncertainty propagation. *Computer Methods in Applied Mechanics and Engineering*, 345, 774–804.

Abdolrasol, M. G., Hussain, S. S., Ustun, T. S., Sarker, M. R., Hannan, M. A., Mohamed, R., Ali, J. A., Mekhilef, S. & Milad, A. (2021). Artificial neural networks based optimization techniques: A review. *Electronics*, 10(21), 2689.

Adamo, N., Al-Ansari, N., Sissakian, V., Laue, J. & Knutsson, S. (2021). Dam Safety: Use of Instrumentation in Dams. *Journal of Earth Sciences and Geotechnical Engineering*, 11(1), 145–202.

Adarsh, S., Dhanya, R., Krishna, G., Merlin, R. & Tina, J. (2012). Prediction of Ultimate Bearing Capacity of Cohesionless Soils Using Soft Computing Techniques [Research article].

Akbari Hamed, A. (2017). *Predictive numerical modeling of the behavior of rockfill dams*. (Ph.D. thesis, École de technologie supérieure).

Akhtarpour, A. & Khodaii, A. (2009). Nonlinear Numerical Evaluation of Dynamic Behavior of an Asphaltic Concrete Core Rockfill Dam (A Case Study). *Journal of Seismology and Earthquake Engineering*, 11(3), 143.

Al-Qaness, M. A., Ewees, A. A., Fan, H. & Abd El Aziz, M. (2020). Optimization method for forecasting confirmed cases of COVID-19 in China. *Journal of Clinical Medicine*, 9(3), 674.

Alonso, E. E. & Cardoso, R. (2010). Behavior of materials for earth and rockfill dams: Perspective from unsaturated soil mechanics. *Frontiers of Structural and Civil Engineering*, 4(1), 1-39.

Alzubaidi, L., Zhang, J., Humaidi, A. J., Al-Dujaili, A., Duan, Y., Al-Shamma, O., Santamaría, J., Fadhel, M. A., Al-Amidie, M. & Farhan, L. (2021). Review of deep learning: Concepts, CNN architectures, challenges, applications, future directions. *Journal of big Data*, 8, 1–74.

Amini, A., Abdollahi, A., Hariri-Ardebili, M. A. & Lall, U. (2021). Copula-based reliability and sensitivity analysis of aging dams: Adaptive Kriging and polynomial chaos Kriging methods. *Applied Soft Computing*, 109, 107524.

Amouzou, G. Y. & Soulaïmani, A. (2021). Numerical algorithms for elastoplacity: Finite elements code development and implementation of the mohr–coulomb law. *Applied Sciences*, 11(10), 4637.

An, J.-S., Kang, K.-N., Kim, S.-H. & Song, K.-I. (2019). Analysis for Applicability of Differential Evolution Algorithm to Geotechnical Engineering Field. *Journal of the Korean Geotechnical Society*, 35(4), 27–35.

An, J.-S., Kang, K.-N., Choi, J.-Y., Sung, W.-S., Suy, V. & Song, K.-I. (2020). Tunnel back analysis based on differential evolution using stress and displacement. *Advances in Civil Engineering*, 2020, 1–10.

Arora, R. K. (2015). *Optimization: algorithms and applications*. CRC Press.

Asteris, P. G., Rizal, F. I. M., Koopialipoor, M., Roussis, P. C., Ferentinou, M., Armaghani, D. J. & Gordan, B. (2022). Slope Stability Classification under Seismic Conditions Using Several Tree-Based Intelligent Techniques. *Applied Sciences*, 12(3), 1753. Number: 3 Publisher: Multidisciplinary Digital Publishing Institute.

Asthana, B. & Khare, D. (2022). *Recent Advances in Dam Engineering*. Springer Nature, SN.

Bao, T., Li, J., Lu, Y. & Gu, C. (2020). IDE-MLSSVR-based back analysis method for multiple mechanical parameters of concrete dams. *Journal of Structural Engineering*, 146(8), 04020155.

Baram, Y. & Sandell, N. (1978). An information theoretic approach to dynamical systems modeling and identification. *IEEE Transactions on Automatic Control*, 23(1), 61-66.

Beale, M., Hagan, M. & Demuth, H. (2019). MATLAB deep learning toolbox™ user's guide: PDF documentation for release R2019a. *The MathWorks, Inc*, 777-798.

Berveiller, M., Sudret, B. & Lemaire, M. (2006). Stochastic finite element: a non intrusive approach by regression. *European Journal of Computational Mechanics/Revue Européenne de Mécanique Numérique*, 15(1-3), 81–92.

Bhutto, A. H., Zardari, S., Zardari, M., Bhurgri, G., Memon, B., Bhanbhro, R. & Babar, M. M. (2019). Mohr-Coulomb and hardening soil model comparison of the settlement of an embankment dam. *Engineering, Technology & Applied Science Research*, 9(5), 4654–4658.

Bishop, C. M. (2006). *Pattern recognition and machine learning*. springer.

Blatman, G. & Sudret, B. (2010a). An adaptive algorithm to build up sparse polynomial chaos expansions for stochastic finite element analysis. *Probabilistic Engineering Mechanics*, 25(2), 183–197.

Blatman, G. & Sudret, B. (2010b). An adaptive algorithm to build up sparse polynomial chaos expansions for stochastic finite element analysis. *Probabilistic Engineering Mechanics*, 25(2), 183-197. Publisher: Elsevier.

Bolzon, G. & Buljak, V. (2011). An effective computational tool for parametric studies and identification problems in materials mechanics. *Computational mechanics*, 48(6), 675–687.

Boumezerane, D. (2022). Recent Tendencies in the Use of Optimization Techniques in Geotechnics: A Review. *Geotechnics*, 2(1), 114–132.

Bowles, L. et al. (1996). *Foundation analysis and design*. McGraw-hill.

Branbo, R. S., Hassan, I. et al. (2020). Seepage Sensitivity Analysis through a Homogeneous Dam within the Unsaturated Soil Zone. *Journal of Engineering and Computer Science (JECS)*, 21(3), 64–74.

Bratley, P. & Fox, B. L. (1988). Algorithm 659: Implementing Sobol's quasirandom sequence generator. *ACM Transactions on Mathematical Software (TOMS)*, 14(1), 88–100.

Breiman, L. (1996). Bagging predictors. *Machine learning*, 24(2), 123–140.

Brinkgreve, R., Kumarswamy, S., Swolfs, W., Waterman, D., Chesaru, A., Bonnier, P. et al. (2016). PLAXIS 2016. *PLAXIS bv, the Netherlands*, 1-16.

Burhenne, S., Jacob, D. & Henze, G. P. (2011). Sampling based on Sobol'sequences for Monte Carlo techniques applied to building simulations. *Proc. Int. Conf. Build. Simulat*, pp. 1816–1823.

Cacuci, D. G., Ionescu-Bujor, M. & Navon, I. M. (2005). *Sensitivity and uncertainty analysis, volume II: applications to large-scale systems*. CRC press.

Calvello, M. & Finno, R. J. (2004). Selecting parameters to optimize in model calibration by inverse analysis. *Computers and Geotechnics*, 31(5), 410–424.

Cao, X., Jiang, C. & Zu, A. (2022). Uncertainty analysis of dam finite element simulation based on a surrogate model. In *Advances in Civil Function Structure and Industrial Architecture* (pp. 594–600). CRC Press.

Carbonari, S., Dezi, F., Arezzo, D. & Gara, F. (2022). A methodology for the identification of physical parameters of soil-foundation-bridge pier systems from identified state-space models. *Engineering Structures*, 255, 113944.

Carrera, J. (1988). State of the art of the inverse problem applied to the flow and solute transport equations. *Groundwater Flow and Quality Modelling*, 549-583.

Cheng, Y. M., Li, L., Sun, Y. & Au, S. (2012). A coupled particle swarm and harmony search optimization algorithm for difficult geotechnical problems. *Structural and Multidisciplinary Optimization*, 45, 489–501.

Chicone, C. et al. (1999). Ordinary Differential Equations with Applications [electronic resource]. 571.

Coello, C. A. C., Lamont, G. B., Van Veldhuizen, D. A. et al. (2007). *Evolutionary algorithms for solving multi-objective problems*. Springer.

Costa, L. & Alonso, E. (2009). Predicting the behavior of an earth and rockfill dam under construction. *Journal of geotechnical and geoenvironmental engineering*, 135(7), 851-862.

Creegan, P. J. & Monismith, C. L. (1996). Asphalt-concrete water barriers for embankment dams. ASCE.

Cui, Z. & Gao, X. (2012). Theory and applications of swarm intelligence. Springer.

Dakoulas, P. (2012). Nonlinear seismic response of tall concrete-faced rockfill dams in narrow canyons. *Soil Dynamics and Earthquake Engineering*, 34(1), 11–24.

Darwin, C. (1857). *Darwin's Theory Of Evolution*.

Darwin, C. (2007). *Theory of evolution*. C. King & S. Scott, Trans.). Encarta-Microsoft Student.

Das, R. & Soulaïmani, A. (2019). Global sensitivity analysis in the design of rockfill dams. In *Sustainable and Safe Dams Around the World/Un monde de barrages durables et sécuritaires* (pp. 950–962). CRC Press.

Das, R. & Soulaimani, A. (2021). Non-deterministic methods and surrogates in the design of rockfill dams. *Applied Sciences*, 11(8), 3699.

Davis, S. E., Cremaschi, S. & Eden, M. R. (2017). Efficient surrogate model development: Optimum model form based on input function characteristics. *Computer aided chemical engineering*, 457–462.

Da'u, A. & Salim, N. (2020). Recommendation system based on deep learning methods: a systematic review and new directions. *Artificial Intelligence Review*, 53(4), 2709–2748.

Deng-gang, W., Ying-xi, L. & Shou-ju, L. (2000). Genetic algorithms for inverse analysis of displacements in geotechnical engineering. *Chinese Journal of Rock Mechanics and Engineering*, 19(2), 979–982.

Dige, N. & Diwekar, U. (2018). Efficient sampling algorithm for large-scale optimization under uncertainty problems. *Computers & Chemical Engineering*, 115, 431–454.

Dimov, I. & Georgieva, R. (2010). Monte Carlo algorithms for evaluating Sobol'sensitivity indices. *Mathematics and Computers in Simulation*, 81(3), 506–514.

Dinescu, C., Smirnov, S., Hirsch, C. & Lacor, C. (2010). Assessment of intrusive and nonintrusive non-deterministic CFD methodologies based on polynomial chaos expansions. *International Journal of Engineering Systems Modelling and Simulation*, 2(1-2), 87–98.

Dou, S.-q., Li, J.-j. & Kang, F. (2019). Health diagnosis of concrete dams using hybrid FWA with RBF-based surrogate model. *Water Science and Engineering*, 12(3), 188–195.

Dou, S., Li, J. & Kang, F. (2017). Parameter identification of concrete dams using swarm intelligence algorithm. *Engineering Computations*, 34(7), 2358–2378.

Duncan, J. M. & Chang, C.-Y. (1970). Nonlinear analysis of stress and strain in soils. *Journal of the soil mechanics and foundations division*, 96(5), 1629–1653.

Duncan, J. M. (1996). State of the art: limit equilibrium and finite-element analysis of slopes. *Journal of Geotechnical engineering*, 122(7), 577–596.

Edwards, A. W. (1974). The history of likelihood. *International Statistical Review/Revue Internationale de Statistique*, 9-15.

Eltaeib, T. & Mahmood, A. (2018). Differential evolution: A survey and analysis. *Applied Sciences*, 8(10), 1945.

Engl, H., Hanke, M. & Neubauer, A. (1996). *Regularization of inverse problems*. Dordrecht, The Netherlands: Kluwert.

Eykhoff, P. (1974). *System identification*. Wiley New York.

Ferdowsi, A., Mousavi, S.-F., Mohamad Hoseini, S., Faramarzpour, M. & Gandomi, A. H. (2022). A survey of pso contributions to water and environmental sciences. In *Computational Intelligence for Water and Environmental Sciences* (pp. 85–102). Springer.

Finno, R. & Calvello, M. (2005). Supported Excavations: Observational Method and Inverse Modeling. *Journal of Geotechnical and Geoenvironmental Engineering*, 131(7), 826–836.

Fletcher, R. [Unconstrained optimization.]. (1981). Practical Methods of Optimization. John Wiley and Sons.

Forrester, A., Sobester, A. & Keane, A. (2008). *Engineering design via surrogate modelling: a practical guide*. John Wiley & Sons.

Gallagher, K., Sambridge, M. & Drijkoningen, G. (1991). Genetic algorithms: An evolution from Monte Carlo Methods for strongly non-linear geophysical optimization problems. *Geophysical Research Letters*, 18(12), 2177–2180.

Gao, W. (2006). Back analysis algorithm in geotechnical engineering based on particle swarm optimization. *Yantu Lixue(Rock and Soil Mechanics)*, 27(5), 795–798.

Georgevici, A. I. & Terblanche, M. (2019). Neural networks and deep learning: a brief introduction. *Intensive Care Medicine*, 45(5), 712–714.

Ghanem, R. (1999). Ingredients for a general purpose stochastic finite elements implementation.

Ghanem, R., Saad, G. & Doostan, A. (2007). Efficient solution of stochastic systems: application to the embankment dam problem. *Structural safety*, 29(3), 238–251.

Ghiocel, D. & Ghanem, R. (2002). Stochastic finite-element analysis of seismic soil–structure interaction. *Journal of Engineering Mechanics*, 128(1), 66–77.

Gioda, G. & Maier, G. (1980). Direct search solution of an inverse problem in elastoplasticity: Identification of cohesion, friction angle andin situ stress by pressure tunnel tests. *International Journal for Numerical Methods in Engineering*, 15(12), 1823-1848.

Gioda, G. & Sakurai, S. (1987). Back analysis procedures for the interpretation of field measurements in geomechanics. *International Journal for Numerical and Analytical Methods in Geomechanics*, 11(6), 555-583. Retrieved from: https://onlinelibrary.wiley.com/doi/abs/10.1002/nag.1610110604.

Godio, A., Pace, F. & Vergnano, A. (2020). SEIR modeling of the Italian epidemic of SARS-CoV-2 using computational swarm intelligence. *International journal of environmental research and public health*, 17(10), 3535.

Goh, A. T. & Zhang, W. (2014). An improvement to MLR model for predicting liquefaction-induced lateral spread using multivariate adaptive regression splines. *Engineering geology*, 170, 1–10.

Goh, A. T. C., Zhang, W., Zhang, Y., Xiao, Y. & Xiang, Y. (2018). Determination of earth pressure balance tunnel-related maximum surface settlement: a multivariate adaptive regression splines approach. *Bulletin of Engineering Geology and the Environment*, 77, 489–500.

Goldberg, D. (1989a). *Genetic Algorithms in Search, Optimization, and Machine Learning*. MA, USA: Addison-Wesley.

Goldberg, D. (1989b). Sizing populations for serial and parallel genetic algorithms. *Proceeding of the 3rd International Conference on Genetic Algorithms*, pp. 70–79.

Goodfellow, I., Bengio, Y. & Courville, A. (2016). *Deep learning*. MIT press.

Gopi, S. (2010). *Basic civil engineering*. Pearson Education India.

Gunantara, N. (2018). A review of multi-objective optimization: Methods and its applications. *Cogent Engineering*, 5(1), 1502242.

Guo, X. & Dias, D. (2020). Kriging based reliability and sensitivity analysis–Application to the stability of an earth dam. *Computers and Geotechnics*, 120, 103411.

Guo, X., Dias, D., Carvajal, C., Peyras, L. & Breul, P. (2018). Reliability analysis of embankment dam sliding stability using the sparse polynomial chaos expansion. *Engineering Structures*, 174, 295–307.

Hacıefendioğlu, K., Bayraktar, A. & Başağa, H. B. (2010). Estimation of stochastic nonlinear dynamic response of rock-fill dams with uncertain material parameters for non-stationary random seismic excitation. *Nonlinear Dynamics*, 61(1-2), 43-55.

Hajihassani, M., Jahed Armaghani, D. & Kalatehjari, R. (2018). Applications of particle swarm optimization in geotechnical engineering: a comprehensive review. *Geotechnical and Geological Engineering*, 36, 705–722.

Han, Z., Jiankang, C., Shengwei, H., Yazi, X. & Beijia, Z. (2016). Deformation characteristics and control techniques at the Shiziping earth core rockfill dam. *Journal of Geotechnical and Geoenvironmental Engineering*, 142(2), 04015069.

Hariri-Ardebili, M. A. & Sudret, B. (2020). Polynomial chaos expansion for uncertainty quantification of dam engineering problems. *Engineering Structures*, 203, 109631.

Hariri-Ardebili, M. A., Mahdavi, G., Abdollahi, A. & Amini, A. (2021). An RF-PCE Hybrid Surrogate Model for Sensitivity Analysis of Dams. *Water*, 13(3), 302.

Hariri-Ardebili, M. A., Chen, S. & Mahdavi, G. (2022). Machine learning-aided PSDM for dams with stochastic ground motions. *Advanced Engineering Informatics*, 52, 101615.

Hashash, Y. M., Levasseur, S., Osouli, A., Finno, R. & Malecot, Y. (2010a). Comparison of two inverse analysis techniques for learning deep excavation response. *Computers and geotechnics*, 37(3), 323–333.

Hashash, Y. M., Levasseur, S., Osouli, A., Finno, R. & Malecot, Y. (2010b). Comparison of two inverse analysis techniques for learning deep excavation response. *Computers and geotechnics*, 37(3), 323-333. Publisher: Elsevier.

Hashemi, S. M. & Rahmani, I. (2018). Numerical comparison of the performance of genetic algorithm and particle swarm optimization in excavations. *Civil Engineering Journal*, 4(9), 2186–2196.

He, X., Wang, F., Li, W. & Sheng, D. (2022). Deep learning for efficient stochastic analysis with spatial variability. *Acta Geotechnica*, 17(4), 1031–1051.

Hicher, P. & Shao, J. (2002). Elastoplasticité des sols et des roches; modèles de comportement des sols et des roches 1. Collection Mécanique et Ingénierie des Matériaux. Hermès Sciences Publications, Lavoisier.

Höeg, K. (1993). Asphaltic concrete cores for embankment dams. *Norwegian Geotechnical Institute Publicatie*, 1-85.

Hoeg, K. (2005). *Earthquake Resistance of Asphalt core Dams*. Norwegian Geotechnical Institute.

Hokes, F., Kral, P., Krnavek, O. & Husek, M. (2017). Improved sensitivity analysis in the inverse identification of the parameters of a nonlinear material model. *Procedia Engineering*, 172, 347–354.

Holland, J. (1975). *Adaptive in Nature and Artificial Systems*. Ann Arbor, MI, USA: University of Michigan Press.

Holland, J. H. et al. (1992). *Adaptation in natural and artificial systems: an introductory analysis with applications to biology, control, and artificial intelligence*. MIT press.

Homma, T. & Saltelli, A. (1996a). Importance measures in global sensitivity analysis of nonlinear models. *Reliability Engineering and System Safety*, 52(1), 1–17.

Homma, T. & Saltelli, A. (1996b). Importance measures in global sensitivity analysis of nonlinear models. *Reliability Engineering & System Safety*, 52(1), 1–17.

Hosder, S., Walters, R. & Balch, M. (2007). Efficient sampling for non-intrusive polynomial chaos applications with multiple uncertain input variables. *48th AIAA/ASME/ASCE/AHS/ASC Structures, Structural Dynamics, and Materials Conference*, pp. 1939.

Hsieh, W. W. (2009). *Machine learning methods in the environmental sciences: Neural networks and kernels*. Cambridge university press.

Huang, C., Radi, B. & El Hami, A. (2016). Uncertainty analysis of deep drawing using surrogate model based probabilistic method. *The International Journal of Advanced Manufacturing Technology*, 86(9), 3229–3240.

Höeg, K., Valstad, T. & AM Ruud, B. (2007). Asphalt core embankment dams: recent case studies and research. *International Journal on Hydropower and Dams*, 13(5), 112-119.

Iyengar, N., Rajaram, D., Decker, K. & Mavris, D. N. (2023). Uncertainty Propagation in High-Dimensional Fields using Non-Intrusive Reduced Order Modeling and Polynomial Chaos. *AIAA SCITECH 2023 Forum*, pp. 1686.

Jacquier, P., Abdedou, A., Delmas, V. & Soulaïmani, A. (2021). Non-intrusive reduced-order modeling using uncertainty-aware deep neural networks and proper orthogonal decomposition: Application to flood modeling. *Journal of Computational Physics*, 424, 109854.

Janbu, N. (1963). Soil compressibility as determined by oedometer and triaxial tests. *Proceedings of the European conference on soil mechanics and foundation engineering*, 1, 19-25.

Jean, T. (2011). Modern technologies in dam construction: Development of la Romaine hep in Northern Quebec, Canada. 1-10.

Jia, Y. & Chi, S. (2015). Back-analysis of soil parameters of the Malutang II concrete face rockfill dam using parallel mutation particle swarm optimization. *Computers and Geotechnics*, 65, 87–96.

Joe, S. & Kuo, F. Y. (2008). Constructing Sobol sequences with better two-dimensional projections. *SIAM Journal on Scientific Computing*, 30(5), 2635–2654.

Kang, F., Wu, Y., Li, J. & Li, H. (2021). Dynamic parameter inverse analysis of concrete dams based on Jaya algorithm with Gaussian processes surrogate model. *Advanced Engineering Informatics*, 49, 101348.

Kang, F., Liu, X., Li, J. & Li, H. (2022). Multi-parameter inverse analysis of concrete dams using kernel extreme learning machines-based response surface model. *Engineering Structures*, 256, 113999.

Kennedy, J. & Eberhart, R. (1995). Particle swarm optimization. *Proceedings of ICNN'95-international conference on neural networks*, 4, 1942–1948.

Kim, S. & Finno, R. J. (2019). Inverse analysis of a supported excavation in Chicago. *Journal of Geotechnical and Geoenvironmental Engineering*, 145(9), 04019050.

Kim, T. & Jung, Y.-H. (2022). Optimizing Material Parameters to Best Capture Deformation Responses in Supported Bottom-up Excavation: Field Monitoring and Inverse Analysis. *KSCE Journal of Civil Engineering*, 26(8), 3384–3401.

Konard, J., Soulaimani, A., Lefebvre, G., Leger, P. & Nguyen, P. (2014a). *Etat de l'art sur les modeles multi-physiques pour la simulation du comportement des barrages en remblai*.

Konard, J., Soulaimani, A., Lefebvre, G., Leger, P. & Nguyen, P. (2014b). *Modélisation Multi-physique Couplee m2c pour less barrages*.

Kondner, R. L. (1963). Hyperbolic stress-strain response: cohesive soils. *Journal of the soil mechanics and foundations division, ASCE*, 89(1), 115-143.

Kovári, K. & Amstad, C. (1993). Fundamentals of deformation measurements. *Proceedings of the International Symposium on Field Measurements in Geomechanics*, pp. 219–239.

Labuz, J. F. & Zang, A. (2012). Mohr–Coulomb failure criterion. In *The ISRM Suggested Methods for Rock Characterization, Testing and Monitoring: 2007-2014* (pp. 227–231). Springer.

Lashin, I., Ghali, M., Smith, M., Verret, D. & Karray, M. (2022). Investigation of small-to large-strain moduli correlations of rockfill materials—application to Romaine-2 dam. *Canadian Geotechnical Journal*, 59(5), 715–725.

Lebrun, R. & Dutfoy, A. (2009). A generalization of the Nataf transformation to distributions with elliptical copula. *Probabilistic Engineering Mechanics*, 24(2), 172–178.

Levasseur, S., Malecot, Y., Boulon, M. & Flavigny, E. (2009). Statistical inverse analysis based on genetic algorithm and principal component analysis: Method and developments using synthetic data. *International Journal for Numerical and Analytical Methods in Geomechanics*, 33(12), 1485-1511.

Levasseur, S., Malécot, Y., Boulon, M. & Flavigny, E. (2008). Soil parameter identification using a genetic algorithm. *International Journal for Numerical and Analytical Methods in Geomechanics*, 32(2), 189–213.

Levasseur, S., Malecot, Y., Boulon, M. & Flavigny, E. (2010). Statistical inverse analysis based on genetic algorithm and principal component analysis: applications to excavation problems and pressuremeter tests. *International journal for numerical and analytical methods in geomechanics*, 34(5), 471–491.

Li, G., Rabitz, H., Yelvington, P. E., Oluwole, O. O., Bacon, F., Kolb, C. E. & Schoendorf, J. (2010). Global sensitivity analysis for systems with independent and/or correlated inputs. *The journal of physical chemistry A*, 114(19), 6022–6032.

Li, S., Zhang, B., Xu, S. & Zhong, Y. (2019). Back-analysis of pavement thickness based on PSO-GA hybrid algorithms. *IOP Conference Series: Earth and Environmental Science*, 252, 052066.

Li, Y., Hariri-Ardebili, M. A., Deng, T., Wei, Q. & Cao, M. (2023). A surrogate-assisted stochastic optimization inversion algorithm: Parameter identification of dams. *Advanced Engineering Informatics*, 55, 101853.

Lin, C., Li, T., Chen, S., Lin, C., Liu, X., Gao, L. & Sheng, T. (2020). Structural identification in long-term deformation characteristic of dam foundation using meta-heuristic optimization techniques. *Advances in Engineering Software*, 148, 102870.

Loeven, G., Witteveen, J. & Bijl, H. (2007). Probabilistic collocation: an efficient non-intrusive approach for arbitrarily distributed parametric uncertainties. pp. 317.

Longtin, H., Péloquin, É., Verret, D., Mathieu, B., Beauséjour, N., Hammanji, Y. & Rattue, A. (2012). Romaine 2 hydroelectric project: Design of the first large asphalt core rockfill dam and dykes in North America. *Proc. of Canadian Dam Association Conf.*

Malecot, Y., Flavigny, E. & Boulon, M. (2004). Inverse analysis of soil parameters for Finite Element simulation of geotechnical structures: Pressuremeter test and excavation problem. In R.B.J, B., H, S., H.F, S. & E, W. (Eds.), *Geotechnical Innovations,* (pp. 659–675). Verlag Glückauf.

Marappan, R. & Sethumadhavan, G. (2020). Complexity analysis and stochastic convergence of some well-known evolutionary operators for solving graph coloring problem. *Mathematics*, 8(3), 303.

Marler, R. T. & Arora, J. S. (2010). The weighted sum method for multi-objective optimization: new insights. *Structural and multidisciplinary optimization*, 41, 853–862.

Martínez, J. L. F., Gonzalo, E. G., Álvarez, J. P. F., Kuzma, H. A. & Pérez, C. O. M. (2010). PSO: A powerful algorithm to solve geophysical inverse problems: Application to a 1D-DC resistivity case. *Journal of Applied Geophysics*, 71(1), 13–25.

MATLAB, G. O. T. U. (2016). Guide (R2016a). *Natick, Massachusetts: The MathWorks Inc*, 1-28.

Mendel, G. (1865). *Experiments in Plant Hybridization*. Brno, Czech Republic: Natural History Society Brno.

Miller, K., Berg, S., Davison, J., Sudicky, E. & Forsyth, P. (2018). Efficient uncertainty quantification in fully-integrated surface and subsurface hydrologic simulations. *Advances in Water Resources*, 111, 381–394.

Moreira, N., Miranda, T., Pinheiro, M., Fernandes, P., Dias, D., Costa, L. & Sena-Cruz, J. (2013). Back analysis of geomechanical parameters in underground works using an Evolution Strategy algorithm. *Tunnelling and Underground Space Technology*, 33, 143–158.

Murata, T. & Ishibuchi, H. (1995). MOGA: multi-objective genetic algorithms. *IEEE international conference on evolutionary computation*, 1, 289–294.

Najafzadeh, M. & Tafarojnoruz, A. (2016). Evaluation of neuro-fuzzy GMDH-based particle swarm optimization to predict longitudinal dispersion coefficient in rivers. *Environmental Earth Sciences*, 75, 1–12.

Nakane, T., Bold, N., Sun, H., Lu, X., Akashi, T. & Zhang, C. (2020). Application of evolutionary and swarm optimization in computer vision: a literature survey. *IPSJ Transactions on Computer Vision and Applications*, 12, 1–34.

Nguyen, T., Kashani, A., Ngo, T. & Bordas, S. (2019). Deep neural network with high-order neuron for the prediction of foamed concrete strength. *Computer-Aided Civil and Infrastructure Engineering*, 34(4), 316–332.

Nocedal, J. & Wright, S. (2006). *Numerical optimization*. Springer Science.

Obrzud, R. (2010). *The Hardening Soil Model: A Practical Guidebook*. Zace Services.

Obrzud, R., Truty, A., Podles, K., Commend, S. & Zimmermann, T. (2018). Z Soil. Reference manual 8.04. 2018. Zace Services Ltd, Software engineering P.O.Box 224, CH-1028 Pr´everenges Switzerland.

Oldecop, L. A. & Alonso, E. (2001). A model for rockfill compressibility. *Géotechnique*, 51(2), 127-139.

Owen, D. & Hinton, E. (1980). *Finite elements in plasticity*.

Özkuzukiran, S., Özkan, M., Özyazicioğlu, M. & Yildiz, G. (2006). Settlement behaviour of a concrete faced rock-fill dam. *Geotechnical & Geological Engineering*, 24, 1665–1678.

Pal, S., Wije Wathugala, G. & Kundu, S. (1996). Calibration of a constitutive model using genetic algorithms. *Computers and Geotechnics*, 19(4), 325-348.

Papaioannou, I., Ehre, M. & Straub, D. (2019). PLS-based adaptation for efficient PCE representation in high dimensions. *Journal of Computational Physics*, 387, 186–204.

Perez, R. E. & Behdinan, K. (2007). Particle swarm approach for structural design optimization. *Computers & Structures*, 85(19-20), 1579–1588.

Pham, T. A., Tran, V. Q. & Vu, H.-L. T. (2021). Evolution of deep neural network architecture using particle swarm optimization to improve the performance in determining the friction angle of soil. *Mathematical Problems in Engineering*, 2021, 1–17.

Phoon, K.-K. & Zhang, W. (2022). Future of machine learning in geotechnics. *Georisk: Assessment and Management of Risk for Engineered Systems and Geohazards*, 1–16.

Phoon, K.-K., Cao, Z.-J., Ji, J., Leung, Y. F., Najjar, S., Shuku, T., Tang, C., Yin, Z.-Y., Ikumasa, Y. & Ching, J. (2022). Geotechnical uncertainty, modeling, and decision making. *Soils and Foundations*, 62(5), 101189.

Pietruszczak, S. (2010). *Fundamentals of plasticity in geomechanics*. Crc Press Boca Raton, FL.

Plaxis, B. (2017). Reference manual for PLAXIS 2D. Netherlands: Delft.

Pramthawee, P., Jongpradist, P. & Kongkitkul, W. (2011). Evaluation of hardening soil model on numerical simulation of behaviors of high rockfill dams. *Songklanakarin Journal of Science & Technology*, 33(3), 325-334.

Puri, N., Prasad, H. D. & Jain, A. (2018). Prediction of Geotechnical Parameters Using Machine Learning Techniques. *Procedia Computer Science*, 125, 509-517.

Rahman, S. (2011). Global sensitivity analysis by polynomial dimensional decomposition. *Reliability Engineering and System Safety*, 96(7), 825–837.

Rahmani, H. & Panah, A. K. (2020). Effect of particle size and saturation conditions on the breakage factor of weak rockfill materials under one-dimensional compression testing. *Geomechanics and Engineering*, 21(4), 315-326.

Ray, R., Kumar, D., Samui, P., Roy, L. B., Goh, A. & Zhang, W. (2021). Application of soft computing techniques for shallow foundation reliability in geotechnical engineering. *Geoscience Frontiers*, 12(1), 375–383.

Rechea, C., Levasseur, S. & Finno, R. (2007). Inverse analysis techniques for parameter identification in simulation of excavation support systems. *Computers and Geothecnics*, 35, 331–345.

Rechea, C., Levasseur, S. & Finno, R. (2008). Inverse analysis techniques for parameter identification in simulation of excavation support systems. *Computers and Geotechnics*, 35(3), 331-345.

Rochon, Y., Morneau, J. & Lefebvre, G. (2001). Hydro-electric power project on the Toulnustouc River; Projet d'amenagement hydroelectrique de la riviere Toulnustouc. 1-105.

Saberi, M., Annan, C.-D. & Konrad, J.-M. (2018). Numerical analysis of concrete-faced rockfill dams considering effect of face slab-cushion layer interaction. *Canadian Geotechnical Journal*, 55(10), 1489-1501.

Salazar, F. & Hariri-Ardebili, M. A. (2022). Coupling machine learning and stochastic finite element to evaluate heterogeneous concrete infrastructure. *Engineering Structures*, 260, 114190.

Salehi, S., Raisee, M., Cervantes, M. & Nourbakhsh, A. (2018). An efficient multifidelity 11-minimization method for sparse polynomial chaos. *Computer Methods in Applied Mechanics and Engineering*, 334, 183–207.

Saltelli, A., Ratto, M., Andres, T., Campolongo, F., Cariboni, J., Gatelli, D., Saisana, M. & Tarantola, S. (2008). *Global sensitivity analysis: the primer*. John Wiley & Sons.

Samek, W., Montavon, G., Lapuschkin, S., Anders, C. J. & Müller, K.-R. (2021). Explaining deep neural networks and beyond: A review of methods and applications. *Proceedings of the IEEE*, 109(3), 247–278.

Santos Rodríguez, C. d. (2015). Backanalysis methodology based on multiple optimization techniques for geotechnical problems. 1-323.

Sargsyan, K. (2017). Surrogate models for uncertainty propagation and sensitivity analysis. In *Handbook of uncertainty quantification* (pp. 673–698).

Saxegaard, H. (2003). Crack self-healing properties of asphalt concrete: laboratory simulation. *International Journal on Hydropower & Dams*, 10(3), 106-109.

Schanz, T. & Vermeer, P. (1996). Angles of friction and dilatancy of sand.

Schanz, T., Vermeer, P. & Bonnier, P. (1999). The hardening soil model: formulation and verification. *Beyond 2000 in computational geotechnics*, 281–296.

Segura, R. L., Miquel, B., Paultre, P. & Padgett, J. E. (2021). Accounting for Uncertainties in the Safety Assessment of Concrete Gravity Dams: A Probabilistic Approach with Sample Optimization. *Water*, 13(6), 855.

Sevieri, G., Andreini, M., De Falco, A. & Matthies, H. G. (2019). Concrete gravity dams model parameters updating using static measurements. *Engineering Structures*, 196, 109231.

Shahriari, M., Pardo, D., Moser, B. & Sobieczky, F. (2020). A deep neural network as surrogate model for forward simulation of borehole resistivity measurements. *Procedia Manufacturing*, 42, 235–238.

Shahzadi, G. & Soulaïmani, A. (2021). Deep neural network and polynomial chaos expansion-based surrogate models for sensitivity and uncertainty propagation: An application to a rockfill dam. *Water*, 13(13), 1830.

Shams, M., Ahmed, E.-B. & Sayyouh, H. (2020). Harmony search optimization applied to reservoir engineering assisted history matching. *Petroleum Exploration and Development*, 47(1), 154–160.

Shang, L., Nguyen, H., Bui, X.-N., Vu, T. H., Costache, R. & Hanh, L. T. M. (2022). Toward state-of-the-art techniques in predicting and controlling slope stability in open-pit mines based on limit equilibrium analysis, radial basis function neural network, and brainstorm optimization. *Acta Geotechnica*, 17(4), 1295–1314.

Sharifzadeh, M., Tarifard, A. & Moridi, M. A. (2013). Time-dependent behavior of tunnel lining in weak rock mass based on displacement back analysis method. *Tunnelling and Underground Space Technology*, 38, 348–356.

Sherard, J. L. & Cooke, J. B. (1987). Concrete-face rockfill dam: I. Assessment. *Journal of geotechnical engineering*, 113(10), 1096-1112.

Shi, L., Gong, J. & Zhai, C. (2022). Application of a hybrid PSO-GA optimization algorithm in determining pyrolysis kinetics of biomass. *Fuel*, 323, 124344.

Smith, M. (2015). Rockfill settlement measurement and modelling of the Romaine-2 dam during construction. *Proceedings of the 25th International Congress on Large Dams, ICOLD*, 98, 468-485.

Sobol, I. M. (1993). Sensitivity analysis for non-linear mathematical models. *Mathematical modelling and computational experiment*, 1, 407–414.

Song, Z., Liu, S., Jiang, M. & Yao, S. (2022). Parameter Determination Method of Soil Constitutive Model Based on Machine Learning. *Wireless Communications and Mobile Computing*, 2022, 1-10.

Sou-Sen, L. & Hsien-Chuang, L. (2004). Neural-network-based regression model of ground surface settlement induced by deep excavation. *Automation in construction*, 13(3), 279–289.

Stateler, L. A. & Sundaram, M. (2013). *Routine Instrumented and Visual Monitoring of Dams Based on Potential Failure Modes Analysis*. United States Society on Dams.

Stephens, D., Gorissen, D., Crombecq, K. & Dhaene, T. (2011). Surrogate based sensitivity analysis of process equipment. *Applied Mathematical Modelling*, 35(4), 1676–1687.

Sterling, R. L. & Lee, C. A. (1992). A neural network-Expert system hybrid approach for tunnel design. *The 33rd US Symposium on Rock Mechanics (USRMS)*.

Storn, R. & Price, K. (1997). Differential evolution–a simple and efficient heuristic for global optimization over continuous spaces. *Journal of global optimization*, 11(4), 341–359.

Su, H., Li, J. & Wu, Z. (2007). Feedback analysis for mechanical parameters of dam and its foundation with optimization algorithm. *Chinese J. Hydrol. Eng*, 38, 129–134.

Sudret, B. (2014). Polynomial chaos expansions and stochastic finite element methods. In *Risk and reliability in geotechnical engineering* (pp. 265–300).

Sun, Y., Jiang, Q., Yin, T. & Zhou, C. (2018). A back-analysis method using an intelligent multi-objective optimization for predicting slope deformation induced by excavation. *Engineering Geology*, 239, 214–228.

Tarantola, A. (2005). *Inverse problem theory and methods for model parameter estimation*. SIAM.

Ti, K. S., Huat, B. B., Noorzaei, J., Jaafar, M. S. & Sew, G. S. (2009). A review of basic soil constitutive models for geotechnical application. *Electronic Journal of Geotechnical Engineering*, 14, 1-18.

Torkashvand, M., Neshat, A., Javadi, S. & Pradhan, B. (2021). New hybrid evolutionary algorithm for optimizing index-based groundwater vulnerability assessment method. *Journal of Hydrology*, 598, 126446.

Vahdati, P. (2014). *Identification of soil parameters in an embankment dam by mathematical optimization*. Luleå. Retrieved from: https://pure.ltu.se/portal/sv/publications/identification-of-soil-parameters-in-an-embankment-dam-by-mathematical-optimization(3d22870a-eb82-40d0-be4d-40f6a215bb75).html.

Vahdati, P., Levasseur, S., Mattsson, H. & Knutsson, S. (2013). Inverse Mohr-Coulomb soil parameter identification of an earth and rockfill dam by genetic algorithm optimization. *The Electronic journal of geotechnical engineering*, 18(X), 5419–5440.

Vahdati, P., Levasseur, S., Mattsson, H. & Knutsson, S. (2014). Inverse Hardening soil parameter identification of an earth and rockfill dam by genetic algorithm optimization. *The Electronic journal of geotechnical engineering*, 19(N), 3327–3349.

van Natijne, A. L., Lindenbergh, R. C. & Bogaard, T. A. (2020). Machine learning: New potential for local and regional deep-seated landslide nowcasting. *Sensors*, 20(5), 1425.

Vannobel, P., Smith, M., Lefebvre, G., Karray, M. & Éthier, Y. (2013). Control of rockfill placement for the romaine-2 asphaltic core dam in northern Quebec. *Canadian Geotechnical Journal*, 1-6.

Varadarajan, A., Sharma, K. & AK Gupta, K. (2003). Testing and modeling two rockfill materials. *Journal of Geotechnical and Geoenvironmental Engineering*, 129(3), 206-218.

Varadarajan, A., Sharma, K. G., Abbas, S. M. & Dhawan, A. K. (2006). Constitutive Model for Rockfill Materials and Determination of Material Constants. *International Journal of Geomechanics*, 6(4), 226-237.

Von Soos, P. (1990). Properties of soil and rock (in German), Grundbau Taschenbuch part 4. *Ernst & Sohn, Berlin*, 1-10.

Wang, W., Höeg, K. & Zhang, Y. (2010). Design and performance of the Yele asphalt-core rockfill dam. *Canadian Geotechnical Journal*, 47(12), 1365–1381.

Wang, Z. Z. (2022). Deep learning for geotechnical reliability analysis with multiple uncertainties. *Journal of Geotechnical and Geoenvironmental Engineering*, 148(4), 06022001.

Wei, Z., Xiaolin, C., Chuangbing, Z. & Xinghong, L. (2010). Creep analysis of high concrete-faced rockfill dam. *International Journal for Numerical Methods in Biomedical Engineering*, 26(11), 1477-1492.

Wiener, N. (1938). The homogeneous chaos. *American Journal of Mathematics*, 60(4), 897–936.

Wood, D. M. (1990). *Soil behaviour and critical state soil mechanics*. Cambridge university press.

Xiang, Z., Swoboda, G. & Cen, Z. (2003). Optimal Layout of Displacement Measurements for Parameter Identification Process in Geomechanics. *International Journal of Geomechanics*, 3(2), 205-216.

Xiao, Y., Meng, M., Daouadji, A., Chen, Q., Wu, Z. & Jiang, X. (2020). Effects of particle size on crushing and deformation behaviors of rockfill materials. *Geoscience Frontiers*, 11(2), 375-388.

Xing, H.-F., Gong, X.-N. & Hai-Feng Fu, X.-G. Z. (2006). Construction of concrete-faced rockfill dams with weak rocks. *Journal of geotechnical and geoenvironmental engineering*, 132(6), 778-785.

Xiu, D. & Karniadakis, G. E. (2002). The Wiener–Askey polynomial chaos for stochastic differential equations. *SIAM journal on scientific computing*, 24(2), 619–644.

Xu, C., Liu, X., Wang, E. & Wang, S. (2021). Prediction of tunnel boring machine operating parameters using various machine learning algorithms. *Tunnelling and Underground Space Technology*, 109, 103699.

Xu, Y. & Wu, Z. (2022). Parameter identification of unsaturated seepage model of core rockfill dams using principal component analysis and multi-objective optimization. *Structures*, 45, 145–162.

Yagiz, S., Yazitova, A. & Karahan, H. (2020). Application of differential evolution algorithm and comparing its performance with literature to predict rock brittleness for excavatability. *International Journal of Mining, Reclamation and Environment*, 1–14.

Yang, L. et al. (2019). Inverse analysis of rock creep model parameters based on improved simulated annealing differential evolution algorithm. *Geotechnical and Geological Engineering*, 37(2), 639–649.

Yang, Y. & Mei, G. (2022). A Deep Learning-Based Approach for a Numerical Investigation of Soil–Water Vertical Infiltration with Physics-Informed Neural Networks. *Mathematics*, 10(16), 2945.

YiFei, L., MaoSen, C., Tran-Ngoc, H., Khatir, S. & Wahab, M. A. (2023). Multi-parameter identification of concrete dam using polynomial chaos expansion and slime mould algorithm. *Computers & Structures*, 281, 107018.

Yin, Z.-Y., Jin, Y.-F., Shen, J. S. & Hicher, P.-Y. (2018). Optimization techniques for identifying soil parameters in geotechnical engineering: comparative study and enhancement. *International Journal for Numerical and Analytical Methods in Geomechanics*, 42(1), 70–94.

Yousefpour, N. & Fallah, S. (2018). Applications of Machine Learning in Geotechnics. *Proceedings of the Civil Engineering Research in Ireland Conference, Dublin, Ireland*, pp. 29–30.

Yu, Y., Zhang, B. & Yuan, H. (2007). An intelligent displacement back-analysis method for earth-rockfill dams. *Computers and Geotechnics*, 34(6), 423–434.

Zentar, R., Hicher, P.-Y. & Moulin, G. (2001). Identification of soil parameters by inverse analysis. *Computers and Geotechnics*, 28(2), 129-144.

Zhang, W. & Phoon, K.-K. (2022). Editorial for Advances and applications of deep learning and soft computing in geotechnical underground engineering. *Journal of Rock Mechanics and Geotechnical Engineering*, 14(3), 671–673.

Zhang, W., Goh, A. T. & Zhang, Y. (2016). Multivariate adaptive regression splines application for multivariate geotechnical problems with big data. *Geotechnical and Geological Engineering*, 34, 193–204.

Zhang, W., Li, H., Li, Y., Liu, H., Chen, Y. & Ding, X. (2021a). Application of deep learning algorithms in geotechnical engineering: a short critical review. *Artificial Intelligence Review*, 54(8), 5633–5673.

Zhang, W., Gu, X., Tang, L., Yin, Y., Liu, D. & Zhang, Y. (2022). Application of machine learning, deep learning and optimization algorithms in geoengineering and geoscience: comprehensive review and future challenge. *Gondwana Research*, 1-17.

Zhang, Y., Xie, Y., Zhang, Y., Qiu, J. & Wu, S. (2021b). The adoption of deep neural network (DNN) to the prediction of soil liquefaction based on shear wave velocity. *Bulletin of Engineering Geology and the Environment*, 80, 5053–5060.

Zhao, H. & Yin, S. (2016). Inverse analysis of geomechanical parameters by the artificial bee colony algorithm and multi-output support vector machine. *Inverse Problems in Science and Engineering*, 24(7), 1266–1281.

Zhou, W., Li, S., Ma, G., Chang, X., Ma, X. & Zhang, C. (2016). Parameters inversion of high central core rockfill dams based on a novel genetic algorithm. *Science China Technological Sciences*, 59(5), 783–794.

Zhou, X., Ma, G. & Zhang, Y. (2019). Grain size and time effect on the deformation of rockfill dams: A case study on the Shuibuya CFRD. *Geotechnique*, 69(7), 606-619.

Zokagoa, J.-M. [Thèse de doctorat, École de technologie supérieure).]. (2011). Modélisation numérique des écoulements à surface libre avec bancs couvrants-découvrants par les volumes finis et la décomposition orthogonale aux valeurs propres.

Zukri, A. & Nazir, R. (2018). Numerical modelling techniques of soft soil improvement via stone columns: A brief review. *IOP Conference Series: Materials Science and Engineering*, 342, 012002.